



Scuola Internazionale Superiore di Studi Avanzati - Trieste

INTERNATIONAL SCHOOL FOR ADVANCED STUDIES

PHD COURSE IN STATISTICAL PHYSICS

ACADEMIC YEAR 2019-2020

**Exact results for critical systems with
and without quenched disorder**

Thesis submitted for the degree of

DOCTOR PHILOSOPHIÆ

CANDIDATE : Noel Lamsen

SUPERVISOR : Gesualdo Delfino

SISSA - Via Bonomea 265 - 34136 TRIESTE - ITALY

Contents

Outlook	vii
List of publications	ix
1 Notions of critical phenomena	1
1.1 Phase transitions and universality	1
1.2 Field theory and renormalization group	4
1.3 Conformal field theory in $d = 2$	9
1.4 Model theories of $d = 2$ criticality	14
1.4.1 $O(N)$ model	15
1.4.2 Potts model	17
1.5 Quenched disorder	19
1.5.1 Replica method	19
1.5.2 Harris criterion	20
2 Scattering formalism	23
2.1 Particles and fields	23
2.2 Elastic scattering in $d = (1 + 1)$ QFT	24
2.3 Scale invariant scattering formalism	27
3 $O(N)$-vector model	29
3.1 Scattering formulation	29
3.2 Critical lines of non-intersecting loops	31

3.3	Critical line at $N = 2$ and the BKT phase	34
3.4	Free solutions and zero temperature critical point for $N > 2$. . .	35
4	Potts model	37
4.1	Scattering formulation	37
4.2	Ferromagnetic critical line	40
4.3	Ferromagnetic tricritical line	41
4.4	Antiferromagnetic case	42
5	Vector-Ising model	45
5.1	Physical context	45
5.2	Scattering formulation	47
5.3	Scattering solutions and classification of multicritical points . . .	49
5.4	Implications for the fully frustrated XY model	53
6	RP^{N-1} model	57
6.1	Physical context	57
6.2	Scattering formulation	59
6.3	Scattering solutions and implications for liquid crystals	62
7	Bond disordered Potts model	65
7.1	Scale invariant scattering and replicas	65
7.2	Solutions of the unitarity equations	69
7.2.1	Generic number of replicas	69
7.2.2	The limit of zero replicas	72
7.3	Properties of the solutions	74
7.3.1	Critical lines with weak disorder limit	74
7.3.2	Critical lines without weak disorder limit	76
7.4	Softening of first order transition by disorder	79
8	Bond disordered $O(N)$ model	83
8.1	Scattering formulation	83
8.2	Solutions of the fixed point equations	86

8.2.1	Generic number of replicas	87
8.2.2	Disorder limit	89
8.3	Properties of solutions for the disordered case	90
8.3.1	Critical lines with varying disorder modulus	90
8.3.2	Critical lines with maximal disorder modulus	92
Bibliography		97

Outlook

Critical behavior in statistical systems is controlled by fixed points of the renormalization group. These are points in coupling space where the divergence of the correlation length allows for scale invariance to emerge. Fixed points are naturally described within the field theoretical framework, which in particular allows to see how their invariance properties actually extend, beyond scale transformations, to conformal transformations (see e.g. [1]). The charm and, at the same time, the difficulty of critical phenomena is that in general they correspond to non-trivial fixed points of the renormalization group, i.e. to interacting field theories that can only be studied within some approximation. An important exception is represented by the two-dimensional case, where conformal symmetry becomes infinite dimensional and conformal field theory (CFT) has provided a plethora of exact results extending to multi-point correlation functions at non-trivial fixed points [1,2]. While this is a fantastic achievement, there are cases in two dimensions in which the sophisticated tools of CFT (e.g. differential equations for correlation functions) are not available, or have been so far too difficult to implement. In this respect, the idea of implementing the infinite dimensional conformal symmetry in a basis of particles rather than fields [3,4] has proved quite useful. The resulting scale invariant scattering approach relies on few basic ingredients, i.e. elasticity of scattering processes, crossing symmetry and unitarity of the scattering matrix. This minimality of means makes the formalism very general and yields exact equations that allow to explore the space of fixed points with a given internal symmetry.

This is extremely fruitful already for the “pure” case (i.e. without disorder), since it allows a global view of fixed points, which emerge from a single set of equations, as well the study of problems that had been too difficult for other analytical approaches. On the other hand, a further particularly remarkable feature of the scale invariant scattering formalism in two dimensions is that it extends to the problem of quenched disorder [5], i.e. to those “random” fixed points that had seemed out of reach for exact methods.

This thesis is organized as follows. The first two chapters are devoted to a synthetic review of main ideas and results to be used in the remaining chapters, which are devoted to the application of scale invariant scattering to various two-dimensional critical systems with and without disorder. More precisely, chapter 1 is a minimal review of the ideas and vocabulary of critical phenomena in pure and disordered systems, while chapter 2 reviews the scale-invariant scattering formalism. Chapters 3, 4, 5, and 6 contain the application of the formalism to pure systems characterized by $O(N)$, permutational (Potts), $O(N) \times Z_2$ and RP^{N-1} symmetry, respectively. Finally, chapters 7 and 8 illustrate the application to the case of quenched disorder, for the Potts and $O(N)$ models, respectively.

List of publications

The thesis is mainly based on the results obtained in the following research articles:

1. Delfino, G., and Lamsen, N. *Exact results for the $O(N)$ model with quenched disorder* J. High Energy Phys. (2018) 77.
2. Delfino, G., and Lamsen, N., *Critical lines in the pure and disordered $O(N)$ model* J. Stat. Mech. (2019) 024001.
3. Delfino, G., and Lamsen, N. *Critical points of coupled vector-Ising systems. Exact results* J. Phys. A: Math. Theor. 52 (2019) 35LT02.
4. Delfino, G., and Lamsen, N. *On the phase diagram of the random bond q -state Potts model* Eur. Phys. J. B 92 (2019) 278.
5. Delfino, G., Diouane, Y., and Lamsen, N. *Absence of nematic quasi-long-range order in two-dimensional liquid crystals with three director components*, arXiv:2005.06307.

Chapter 1

Notions of critical phenomena

We provide basic notions of the theory of critical phenomena in pure and disordered systems to be used in the following chapters.

1.1 Phase transitions and universality

The physics of a statistical system is governed by its Hamiltonian $\mathcal{H} = \mathcal{H}(\mathcal{K}, \mathcal{C})$, which is a function of a list $\mathcal{K} = \{K_j\}_{j=1}^s$ of coupling parameters and of the configurations $\mathcal{C} = \{w_i\}_{i=1}^N$ of the degrees of freedom w_i . Expectation values of observables, $\mathcal{O} = \mathcal{O}(\mathcal{C})$, are computed over the Boltzmann weight at a given temperature T (setting $k_B = 1$).

$$\langle \mathcal{O} \rangle = \frac{1}{Z(T, \mathcal{K})} \sum_{\mathcal{C}} \mathcal{O}(\mathcal{C}) e^{-\frac{1}{T} \mathcal{H}(\mathcal{K}, \mathcal{C})}, \quad (1.1.1)$$

where $Z(T, \mathcal{K})$ is the partition function,

$$Z(T, \mathcal{K}) = \sum_{\mathcal{C}} e^{-\frac{1}{T} \mathcal{H}(\mathcal{K}, \mathcal{C})} = e^{-\frac{1}{T} F(T, \mathcal{K})}, \quad (1.1.2)$$

with the free energy defined as $F = -T \ln Z$. In general, to compute meaningful thermodynamic quantities, we expect this free energy to be extensive in the limit

of large number of degrees of freedom. This enables us to define the bulk free energy density, f in the thermodynamic limit,

$$f = \lim_{N \rightarrow \infty} \frac{F}{N}. \quad (1.1.3)$$

This encodes the thermodynamic properties of the system in its derivatives, in particular,

$$E = -T^2 \frac{\partial}{\partial T} \left(\frac{f}{T} \right), \quad C = -T \frac{\partial^2 f}{\partial T^2}, \quad (1.1.4)$$

where E and C are the energy density and specific heat capacity of the system, respectively. We will be concerned with the thermodynamic limit, and will refer to f . Phase transitions manifest as some singular behavior of f .

An important tool in understanding phase transitions is the idea of *order parameter* and the symmetry it reflects. The underlying Hamiltonian $\mathcal{H}(\mathcal{K}, \mathcal{C})$ is symmetric under a symmetry group G if there is a representation of the group, in the form of transformations \mathcal{T} operating on the configuration space $\{\mathcal{C}\}$, which leaves the Hamiltonian invariant,

$$\mathcal{H}(\mathcal{C}') = \mathcal{H}(\mathcal{C}), \quad \mathcal{C}' = \mathcal{T}\mathcal{C}. \quad (1.1.5)$$

The symmetry transformations can directly act on the microscopic variables (*internal* symmetries) or may also involve moving the microscopic variables around in the physical space (*spatial* symmetries). The internal symmetry is *global* if it acts on the entire system uniformly, otherwise it is *local*. A common mechanism for phase transition is *spontaneous symmetry breaking* (SSB) of global internal symmetries. This happens when the system chooses one of several degenerate ground state configurations as $T \rightarrow 0$. In a spontaneously broken phase, the order parameter, which transforms under a representation of the symmetry, acquires a non-vanishing value. This low temperature state called the *ordered phase* can persist up to a critical temperature, $T_c \geq 0$. Above T_c , the order parameter vanishes and the system enters a symmetric *disordered phase*. The change in

the order parameter at T_c can be discontinuous, and we call this a *first order transition*. Instead, if the order parameter vanishes continuously as $T \rightarrow T_c$ from the ordered phase, we have a second-order or *continuous phase transition*. In this case, at $T = T_c$, the system achieves *criticality* and we call the associated properties and observations as *critical phenomena*.

In some cases, the identification of the order parameter and the symmetry it breaks during phase transitions may not be straightforward. For paramagnetic-ferromagnetic transitions, the order parameter is usually the averaged site variable – magnetization per site. For liquid-gas transitions, the order parameter is usually chosen to be the density difference between the liquid and gas phase, $(\rho_l - \rho_g)$, but the underlying broken symmetry is not physically apparent. Nevertheless, at the critical point, the liquid-gas system emerges with an effective two-fold symmetry. In superfluid transitions, the order parameter takes on exotic forms such as the complex phase of a macroscopic wavefunction. It is instructive to study simplified models with order parameter transforming under a given symmetry to provide insight into corresponding physical systems at criticality.

It is convenient to consider model Hamiltonians where the order parameter is the averaged localized variable, as in the case of magnetic systems. We consider the system as discretized on a d -dimensional lattice with sites indexed by $i = 1, 2, \dots, N$, and assign to each site a classical “spin” variable σ_i transforming according to a representation of a given symmetry G . The order parameter is the average magnetization per site, $m = \langle \sum_i \sigma_i \rangle / N$ in the thermodynamic limit. In addition, we can couple the spins to an external magnetic field h by adding a term $h \sum_i \sigma_i$ in the Hamiltonian. Spin fluctuation can be computed using the two-point connected correlation function,

$$\Gamma(r_{i,j}) = \langle \sigma_i \sigma_j \rangle - \langle \sigma_i \rangle \langle \sigma_j \rangle, \quad (1.1.6)$$

where $r_{i,j}$ is the distance between the lattice sites i and j . Away from criticality, this decays as $\Gamma(r) \sim e^{-r/\xi}$ for $r \gg \xi$, where ξ is the *correlation length*.

Exponent	Definition	Name
α	$C \sim T - T_c ^{-\alpha}, h = 0$	heat capacity
β	$m \sim (T_c - T)^\beta, T < T_c, h = 0$	order parameter
δ	$m \sim h^{\frac{1}{\delta}}, T = T_c$	equation of state
γ	$\chi = \frac{\partial m}{\partial h} \sim T - T_c ^{-\gamma}, h = 0$	susceptibility
η	$\Gamma(r) \sim r^{2-d-\eta}, T = T_c, h = 0$	two-point function
ν	$\xi \sim T - T_c ^{-\nu}, h = 0$	correlation length

Table 1.1: Definition of critical exponents for magnetic systems.

However, at a second order critical point, the correlation length diverges and the correlation function assumes a power law decay of the form $\Gamma(r) \sim r^{2-d-\eta}$. This power law decay of the correlation function manifests, for example, in the observed divergence of the susceptibility $\chi = \langle \sum_j \sigma_i \sigma_j \rangle / N$ for critical systems. These power law singularities occur also in other physical quantities as a function of the external parameters like temperature and conjugate external fields. The exponents appearing in these power law relations are called *critical exponents*. Remarkably, critical exponents are insensitive to microscopic details and depend only on a set of global properties of the system such as symmetries, order parameter dimension, and space dimensionality – an observation referred to as *universality*. Thus, systems with different microscopic details may produce the same critical exponents near the critical point. Such systems belong to the same *universality class*.

1.2 Field theory and renormalization group

The divergence of correlation length and the power law relations observed at the critical point suggests the absence of characteristic length scale in a critical system. There is no separation of length scales mediated by the correlation length. Fluctuations on smaller scales cascade into increasingly larger scales re-

sulting in divergent behavior of susceptibilities at criticality. Addressing this is the origin of the *renormalization group* idea. Instead of performing the partition function sum for all the variable configurations, the system is described in a successively coarse-grained manner by selectively summing configurations at an increasing scale without affecting the large distance physics. This is implemented via transformations generally referred to as renormalization group transformations. This idea was initially formulated in real space [6] via block spin transformations, $\sigma_B = \sum_{i \in B} \sigma_i / \Lambda_B$ where B is a block of neighboring sites of size Λ_B in the lattice such that

$$Z = \sum_{\{\sigma_i\}} e^{-\frac{1}{T} \mathcal{H}[\mathcal{K}, \{\sigma_i\}]} = \sum_{\{\sigma_B\}} e^{-\frac{1}{T} \mathcal{H}[\mathcal{K}', \{\sigma_B\}]}, \quad (1.2.1)$$

where $\mathcal{K}' = \mathcal{R}\mathcal{K}$ is the induced renormalization transformation \mathcal{R} acting on the coupling parameters. Essentially, the quantities are measured at a scaled metric without changing their value. For instance, the physical value of correlation length is successively measured through some scale factor $b > 1$ of the lattice spacing a such that $\xi_{\text{phys}} = \xi a = \xi'(ba)$ so that $\xi' = \mathcal{R}\xi = \xi/b$. The expression “renormalization group” refers to the semigroup features (absence of inverse) under composition of two transformations. Successive application of renormalization group transformations generates a flow in the parameter space spanned by all possible coupling parameter values \mathcal{K} . A main goal is to determine renormalization group flow *fixed points* \mathcal{K}^* where application of renormalization group transformations does not change the coupling parameters, i.e. $\mathcal{K}^* = \mathcal{R}\mathcal{K}^*$. These parameters, \mathcal{K}^* , correspond to an effective fixed point Hamiltonian, \mathcal{H}^* . Since renormalization group transformations involve a change of scale, a fixed point Hamiltonian enjoys *scale invariance* and corresponds to infinite correlation length.

At the vicinity of a fixed point, the divergence of correlation length suggests that the lattice spacing a can be treated as $a \rightarrow 0$, thereby motivating a continuum description. This corresponds to a homogeneous and isotropic *field the-*

ory. The lattice site label i is replaced by $x = (x^1, x^2, \dots, x^d)$, coordinate in a d -dimensional Euclidean space \mathbb{R}^d , while the spin variables σ_i are effectively replaced by the spin or *order parameter field*, $\sigma(x)$. The reduced Hamiltonian \mathcal{H}/T is replaced by a *Euclidean action* \mathcal{A} . The field theory contains an infinite set of local *scaling fields*, $\{\Phi_i(x)\}$. Expectation values are formally computed by averaging over the field configurations, an operation that we formally write as

$$\langle(\dots)\rangle = \frac{1}{Z} \sum_{\substack{\text{field} \\ \text{configs}}} (\dots) e^{-\mathcal{A}}, \quad Z = \sum_{\substack{\text{field} \\ \text{configs}}} e^{-\mathcal{A}}. \quad (1.2.2)$$

A *fixed point field theory* corresponds in the continuum to a fixed point Hamiltonian \mathcal{H}^* . Scale invariance of such a field theory constrains (along with translation and rotation invariance in Euclidean space) the two-point correlation function of a scaling field Φ to decay as a power law of the distance,

$$\langle\Phi(x)\Phi(0)\rangle \sim \frac{1}{|x|^{2X_\Phi}}, \quad (1.2.3)$$

where X_Φ is the *scaling dimension* of the field. Scaling dimensions determine the behavior of correlation functions under a scale transformation $x \rightarrow x' = x/b$:

$$\langle\Phi_1(x'_1)\Phi_2(x'_2)\dots\Phi_k(x'_k)\rangle = b^{\sum_{i=1}^k X_i} \langle\Phi_1(x_1)\Phi_2(x_2)\dots\Phi_k(x_k)\rangle, \quad (1.2.4)$$

formally implying $\Phi' = \mathcal{R}\Phi \sim b^X\Phi$. The existence of a set of infinite scaling fields $\{\Phi_i\}$ postulates the possibility of expanding a product of fields $\Phi_i(x)\Phi_j(0)$ with $x \rightarrow 0$ as a linear combination of fields at $x = 0$. For fixed point theories, this can be represented by an *operator product expansion* (OPE) of the form

$$\langle\Phi_i(x)\Phi_j(0)\dots\rangle = \sum_k \frac{C_{i,j}^k}{|x|^{X_i+X_j-X_k}} \langle\Phi_k(0)\dots\rangle, \quad (1.2.5)$$

with numerical coefficients $C_{i,j}^k$ as structure constants peculiar to a given field theory.

To explain universality at critical temperature T_c , the action \mathcal{A} can be expanded in the vicinity of a fixed point action \mathcal{A}^* incorporating perturbations consistent with the symmetry group of interest G [7]. A generic expansion around the fixed point action can be represented as

$$\mathcal{A} = \mathcal{A}^* + K_i \int d^d x \Phi_i(x). \quad (1.2.6)$$

Since the action is dimensionless, a coupling parameter K_i scales as $K'_i \sim b^{d-X_i} K_i$. The perturbation of the fixed point action by a scaling field Φ_i is said to be:

1. *Irrelevant* if $X_i > d$, so that the conjugate coupling flows to zero giving back the fixed point action.
2. *Marginal* if $X_i = d$, and further analysis is needed to see how it affects the fixed point.
3. *Relevant* if $X_i < d$, so that the conjugate coupling grows and the theory flows away from the fixed point.

A lattice model contains parameters $\mathbf{K} = \{K_1, K_2, \dots, K_s\}$. For a given fixed point theory, there will be infinitely many irrelevant fields whose corresponding conjugate couplings span a hypersurface basin of attraction of renormalization group flows towards the fixed point, \mathcal{K}^* . A particular model intersects this critical hypersurface at the critical parameter values \mathbf{K}_c , which will flow to \mathcal{K}^* . All points in this critical hypersurface must necessarily have $\xi_c = \infty$, so that they can flow to the fixed point correlation length $\xi^* = \infty$. Thus, these points characterize the critical points of various models intersecting the critical hypersurface. This accounts for the observed universality at \mathbf{K}_c of different models whose long distance (infrared) behaviour is governed by the fixed point theory at \mathcal{K}^* .

In the presence of a single relevant field $\varepsilon(x)$ invariant under the symmetry group

G , we consider the scaling action

$$\mathcal{A} = \mathcal{A}^* + \tau \int d^d x \varepsilon(x), \quad (1.2.7)$$

where $\tau \sim T - T_c$ measures the deviation from criticality. The regions $\tau > 0$ and $\tau < 0$ correspond to different phases across the phase transition at $\tau = 0$. The energy density field $\varepsilon(x)$ is the most relevant G -invariant field in the fixed point theory. Simplest theories only contain one G -invariant relevant field. More generally, however, multiple G -invariant relevant fields can occur. In this case, several parameters have to be tuned to achieve criticality, and the corresponding fixed points are referred to as *multicritical*. The outflow directions generated by the other relevant G -invariant fields can lead to another G symmetric fixed points of lesser order. Another scenario that can occur is the presence of marginal G -invariant fields in the theory. On closer inspection, these marginal fields are often just marginally relevant or marginally irrelevant, generating flows much slower than usual relevant and irrelevant fields. Adding marginally irrelevant fields to the action contributes logarithmic corrections to scaling. On the other hand, a *truly marginal* G -invariant field preserves scale-invariance, and the conjugate coupling parametrizes a line of G -symmetric fixed points in coupling space.

Adding G -symmetry breaking fields in the action amounts to switching on an external field h . The order parameter field $\sigma(x)$ is the most relevant G -covariant field. The scaling dimensions of the energy density and order parameter fields determine the critical exponents. For instance, combining the scaling of temperature parameter $\tau' \sim b^{d-X_\varepsilon} \tau$ with the correlation length $\xi' \sim b^{-1} \xi$ yields $\xi \sim \tau^{-\frac{1}{d-X_\varepsilon}}$. Comparing with $\xi \sim \tau^{-\nu}$ gives

$$\nu = \frac{1}{d - X_\varepsilon}. \quad (1.2.8)$$

Similarly, the anomalous dimension follows from the power-law decay of the critical two-point correlation function of the order parameter field $\langle \sigma(x) \sigma(0) \rangle \sim$

$|x|^{2-d-\eta}$, and then is given by

$$\eta = 2 - d + 2X_\sigma. \quad (1.2.9)$$

Similar relations for the other critical exponents can be derived. Scaling analysis of σ , ε , h , τ , $\chi \sim \int d^d x \langle \sigma(x)\sigma(0) \rangle$, $C \sim \int d^d x \langle \varepsilon(x)\varepsilon(0) \rangle$, and $m = \langle \sigma(x) \rangle$ yield

$$\alpha = \frac{d - 2X_\varepsilon}{d - X_\varepsilon}, \quad \beta = \frac{X_\sigma}{d - X_\varepsilon}, \quad \delta = \frac{d - X_\sigma}{X_\sigma}, \quad \gamma = \frac{d - 2X_\sigma}{d - X_\varepsilon}. \quad (1.2.10)$$

Hence, we see that the scaling dimensions X_ε and X_σ specify the critical exponents, and thus the universality class of the model.

1.3 Conformal field theory in $d = 2$

Field theory allows to show [1] that, besides global scale invariance, fixed point theories are invariant under smooth point dependent scale transformations. In place of (1.2.4) one considers the transformation of correlation functions with a local scaling factor $b(x)$ [1, 8],

$$\langle \Phi_1(x'_1)\Phi_2(x'_2)\dots\Phi_n(x'_n) \rangle = \left(\prod_{i=1}^n b(x_i)^{X_i} \right) \langle \Phi_1(x_1)\Phi_2(x_2)\dots\Phi_n(x_n) \rangle. \quad (1.3.1)$$

Along with translations, rotations, and dilatations, the relation above is consistent with the so called special conformal transformations – composition of a translation in between two spatial inversions. Altogether, they generate the group of *conformal transformations* [9]. For this reason the fixed point theory is called a *conformal field theory* (CFT). For generic dimension $d > 2$, conformal symmetry only provides a finite set of constraints to the possible form of n -point correlation functions. In $d = 2$, conformal symmetry has instead infinitely many generators. This sufficiently constraints the CFT to allow in many cases the exact calculation of correlation functions [2].

In two dimensions, it is convenient to work in terms of complex coordinates

$z = x^1 + ix^2$ and $\bar{z} = x^1 - ix^2$ transforming under spatial rotation as $z \rightarrow ze^{i\alpha}$ and $\bar{z} \rightarrow \bar{z}e^{-i\alpha}$ for some angle α . Scaling fields can, in general, transform under rotation by gaining some complex phase $\Phi(z, \bar{z}) \rightarrow e^{-is_\Phi\alpha}\Phi(z, \bar{z})$, where s_Φ is called the *Euclidean spin* of Φ . As a consequence, the two-point correlation function of Φ can be generally written as

$$\langle \Phi(z, \bar{z})\Phi(0, 0) \rangle \sim \frac{1}{(z\bar{z})^{X_\Phi}} \left(\frac{\bar{z}}{z}\right)^{s_\Phi} = \frac{1}{z^{2\Delta}\bar{z}^{2\bar{\Delta}}}, \quad (1.3.2)$$

where the conformal dimensions $(\Delta_\Phi, \bar{\Delta}_\Phi)$ are introduced such that $X_\Phi = \Delta_\Phi + \bar{\Delta}_\Phi$ and $s_\Phi = \Delta_\Phi - \bar{\Delta}_\Phi$. Two fields Φ_i and Φ_j are said to be *mutually local* if the expectation value $\langle \Phi_i(z_1, \bar{z}_1)\Phi_j(z_2, \bar{z}_2) \dots \rangle$ is single-valued. The OPE (1.2.5) can now be generalized to (suppressing the expectation value in subsequent equations for brevity)

$$\Phi_i(z, \bar{z})\Phi_j(0, 0) = \sum_k \frac{C_{i,j}^k}{z^{\Delta_i+\Delta_j-\Delta_k}\bar{z}^{\bar{\Delta}_i+\bar{\Delta}_j-\bar{\Delta}_k}}\Phi_k(0, 0), \quad (1.3.3)$$

and the mutual locality condition for the two fields can be written as

$$s_i + s_j - s_k \in \mathbb{Z} \quad (1.3.4)$$

for every k in the expansion. Mutual locality with the energy density field $\varepsilon(x)$ is generally expected.

A field theory has a conserved symmetric energy-momentum tensor $T_{\mu\nu}(x)$. For infinitesimal coordinate transformation $x^\mu \rightarrow x'^\mu = x^\mu + a^\mu(x)$, $T_{\mu\nu}$ generates the variation of the action as, $\delta\mathcal{A} \sim -\int d^d x T_{\mu\nu}\partial^\mu a^\nu$. In $d = 2$, in the basis of complex coordinates, infinitesimal coordinate transformations associated with conformal symmetry decouple into $z \rightarrow z + a(z)$ and $\bar{z} \rightarrow \bar{z} + \bar{a}(\bar{z})$, where a and \bar{a} are analytic functions. The three independent components of the energy-momentum tensor are $T = T_{zz}$, $\bar{T} = T_{\bar{z}\bar{z}}$ and $-\Theta = T_{z\bar{z}} = T_{\bar{z}z}$, with conformal dimensions $(\Delta, \bar{\Delta})$ given by $(2, 0)$, $(0, 2)$, and $(1, 1)$, respectively. The conserva-

tion law can be written as

$$\bar{\partial}T = \partial\Theta, \quad \partial\bar{T} = \bar{\partial}\bar{\Theta}, \quad (1.3.5)$$

with $\partial = \partial_z$ and $\bar{\partial} = \partial_{\bar{z}}$. Scale-invariance at criticality implies a traceless energy-momentum tensor. In two dimensions, this decouples the remaining non-vanishing components into analytic functions as $T = T(z)$ and $\bar{T} = \bar{T}(\bar{z})$. Physically relevant fields must be mutually local with the energy-momentum tensor. Since T is analytic, the OPE with a scaling field Φ can be expanded as a Laurent series,

$$T(z)\Phi(0) = \sum_{n=-\infty}^{\infty} \frac{1}{z^{n+2}} L_n \Phi(0), \quad (1.3.6)$$

where the fields $L_n\Phi$ have conformal dimensions $(\Delta_\Phi - n, \bar{\Delta}_\Phi)$, with n integers as required by mutual locality. Similar relation holds for \bar{T} and \bar{L}_n with conformal dimensions $(\Delta_\Phi, \bar{\Delta}_\Phi - n)$ for fields $\bar{L}_n\Phi$. For instance, $L_0\Phi = \Delta_\Phi\Phi$ and $L_{-1}\Phi = \partial\Phi$. The space of fields can be organized into several *conformal families*. A conformal family, denoted by $[\phi]$, consists of a field with lowest conformal dimension ϕ called *primary* with the property $L_n\phi = 0$ for $n > 0$, along with its *descendants* $L_n\phi$ with $n < 0$. The shift operators L_n and \bar{L}_n in the space of fields graded by the conformal dimension $(\Delta, \bar{\Delta})$ satisfy the Virasoro algebra [1, 8]

$$[L_n, L_m] = (n - m)L_{n+m} + \frac{c}{12}(n^3 - n)\delta_{n,-m}, \quad (1.3.7)$$

with the same relation for \bar{L}_n operators and the decoupling $[L_n, \bar{L}_m] = 0$. Primary fields satisfy the OPE

$$T(z)\phi(0) = \frac{\Delta_\phi}{z^2}\phi(0) + \frac{1}{z}\partial\phi(0) + \dots \quad (1.3.8)$$

The energy-momentum field T is not a primary but a descendant of the identity field I , $T = L_{-2}I$. The constant c , called the *central charge*, in the Virasoro algebra is fundamental to the theory and manifests in the OPE of the energy-

momentum tensor with itself,

$$T(z)T(0) = \frac{c}{2z^4} + \frac{2}{z^2}T(0) + \frac{1}{z}\partial T(0) + \dots \quad (1.3.9)$$

The central charge provides a measure for the number of effective degrees of freedom of a critical theory [10]. It is also additive, in the sense that a theory composed of decoupled sectors, each with central charge c_i , will have a central charge $c = \sum_i c_i$.

The family of fields $[\phi]$ by construction provides a lowest weight representation of the Virasoro algebra. The primary ϕ is the lowest weight vector with its conformal dimension Δ_ϕ , while the descendants form *levels*, indexed by integer $l > 0$, i.e, subspaces of fields with conformal dimension $\Delta_\phi + l$ spanned by $\{L_{-j_1} \dots L_{-j_k} \phi\}$ with $0 < j_1 \leq \dots \leq j_k$ and $\sum_{i=1}^k j_i = l$. In some cases it is possible to obtain irreducible representations starting from a reducible representation, i.e., a family $[\phi]$ containing an embedded family $[\phi_0]$ whose primary ϕ_0 is a descendant of ϕ at level l_0 . Then, one factors out the $[\phi_0]$ representation from $[\phi]$ to give an irreducible representation *degenerate* at level l_0 . The primary, ϕ , of the irreducible representation is called *degenerate primary*. The process of factoring out $[\phi_0]$ corresponds to setting ϕ_0 to zero, leading to constraints in the form of linear partial differential equation for the expectation values involving the now degenerate primary ϕ [2].

Simplest universality classes in two dimensions are associated with CFT's with central charge $c \leq 1$. This can be formulated in terms of the Gaussian action of a free scalar boson field [11]

$$\mathcal{A}_0 = \frac{1}{4\pi} \int d^2x (\nabla\varphi)^2. \quad (1.3.10)$$

The components of the energy-momentum tensor can be written as

$$T(z) = -(\partial\varphi)^2 + iQ\partial^2\varphi, \quad \bar{T}(\bar{z}) = -(\bar{\partial}\varphi)^2 + iQ\bar{\partial}^2\varphi, \quad (1.3.11)$$

where the term proportional to Q does not affect the conservation laws $\bar{\partial}T = \partial\bar{T} = 0$ due to the equation of motion $\partial\bar{\partial}\phi = 0$. The equation of motion also allows the decomposition of the scalar field φ into

$$\varphi(x) = \phi(z) + \bar{\phi}(\bar{z}), \quad (1.3.12)$$

and is consistent with the logarithmic correlation function

$$\langle \varphi(x)\varphi(0) \rangle = -\ln|x| = -\frac{1}{2}(\ln z + \ln \bar{z}). \quad (1.3.13)$$

This motivates using the exponentials of ϕ and $\bar{\phi}$ as the primary fields $V_{q,\bar{q}} = V_q\bar{V}_{\bar{q}}$, with

$$V_q(z) = e^{2iq\phi(z)}, \quad \bar{V}_{\bar{q}}(\bar{z}) = e^{2i\bar{q}\bar{\phi}(\bar{z})}. \quad (1.3.14)$$

The additional Q term in the energy-momentum tensor modifies the central charge and conformal dimensions of the primary fields as

$$c = 1 - 6Q^2, \quad \Delta_q = q(q - Q), \quad \bar{\Delta}_{\bar{q}} = \bar{q}(\bar{q} - Q). \quad (1.3.15)$$

For $Q = 0$, we have the $c = 1$ free Gaussian critical theory whose primaries follow the OPE

$$V_{q,\bar{q}}V_{q',\bar{q}'} = [V_{q+q',\bar{q}+\bar{q}'}], \quad (1.3.16)$$

where the structure constants and z -dependence are suppressed and $[\dots]$ denotes the conformal family. Mutual locality of the two fields requires

$$2(qq' - \bar{q}\bar{q}') \in \mathbb{Z} \quad (1.3.17)$$

For general $Q \in \mathbb{R}$, the following parametrization is convenient,

$$Q = \beta^{-1} - \beta, \quad \beta^2 = \frac{p}{p+1}, \quad (1.3.18)$$

along with the following notation for the fields

$$\Phi_{\mu,\nu}(z) = V_{q_{\mu,\nu}}(z), \quad \bar{\Phi}_{\mu,\nu}(\bar{z}) = \bar{V}_{q_{\mu,\nu}}(\bar{z}), \quad (1.3.19)$$

where q is further parametrized by (μ, ν) and β as

$$q_{\mu,\nu} = \frac{1}{2} [(1 - \mu)\beta^{-1} + (1 - \nu)\beta]. \quad (1.3.20)$$

This ultimately parametrizes the central charge and conformal dimensions following the Kac formula [1]

$$c = 1 - \frac{6}{p(p+1)}, \quad \Delta_{\mu,\nu} = \frac{[(p+1)\mu - p\nu]^2 - 1}{4p(p+1)}. \quad (1.3.21)$$

For positive integer values $\mu = m$ and $\nu = n$, the fields $\Phi_{m,n}$ are degenerate primaries [2]. The degenerate-nondegenerate and degenerate-degenerate OPE's take the form

$$\Phi_{m,n} \Phi_{\mu,\nu} = \sum_{k=0}^{m-1} \sum_{l=0}^{n-1} [\Phi_{\mu-m+1+2k, \nu-n+1+2l}], \quad (1.3.22)$$

$$\Phi_{m,n} \Phi_{m',n'} = \sum_{k=0}^{\min(m,m')-1} \sum_{l=0}^{\min(n,n')-1} [\Phi_{|m-m'|+1+2k, |n-n'|+1+2l}], \quad (1.3.23)$$

respectively.

1.4 Model theories of $d = 2$ criticality

The universality class of a given model at criticality depends on the identification of energy density and order parameter fields. Here, two main statistical models, one with continuous and the other with discrete symmetry, are considered as an illustration.

1.4.1 $O(N)$ model

A basic example of continuous symmetry is the orthogonal symmetry $G = O(N)$. This can be realized in the $O(N)$ vector model, defined on a lattice by the Hamiltonian

$$\mathcal{H}_{O(N)} = - \sum_{\langle i,j \rangle} J_{i,j} \boldsymbol{\sigma}_i \cdot \boldsymbol{\sigma}_j \quad (1.4.1)$$

with N -component unit vectors $\boldsymbol{\sigma}_i = (\sigma_i^1, \dots, \sigma_i^N)$ and $\langle i, j \rangle$ denoting the sum over nearest neighbors. The homogeneous case, to which we refer for the time being, is given by $J_{i,j} = J$. Known models correspond to particular values of N , i.e., $N = 1$ for Ising, $N = 2$ for XY, and $N = 3$ for Heisenberg model. An important result comes from rewriting the partition function of a related model with the same $O(N)$ symmetry into a form of loop expansion in a lattice,

$$Z_{\text{loops}} = \sum_{\mathcal{C}_{\text{loops}}} N^{n_l} K^{n_b}, \quad (1.4.2)$$

with $K \sim J/T$, the summation running over all possible configurations $\mathcal{C}_{\text{loops}}$ obtained by drawing n_l closed loops for a total of n_b edges of the lattice [8]. A remarkable property of the expansion is the new role played by N as loop fugacity which may be taken to vary continuously. The model is solvable on the hexagonal lattice (non-intersecting loops) [12–14] and allows exact calculations as $N \rightarrow 0$ for self-avoiding walks [15] – a completely geometric problem not directly involving temperature. The critical $O(N)$ model was identified for $-2 \leq N \leq 2$ as [11] with the CFT with central charge (1.3.21), via the correspondence

$$N = 2 \cos \frac{\pi}{p}. \quad (1.4.3)$$

At $N = 2$, the model displays critical behavior differing from the usual SSB picture. It is known that for continuous symmetries in $d = 2$, ordering is unstable for $T > 0$, so that a spontaneously broken phase cannot occur [16–18], and the order parameter remains zero for any temperature. However, the $O(2)$

model undergoes a transition of the Berezinsky-Kosterlitz-Thouless (BKT) type at a temperature $T_{\text{BKT}} > 0$, signaling the onset of quasi-long range ordering (QLRO) for $T < T_{\text{BKT}}$ [19, 20]. This low temperature phase is characterized by an algebraic decay of correlations, in contrast with the exponential decay for the high temperature phase. The critical behavior around T_{BKT} is captured by the $c = 1$ Gaussian action (1.3.10) perturbed as in (1.2.7) by an energy density field $\varepsilon = \cos 2b\phi \propto V_{b,b} + V_{-b,-b}$ with conformal dimension $\Delta_\varepsilon = \bar{\Delta}_\varepsilon = b^2$. This is known as the sine-Gordon model. It follows from (1.3.17) that a field $V_{q,\bar{q}}$ is mutually local with ε if the field parameters satisfy

$$q - \bar{q} = \frac{m}{2b}, \quad m \in \mathbb{Z}. \quad (1.4.4)$$

Starting with the choice $m = 1$, a two-component complex Dirac fermion can be constructed,

$$\Psi = \begin{pmatrix} \psi \\ \bar{\psi} \end{pmatrix} = \begin{pmatrix} V_{\frac{1}{4b} + \frac{b}{2}, -\frac{1}{4b} + \frac{b}{2}} \\ V_{\frac{1}{4b} - \frac{b}{2}, -\frac{1}{4b} - \frac{b}{2}} \end{pmatrix} \quad (1.4.5)$$

with spin $q^2 - \bar{q}^2 = \pm \frac{1}{2}$ for ψ and $\bar{\psi}$, respectively. This can be written in terms of real Majorana fermions

$$\Psi = \Psi_1 + i\Psi_2 = \begin{pmatrix} \psi_1 \\ \bar{\psi}_1 \end{pmatrix} + i \begin{pmatrix} \psi_2 \\ \bar{\psi}_2 \end{pmatrix}. \quad (1.4.6)$$

This is at the origin of the result, known as *bosonization*, that the Gaussian bosonic action (1.3.10) can be mapped into the Thirring model for fermions [21, 22]

$$\mathcal{A}_0 = \int d^2x \left(\sum_{i=1}^2 (\psi_i \bar{\partial} \psi_i + \bar{\psi}_i \partial \bar{\psi}_i) + g(b^2) \psi_1 \bar{\psi}_1 \psi_2 \bar{\psi}_2 \right). \quad (1.4.7)$$

The fermionic counterpart for the energy density $\varepsilon = \cos 2b\phi$ is given by $\psi_1 \bar{\psi}_1 + \psi_2 \bar{\psi}_2$. The fermionic action is interacting except at the decoupling point $g(b^2 = \frac{1}{2}) = 0$. Symmetry in the action corresponds to invariance under $O(2)$ rotation

of (ψ_1, ψ_2) , or $U(1)$ transformation of complex fermion ψ with $m = 1$ as the $U(1)$ charge. The order parameter field associated to this symmetry can be built from $m = \pm 1$ spin-0 fields $\sigma_{\pm} = V_{\pm \frac{1}{4b}, \mp \frac{1}{4b}}$ with conformal dimension $\Delta_{\pm} = \bar{\Delta}_{\pm} = \frac{1}{16b^2}$. Other $O(2)$ -invariant fields must also be mutually local with both ε and σ_{\pm} . These can be constructed from $V_{q,q}$ with $q = kb$ ($k \in \mathbb{Z}$) with conformal dimension $\Delta_k = \bar{\Delta}_k = k^2 b^2$. Aside from the trivial field, $k = 0$, all these $O(2)$ -invariant fields including ε are irrelevant for $b^2 > 1$. This accounts for the BKT phase of $O(2)$ models and $b^2 = 1$ corresponds to the critical temperature T_{BKT} .

$O(N)$ symmetric theories can also be trivially built from N free bosonic ($c = 1$) or fermionic ($c = \frac{1}{2}$) fields, i.e.

$$\mathcal{A}_0^{N\text{-boson}} \propto \sum_{i=1}^N \int d^2x (\nabla \varphi_i)^2, \quad (1.4.8)$$

$$\mathcal{A}_0^{N\text{-fermion}} \propto \sum_{i=1}^N \int d^2x (\psi_i \bar{\partial} \psi_i + \bar{\psi}_i \partial \bar{\psi}_i), \quad (1.4.9)$$

with central charge N and $\frac{N}{2}$, respectively. There is however, a non-trivial realization in the form of the non-linear sigma model

$$\mathcal{A}_{\text{SM}} = \frac{1}{T} \sum_{i=1}^N \int d^2x (\nabla \varphi_i)^2, \quad \sum_{i=1}^N \varphi_i = 1, \quad (1.4.10)$$

which differs from (1.4.8) for the constraint on the length of the vector $(\varphi_1, \dots, \varphi_N)$. This model provides a realization of *asymptotic freedom* in the short-distance limit [8]. This corresponds to a fixed point at $T = 0$ with central charge $c = N - 1$, marginally relevant energy density and exponentially diverging correlation length for $T \rightarrow 0$.

1.4.2 Potts model

An important example of discrete symmetry is the permutation group of q objects \mathbb{S}_q . A realization of a statistical model with permutation symmetry is the Potts

model. It is defined by the lattice Hamiltonian

$$\mathcal{H}_{\text{Potts}} = - \sum_{\langle i,j \rangle} J_{i,j} \delta_{\sigma_i, \sigma_j} \quad (1.4.11)$$

where the variables σ_i take q different values $\sigma \in \{1, \dots, q\}$, which can be conveniently referred to as “colors”. The homogeneous case, to which we refer for the time being, corresponds to $J_{i,j} = J$. The order parameter can be built with the q spin-like variables,

$$s_{\sigma_i, \alpha} = \delta_{\sigma_i, \alpha} - \frac{1}{q}, \quad \alpha = 1, \dots, q, \quad (1.4.12)$$

whose expectation values vanish in the high temperature phase. The model corresponds to Ising at $q = 2$, and to a particular case of Ashkin-Teller model for $q = 4$. The lattice partition function also allows a geometric expansion in terms of clusters [8, 23] known as Fortuin-Kasteleyn expansion [24],

$$Z_{\text{Potts}} \propto \sum_{\mathcal{C}_{\text{graphs}}} q^{n_c} p^{n_b} (1-p)^{\bar{n}_b}, \quad (1.4.13)$$

where one sums over all graph configurations with (\bar{n}_b) n_b (un-) occupied bonds and n_c clusters (including isolated sites). The parameter $p = 1 - e^{-J/T}$ plays the role of bond occupation probability. In particular, for $q \rightarrow 1$, (1.4.13) corresponds to bond percolation [23]. The model has been shown, through exact lattice calculations, to display a continuous phase transition for $q \leq 4$ in the ferromagnetic case ($J \geq 0$) [25]. For $q > 4$ the continuous transition gives way to a first-order transition [23, 25]. These results point to a CFT with continuous parameter q for $0 \leq q \leq 4$. This corresponds to the central charge (1.3.21) with [11, 12]

$$\sqrt{q} = 2 \cos \frac{\pi}{p+1}. \quad (1.4.14)$$

1.5 Quenched disorder

Statistical systems may contain a fraction of degrees of freedom (let us call them “impurities” or “disorder”) which take too long to reach thermal equilibrium as compared to the other (let us call them “ordinary”) degrees of freedom. It then makes sense to consider the impurities as random variables $\mathcal{J} = \{J_{i,j}\}$ (to be definite, we refer to random bonds) distributed with probability $P(\mathcal{J})$. One computes the equilibrium partition function $Z(\mathcal{J})$ summing over the ordinary degrees of freedom $\mathcal{S} = \{\sigma_i\}$ with an assigned configuration of the impurities. Then the average over disorder is performed on the free energy $F(\mathcal{J}) = -T \ln Z(\mathcal{J})$, i.e., one considers

$$\bar{F} = \sum_{\mathcal{J}} P(\mathcal{J}) F(\mathcal{J}). \quad (1.5.1)$$

This type of disorder, known as *quenched disorder*, plays a relevant role and is able to change the critical properties of a system.

1.5.1 Replica method

If one is able to evaluate the quenched averaged free energy, the thermodynamic properties can be computed from its derivatives. To start with, we have to perform the quenched average of the logarithm of the partition function. For this, a mathematical identity can conveniently be used,

$$\overline{\ln Z} = \lim_{n \rightarrow 0} \frac{\overline{Z^n} - 1}{n}. \quad (1.5.2)$$

This allows us to formally proceed with the quenched average of a simpler object Z^n , a procedure referred to as the *replica trick*. One considers n copies of the system indexed by $a = 1, 2, \dots, n$. Each replica has identical disorder configuration $\mathcal{J} = \{J_{i,j}\}$, so that each Hamiltonian has the form $\mathcal{H}(\mathcal{J}, \mathcal{S}_a)$. The replicated partition function is given by

$$Z^n = \sum_{\mathcal{S}_1, \dots, \mathcal{S}_n} e^{-\frac{1}{T} \sum_{a=1}^n \mathcal{H}(\mathcal{J}, \mathcal{S}_a)}. \quad (1.5.3)$$

The quenched average $\overline{Z^n}$ can be effectively described by a replica Hamiltonian \mathcal{H}_n , namely

$$\overline{Z^n} = \sum_{\mathcal{J}} P(\mathcal{J}) \sum_{S_1, \dots, S_n} e^{-\frac{1}{T} \sum_{a=1}^n \mathcal{H}(\mathcal{J}, S_a)} = \sum_{S_1, \dots, S_n} e^{-\frac{1}{T} \mathcal{H}_n(S_1, \dots, S_n)}. \quad (1.5.4)$$

The effective replicated system now corresponds to a homogenous and isotropic Hamiltonian \mathcal{H}_n . This comes at the cost of having the different replicas coupled by the disorder \mathcal{J} . Nevertheless, it allows to use methods known for pure systems (i.e. without disorder), as we are going to illustrate.

1.5.2 Harris criterion

Let \mathcal{A}^* be the fixed point action of the pure system. Random bonds correspond in the continuum to a variable $\chi(x)$ coupled to the energy density field, so that we have

$$\mathcal{A} = \mathcal{A}^* + \int d^2x \chi(x) \varepsilon(x). \quad (1.5.5)$$

The equivalent of (1.5.4) is now

$$\overline{Z^n} = \sum_{\{\chi(x)\}} P(\chi(x)) \sum_{\substack{\text{field} \\ \text{configs}}} e^{-\sum_a [\mathcal{A}_a^* + \int d^2x \chi(x) \varepsilon_a(x)]}, \quad (1.5.6)$$

where $\varepsilon_a(x)$ is the energy density field in replica a . To proceed with formally evaluating the disorder average, a cumulant expansion for the probability distribution $P(\chi(x))$ can be written as

$$\ln \left(\overline{e^{-\int d^2x \chi(x) f(x)}} \right) = -C_1 \int d^2x f(x) - \int d^2x d^2x' C_2(x, x') f(x) f(x') + \dots \quad (1.5.7)$$

with first and second cumulant C_1 and $C_2(x, x')$, respectively. In the replica partition function, χ is conjugate to

$$f(x) = \sum_{a=1}^n \varepsilon_a(x). \quad (1.5.8)$$

It is usually sufficient to consider uncorrelated disorder, i.e., $C_2(x, x') \propto \delta(x - x')$. This means that the perturbation to the pure fixed point action comes from the fields of the form ε_a , $\varepsilon_a \varepsilon_a$, and $\varepsilon_a \varepsilon_b$ with $a \neq b$. ε_a and $\varepsilon_a \varepsilon_a$ contribute only to a shift of critical temperature, and are not particularly interesting. The perturbation $\varepsilon_a \varepsilon_b$, on the other hand, couples different replicas and is nontrivial. It is irrelevant in the pure fixed point action if $X_{\varepsilon\varepsilon} = 2X_\varepsilon > d = 2$. Recalling that the specific heat critical exponent of the pure systems is given by $\alpha = (d - 2X_\varepsilon)\nu$, this leads to the Harris criterion [26]

$$\alpha < 0 \tag{1.5.9}$$

for the irrelevance of weak disorder. Higher order terms in the cumulant expansion are less relevant compared to the $\varepsilon_a \varepsilon_b$ contribution. Thus, if the Harris criterion is satisfied, the addition of quenched bond disorder is irrelevant and disorder does not change the critical exponents. If it is not satisfied, the fixed point of the pure model will be unstable under the addition of disorder. This may lead to a new fixed point. One possible strategy is to impose the properties of a CFT directly on the replica action corresponding to the scaling limit of the replica Hamiltonian in (1.5.4). This will be of main interest in the thesis, as this idea paves the way to a non-perturbative approach to random fixed points [5].

Chapter 2

Scattering formalism

We briefly review the scale invariant scattering formalism [3] to be used in the next chapters to obtain exact access to critical points of pure and disordered two-dimensional systems.

2.1 Particles and fields

The scaling limit of a statistical lattice model yields an Euclidean field theory. In a generic dimension d , an analytic continuation can be made by taking one of the coordinate as imaginary time, i.e. $x = (x^1, \dots, x^d)$ with $x^d = it$. This is often referred to as Wick rotation. In $d = 2$, this results in a $(1 + 1)$ -dimensional *quantum field theory* (QFT). The spatial symmetries in the form of rotation and translation invariance of Euclidean field theory translate into space-time Poincare symmetries, i.e. invariance under space-time translations and Lorentz boosts. The field content is the same in the two pictures and correlation functions are related by the analytic continuation between real and imaginary time. On the other hand, the QFT allows a description in terms of relativistic particles, which correspond to elementary excitations over the quantum vacuum or ground state.

The particle description of a QFT can be expressed in terms of the S-matrix [27]. Far away from the interaction region, one has asymptotic states containing free particles. In a scattering process, we distinguish the “in” state at $t = -\infty$ from the “out” state at $t = +\infty$. The relativistic particles obey the dispersion relation

$$E = \sqrt{p^2 + m^2}, \quad (2.1.1)$$

relating the energy E , momentum $p = (p^1, \dots, p^{d-1})$, and mass m . The entries of the S-matrix are the probability amplitudes of an in state evolving into an out state. A generic amplitude has the form

$$S_{\mu_1, \dots, \mu_m}^{\nu_1, \dots, \nu_n}(p_1, \dots, p_n | q_1, \dots, q_m) = {}_{\nu_1, \dots, \nu_n} \langle p_1, \dots, p_n | \mathbf{S} | q_1, \dots, q_m \rangle_{\mu_1, \dots, \mu_m} \quad (2.1.2)$$

where \mathbf{S} is the scattering operator and μ_i, ν_i label particle species.

2.2 Elastic scattering in $d = (1 + 1)$ QFT

The simplest realization of scattering involves preservation of particle masses and particle number in addition to conservation of total energy and momentum. This is referred to as *elastic* scattering. For the case of two-particle elastic scattering with identical masses, the scattering amplitude is $S_{\mu, \nu}^{\rho, \sigma}$. In $d = 2$, the identical masses make the momenta of ingoing and outgoing particles to be individually conserved as in figure 2.1. The scattering amplitude $S_{\mu, \nu}^{\rho, \sigma}$ is relativistically invariant. There is a single relativistic invariant variable,

$$s = (E_1 + E_2)^2 - (p_1 + p_2)^2, \quad (2.2.1)$$

which is the square of the center of mass energy. Various properties of a QFT may be written as constraints on scattering amplitudes as analytic functions of complex s [27]. The simplest requirements are the symmetries of spatial reflection and time reversal invariance of the QFT. These conditions only restrict the number of independent components of the S-matrix and not the s dependence,

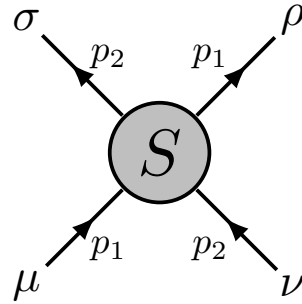


Figure 2.1: A two-particle elastic scattering process of particles corresponding to the scattering amplitude $S_{\mu,\nu}^{\rho,\sigma}$. Time runs upwards.

i.e.

$$S_{\mu,\nu}^{\rho,\sigma}(s) = S_{\nu,\mu}^{\sigma,\rho}(s), \quad S_{\mu,\nu}^{\rho,\sigma}(s) = S_{\rho,\sigma}^{\mu,\nu}(s). \quad (2.2.2)$$

The next requirement is probability conservation which manifests in the S-matrix as *unitarity*. This imposes in general branch cuts originating from possible k -particle production thresholds $s_k = (km)^2 \in \mathbb{R}$ and extending to infinity along the positive real axis. Below the lowest inelastic particle production threshold s' , the unitarity condition can be written as

$$\sum_{\lambda,\tau} S_{\mu,\nu}^{\lambda,\tau}(s+i\epsilon) [S_{\lambda,\tau}^{\rho,\sigma}(s+i\epsilon)]^* = \delta_{\mu}^{\rho} \delta_{\nu}^{\sigma}, \quad 4m^2 < s < s', \quad (2.2.3)$$

as depicted in figure 2.2.

There is also *crossing symmetry* associated with the exchange of space and time directions. In the elastic two-particle amplitude the crossing channel is obtained by exchanging particles ν and σ along with their arrows in figure 2.1. This corresponds to switching the sign of energy and momentum of the second particle, i.e., $(E_2, p_2) \rightarrow (-E_2, -p_2)$, which translates to $s \rightarrow 4m^2 - s$. For self-conjugated particles, which is the case relevant for our future applications, the crossing symmetry relation can be written as

$$S_{\mu,\nu}^{\rho,\sigma}(s+i\epsilon) = [S_{\mu,\sigma}^{\rho,\nu}(4m^2 - s + i\epsilon)]^*. \quad (2.2.4)$$

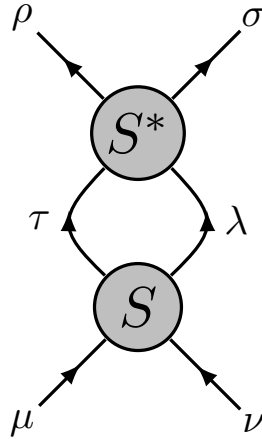


Figure 2.2: The product entering the l.h.s. of (2.2.3).

This induces branch cuts along the negative real axis from $s = 0$ to $s = -\infty$, which are the crossed image of those discussed above.

The space-time translation generators are the quantum Hamiltonian H and momentum operator P , such that $H|p\rangle = E|p\rangle$ and $P|p\rangle = p|p\rangle$, and a generic field in QFT satisfies

$$\Phi(x, t) = e^{-i(Px - Ht)} \Phi(0, 0) e^{i(Px - Ht)}. \quad (2.2.5)$$

The fields are characterized by their matrix elements on the asymptotic particle states. In particular, we define the *form factors*

$$\mathcal{F}_n^\Phi(p_1, \dots, p_n) = \langle 0 | \Phi(0) | p_1, \dots, p_n \rangle, \quad (2.2.6)$$

where $|0\rangle$ is the state without particles (vacuum). An Euclidean correlator can be expanded as

$$\begin{aligned} \langle \Phi(x) \Phi(0) \rangle &= \langle 0 | \Phi(x) \Phi(0) | 0 \rangle \\ &= \sum_{n=0}^{\infty} \frac{1}{n!} \int \frac{dp_1}{2\pi E_1} \cdots \frac{dp_n}{2\pi E_n} |\mathcal{F}_n^\Phi(p_1, \dots, p_n)|^2 e^{-r \sum_{i=1}^n E_i}, \end{aligned} \quad (2.2.7)$$

with $r = |x|$. For $\mathcal{F}_1^\Phi(p) \neq 0$, the leading contribution for large r decays as $\sim e^{-rm}$. This shows that the mass m is the inverse of the correlation length ξ ,

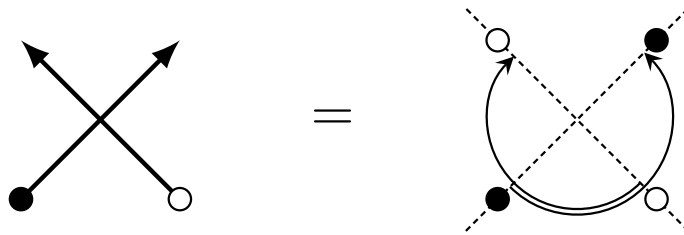


Figure 2.3: Pictorial representation of (2.3.2).

and means that the divergence of the correlation length at criticality corresponds to massless particles.

2.3 Scale invariant scattering formalism

For a fixed point theory in $d = 2$, conformal invariance has infinitely many generators which induce infinitely many conservation laws on scattering processes, forcing them to be completely elastic. The dispersion relation (2.1.1) with $m = 0$ allows for left ($E = -p > 0$) and right ($E = p > 0$) movers, created by fields $\bar{\eta}$ and η , respectively. Their form factors for a single particle

$$\langle 0 | \eta(x) | p \rangle \sim e^{iE(x^1 + ix^2)} = e^{iEz}, \quad \langle 0 | \bar{\eta}(x) | p \rangle \sim e^{iE(x^1 - ix^2)} = e^{iE\bar{z}}, \quad (2.3.1)$$

illustrate that $\eta = \eta(z)$ and $\bar{\eta} = \bar{\eta}(\bar{z})$ are *chiral fields* with conformal dimensions $\Delta_{\bar{\eta}} = \bar{\Delta}_{\eta} = 0$ and $\Delta_{\eta} = \bar{\Delta}_{\bar{\eta}}$, and spin $s_{\eta} = -s_{\bar{\eta}} = \Delta_{\eta}$.

Since the relativistic invariant s is dimensionful, scale invariance forces the amplitude S for the scattering of a right-mover with a left-mover to be s independent. By unitarity, S is a phase without dynamical dependence [3].

The scattering process involves position exchange between the two particles in one spatial dimension, and this produces a statistical phase. In the Euclidean picture, this can also be achieved by a π rotation (figure 2.3), so that the scattering phase can be written as

$$S = e^{-i\pi(s_{\eta} - s_{\bar{\eta}})} = e^{-i2\pi\Delta_{\eta}}. \quad (2.3.2)$$

The particles created by the chiral fields follow bosonic and fermionic exchange statistics for integer and half-integer Δ_η , respectively. In general however, Δ_η and thus s_η can be any real number, and the particles have generalized statistics.

So far we referred to a single species of particles. More generally, the particles carry a representation of the group of internal symmetry [3]. This may be implemented in terms of a multiplet of chiral fields η_μ transforming under the group. The particles may be conveniently labeled with index μ corresponding to the multiplet components η_μ , and the amplitudes can conveniently be written as

$$S_{\mu,\nu}^{\rho,\sigma} = \langle \rho \sigma | \mathbf{S} | \mu \nu \rangle \in \mathbb{C}, \quad (2.3.3)$$

taking into account their momentum independence.

A summary of properties satisfied by the scale-invariant S-matrix can now be written:

$$S_{\mu,\nu}^{\rho,\sigma} = S_{\nu,\mu}^{\sigma,\rho}, \quad (\text{Spatial reflection}) \quad (2.3.4)$$

$$S_{\mu,\nu}^{\rho,\sigma} = S_{\rho,\sigma}^{\mu,\nu}, \quad (\text{Time reversal}) \quad (2.3.5)$$

$$S_{\mu,\nu}^{\rho,\sigma} = [S_{\mu,\sigma}^{\rho,\nu}]^*, \quad (\text{Crossing symmetry}) \quad (2.3.6)$$

$$\sum_{\lambda,\tau} S_{\mu,\nu}^{\lambda,\tau} [S_{\lambda,\tau}^{\rho,\sigma}]^* = \delta_\mu^\rho \delta_\nu^\sigma. \quad (\text{Unitarity}) \quad (2.3.7)$$

This is a system of at most quadratic equations for scattering amplitudes for a given symmetry representation. The solutions of these equations are the allowed renormalization group fixed points for the given symmetry. This will be illustrated in the next chapters.

Chapter 3

$O(N)$ -vector model

We consider $O(N)$ symmetry within the exact framework of scale invariant scattering theory. A global pattern emerges in which the different critical lines are located within the same parameter space. In particular, we show how the critical lines for non-intersecting loops ($-2 \leq N \leq 2$) are connected to the zero temperature critical line ($N > 2$) via the BKT line at $N = 2$.

3.1 Scattering formulation

The lattice definition of the $O(N)$ model was given in (1.4.1). We now consider the homogeneous case $J_{i,j} = J$ and use the scale invariant scattering formalism previously introduced in order to determine the renormalization group fixed points in two dimensions [3, 28]. The first step is the identification of the particle basis, which is naturally identified with a vector multiplet of neutral excitations labeled by an index $a = 1, 2, \dots, N$. The S-matrix takes the $O(N)$ -covariant form

$$S_{a,b}^{c,d} = S_1 \delta_{a,b} \delta_{c,d} + S_2 \delta_{a,c} \delta_{b,d} + S_3 \delta_{a,d} \delta_{b,c}, \quad (3.1.1)$$

where S_i , $i = 1, 2, 3$, are the scattering amplitudes corresponding to annihilation, transmission, and reflection, respectively (figure 3.1). Spatial reflection and time

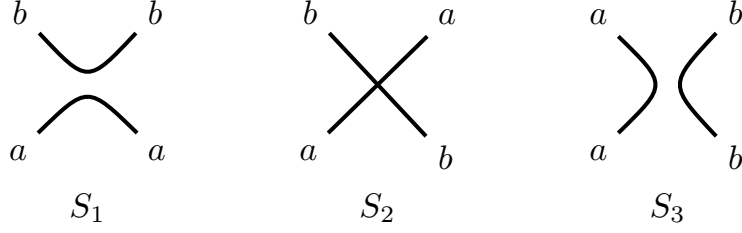


Figure 3.1: $O(N)$ -symmetric S-matrix components corresponding to the three terms in (3.1.1).

reversal symmetry of the S-matrix are already satisfied. Crossing symmetry gives

$$S_1 = S_3^* \equiv \rho_1 e^{i\phi}, \quad S_2 = S_2^* \equiv \rho_2, \quad (3.1.2)$$

where we introduced parametrizations of the amplitudes in terms of ϕ and ρ_2 real, and ρ_1 non-negative. The unitarity equations take the form

$$1 = \rho_1^2 + \rho_2^2 \quad (3.1.3)$$

$$0 = \rho_1 \rho_2 \cos \phi \quad (3.1.4)$$

$$0 = N\rho_1^2 + 2\rho_1 \rho_2 \cos \phi + 2\rho_1^2 \cos 2\phi. \quad (3.1.5)$$

Equation (3.1.3) imposes the restrictions $0 \leq \rho_1 \leq 1$ and $-1 \leq \rho_2 \leq 1$. There are three ways of satisfying equation (3.1.4). This leads to three classes of scale invariant scattering solutions [3, 28], which are listed in table 3.1.

It follows from (3.1.1) that the superposition of two-particle states $\sum_a |aa\rangle$ scatters into itself with the amplitude

$$S = NS_1 + S_2 + S_3 \quad (3.1.6)$$

which has to be a phase by unitarity. Similarly for $a \neq b$, the superpositions $|aa\rangle - |bb\rangle$ and $|ab\rangle + |ba\rangle$ scatter with phase $S_2 + S_3$, while $|ab\rangle - |ba\rangle$ scatters with phase $S_2 - S_3$.

Solution	N	ρ_1	ρ_2	$\cos \phi$
P1 $_{\pm}$	$(-\infty, \infty)$	0	± 1	-
P2 $_{\pm}$	$[-2, 2]$	1	0	$\pm \frac{1}{2} \sqrt{2 - N}$
P3 $_{\pm}$	2	$[0, 1]$	$\pm \sqrt{1 - \rho_1^2}$	0

Table 3.1: Solutions of equations (3.1.3)–(3.1.5). They give the renormalization group fixed points with $O(N)$ symmetry.

3.2 Critical lines of non-intersecting loops

The solutions P2 $_{\pm}$ were identified in [3, 29]; here we summarize the main steps of the derivation and the results. For $N = 2$ these solutions coincide with the point $S_2 = 0$ of the solution P3 that, as we will see below, corresponds to a CFT with central charge $c = 1$. Since the central charge grows with N , the CFT's describing the solutions P2 $_{\pm}$ will have $c \leq 1$. As we saw, in this subspace of CFT a main physical role is played by the “degenerate” primary fields $\Phi_{m,n}$ with conformal dimensions given by the Kac formula (1.3.21).

The energy density field $\varepsilon(x)$ is expected to be a degenerate field, and at $N = 1$ for one of the two solutions should have the conformal dimension $\Delta_{\varepsilon} = 1/2$ of the Ising model ($p = 3$). This leads to the identification $\varepsilon = \Phi_{1,3}$, while, as we will see later, the alternative choice $\Phi_{2,1}$ corresponds to the q -state Potts model. The requirement that the chiral field η entering (2.3.2) is local with respect to ε then leads to the identification $\eta = \Phi_{2,1}$, i.e. to the determination of Δ_{η} as a function of p . On the other hand, Δ_{η} is given as function of N by the relation (2.3.2) and (3.1.6), in which $S = NS_1 + S_3 = -e^{3i\phi}$ for the solutions P2 $_{\pm}$. For $N = 1$ the solution we are discussing corresponds to Ising, i.e. to a free fermion theory with $S = -1$, and this selects P2 $_{-}$. Comparing the two results for Δ_{η} (one as a function of p and one as a function of N) we obtain the relation $N = 2 \cos \frac{\pi}{p}$ for the solution P2 $_{-}$. A slightly more general analysis involving nondegenerate fields [3] yields also $\Delta_s = \Delta_{1/2,0}$ for the conformal dimension of the spin field.

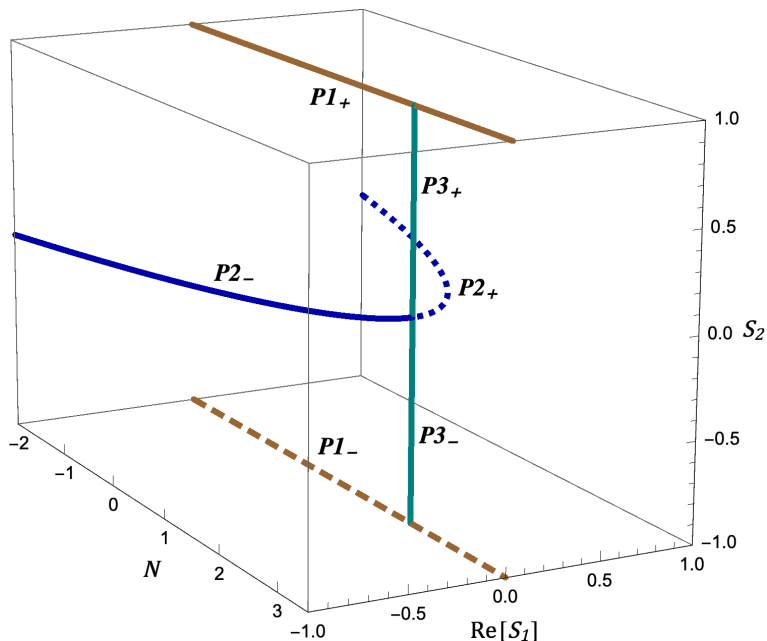


Figure 3.2: Solutions of fixed point equations in the pure $O(N)$ model. Those with $S_2 = 0$ correspond to the critical lines for the dilute (continuous) and dense (dotted) phases of non-intersecting loops. The piece $P3_+$ of the line of fixed points for $N = 2$ accounts for the BKT phase of the XY model. The solution $P1_+$ corresponds to the zero temperature critical point of the $N > 2$ ferromagnet.

The simplest way to identify the solution $P2_+$ is to recall that the perturbation by the field $\Phi_{1,3}$ of the CFT's with central charge (1.3.21) yields (for one sign of the coupling) flows to infrared fixed points with central charge corresponding to $p - 1$ [30]. Since the $\Phi_{1,3} = \varepsilon$ perturbation preserves $O(N)$ symmetry, the infrared line of fixed points corresponds to $P2_+$, and has $N = 2 \cos \frac{\pi}{p+1}$. Together with (2.3.2), this relation yields $\Delta_\eta = \Delta_{1,2}$, a result differing from that for $P2_-$ for the interchange of the indices m, n . This interchange is preserved by the mutual locality arguments (which exploit the operator product expansion), and leads to $\Delta_\varepsilon = \Delta_{3,1}$ and $\Delta_s = \Delta_{0,1/2}$ for the critical line $P2_+$. The results for the solutions $P2_\pm$ are summarized in table 3.2.

It is natural to think of the particle trajectories as those of walks of N different colors on the Euclidean plane. Then the solutions $P2_\pm$ are characterized by

Solution	N	c	Δ_η	Δ_ε	Δ_s
P1 ₋	\mathbb{R}	$\frac{N}{2}$	$\frac{1}{2}$	$\frac{1}{2}$	$\frac{1}{16}$
P1 ₊	\mathbb{R}	$N - 1$	0	1	0
P2 ₋	$2 \cos \frac{\pi}{p}$	$1 - \frac{6}{p(p+1)}$	$\Delta_{2,1}$	$\Delta_{1,3}$	$\Delta_{\frac{1}{2},0}$
P2 ₊	$2 \cos \frac{\pi}{p+1}$	$1 - \frac{6}{p(p+1)}$	$\Delta_{1,2}$	$\Delta_{3,1}$	$\Delta_{0,\frac{1}{2}}$
P3 _±	2	1	$\frac{1}{4b^2}$	b^2	$\frac{1}{16b^2}$

Table 3.2: Central charge and conformal dimensions for the pure $O(N)$ fixed point solutions. The conformal dimensions $\Delta_{\mu,\nu}$ are specified by the Kac formula (1.3.21). Other specifications are discussed in the text.

$S_2 = 0$, i.e. by the absence of intersection of particle trajectories (see figure 3.2). We saw that it is possible to map the partition function of an $O(N)$ invariant ferromagnet on the loop gas partition function (1.4.2), and that a noticeable feature of the loop formulation is that it implements on the lattice the continuation to non-integer values of N ; in particular, for $N \rightarrow 0$ it describes the statistics of self-avoiding walks [15]. The loop model can be solved exactly on the honeycomb lattice [12, 13], on which the loops cannot intersect. The solution yields two critical lines that are defined in the interval $N \in [-2, 2]$, coincide at $N = 2$, and have critical exponents that were first identified in [11] as corresponding to the conformal dimensions Δ_s and Δ_ε deduced above for the scattering solutions P2_±. The two critical lines are often referred to as “dilute” and “dense” with reference to the loop properties they control¹, and correspond to the solutions P2₋ and P2₊, respectively. The analogy between loop paths and particle trajectories was originally observed in [32] for the off-critical case.

¹See [31] about the renormalization group properties of the dense phase on lattices allowing for loop intersections.

3.3 Critical line at $N = 2$ and the BKT phase

The solutions $P3_{\pm}$ can be rewritten as

$$\rho_1 = \sin \alpha, \quad \rho_2 = \cos \alpha, \quad \phi = -\frac{\pi}{2}. \quad (3.3.1)$$

The presence of a free parameter (α in the formulation (3.3.1)) leads to a line of fixed points with $N = 2$. This is not surprising since we saw that the realization of $O(2)$ symmetry with smallest central charge in two-dimensional CFT is provided by the free bosonic theory with action (1.3.10) which indeed describes a line of fixed points with central charge $c = 1$. The energy density field $\varepsilon(x) = \cos 2b\varphi(x)$, with conformal dimension $\Delta_{\varepsilon} = b^2$, contains the parameter b providing the coordinate along the line of fixed points. It was shown in [3] that $\Delta_{\eta} = 1/4b^2$ on this line. Since (3.1.6) gives $S = e^{-i\alpha}$, (2.3.2) yields the relation

$$\alpha = \frac{\pi}{2b^2}, \quad (3.3.2)$$

which satisfies $S = -1$ at the point $b^2 = 1/2$. This is necessary because we saw that the theory (1.3.10) possesses also a fermionic (Thirring) formulation with action (1.4.7) with $b^2 = 1/2$ corresponding to free fermions ($g(1/2) = 0$). The particles $a = 1, 2$ of the scattering theory correspond to the two neutral fermions in (1.4.7). We saw that $O(2)$ symmetry of the action (1.4.7) also yields $\Delta_s = 1/16b^2$ for the conformal dimension of the spin field.

The intervals $\alpha \in [0, \pi/2]$ and $\alpha \in [\pi/2, \pi]$ correspond to solutions $P3_+$ and $P3_-$, respectively, and have in common the point $\alpha = \pi/2$, which is also the merging point of the solutions $P2_{\pm}$ (see figure 3.2). Since the field $\varepsilon = \cos 2b\phi$ is irrelevant in the renormalization group sense ($\Delta_{\varepsilon} = b^2 > 1$) for $\alpha \in [0, \pi/2]$, $P3_+$ accounts for the BKT phase [19, 20] of the XY ferromagnet. The point $\alpha = \pi/2$ is the BKT transition point, where the field ε becomes marginal ($\Delta_{\varepsilon} = 1$).

Since ϕ is fixed in (3.3.1), ρ_1 does not need to be positive. The part of the $c = 1$ line with $b^2 < 1/2$ (i.e. $\alpha > \pi$) is then also mapped on (3.3.1), and corresponds

to $P3_+$ or $P3_-$ depending on the sign of ρ_2 .

3.4 Free solutions and zero temperature critical point for $N > 2$

The solutions $P1_+$ and $P1_-$ are purely transmissive and correspond to free bosons and fermions, respectively. $P1_-$ can straightforwardly be identified as corresponding to N free neutral fermions, for a total central charge $c = N/2$. For $N = 2$ one recovers the $c = 1$ free fermion point described by (1.4.7) with $g = 0$; this is the contact point between $P1$ and $P3_-$ in figure 3.2. For $N = 1$ one recovers the Ising central charge $1/2$. Notice, however, that this Ising point on $P3_-$ does not coincide in the scattering space with that on $P2_-$, which is realized non-transmissively: indeed, for $N = 1$ there are no particle indices to distinguish between S_1 , S_2 and S_3 , and only $S = S_1 + S_2 + S_3 = -1$ matters for a free fermion. The value of the conformal dimension $\Delta_s = 1/16$ we report in table 3.2 for $P1_-$ is that of the multiplet $(\sigma_1, \dots, \sigma_N)$ containing the spin fields of the N decoupled Ising copies. When comparing with the free fermion point $b^2 = 1/2$ of $P3_-$ one has to consider that the spin vector field along the $N = 2$ line has a specific representation [3], which at $b^2 = 1/2$ corresponds to the conformal dimension² $\Delta_{s_1 s_2} = 2\Delta_{s_1} = 1/8$.

The solution $P1_+$ can certainly describe N free bosons, namely a theory characterized by the action (1.4.8), with $\Delta_\varepsilon = \Delta_{\varphi_j^2} = 0$, and $c = N$. However, the fact that the point $N = 2$ of $P1_+$ can also be seen as the limit $b^2 \rightarrow \infty$ of $P3_+$ (which has $c = 1$) says that $P1_+$ must also allow for a different interpretation. We recall that scattering on the line involves position exchange, and mixes statistics with interaction. This is why for $N = 2$ the interacting fermions of the theory (1.4.7) can appear for $b^2 \rightarrow \infty$ as two free bosons ($S_2 = 1$). Interaction is known to play a peculiar role also for the critical properties of the $O(N)$ invariant ferromagnet for $N > 2$ (see e.g. [8]). In this case there is a zero temperature critical point

²See also [33, 34] on spin fields in the fermionic theory (1.4.7) with $N = 2$.

and the scaling properties are described by the non-linear sigma model with action (1.4.10). The theory turns out to be asymptotically free, meaning that the short distance fixed point (which describes the $T = 0$ critical point of the ferromagnet) is a theory of free bosons with marginally relevant energy density field ($\Delta_\varepsilon = 1$, implying exponentially diverging correlation length as $T \rightarrow 0$) and $\Delta_s = \Delta_{\varphi_j} = 0$. The constraint gives a central charge $c = N - 1$ instead of N . The results for c and Δ_s match those for $N = 2$, $b^2 \rightarrow \infty$. Also $\Delta_\varepsilon = 1$ is recovered once we notice that for $b^2 > 1$ the field $\cos 2b\varphi$ becomes irrelevant, so that the most relevant $O(2)$ invariant field is the marginal one that generates the line of fixed points at $N = 2$. It is this sigma model interpretation of the solution Pl_+ that we report in table 3.2 together with the other data discussed in this section.

Chapter 4

Potts model

We review the scale invariant scattering description of the q -state Potts model, showing in particular how the critical lines for both ferromagnetic and antiferromagnetic interactions emerge from a single set of equations.

4.1 Scattering formulation

The q -state Potts model is defined on the lattice by the Hamiltonian (1.4.11) and is characterized by the permutational symmetry \mathbb{S}_q . We now consider the case of homogeneous couplings $J_{i,j} = J$ and implement the scale invariant scattering description for the case of \mathbb{S}_q symmetry in two dimensions, with the goal of obtaining the Potts renormalization group fixed points [3, 29]. As usual, the first step is to introduce a particle basis carrying a representation of the symmetry. For \mathbb{S}_q this is achieved considering particles $A_{\alpha\beta}$ with $\alpha, \beta = 1, 2, \dots, q$, and $\alpha \neq \beta$. For the Potts ferromagnet ($J > 0$) below critical temperature these particles correspond to the kinks that interpolate between pairs of the q degenerate ground states [35]. It was argued in [3, 5] that this particle basis has to be identified as the fundamental way of representing \mathbb{S}_q symmetry also at criticality (where the ground states coalesce and there are no kinks) and in the antiferromagnetic case ($J < 0$).

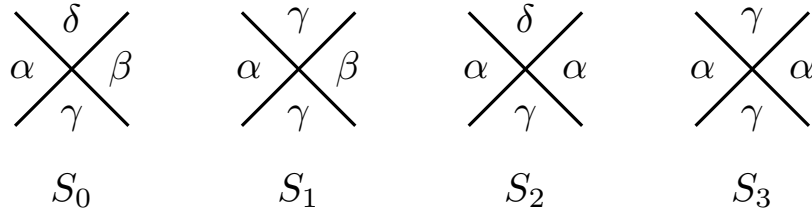


Figure 4.1: Amplitudes S_0 , S_1 , S_2 and S_3 of the \mathbb{S}_q -invariant theory. Different letters correspond to different colors.

In general, we think of the trajectory of the particle $A_{\alpha\beta}$ as a line separating a region of the plane characterized by the color α from a region characterized by the color β . Permutational invariance then yields the four inequivalent amplitudes S_0 , S_1 , S_2 and S_3 depicted in Fig. 4.1. For these the crossing relations (2.3.6) yield

$$S_0 = S_0^* \equiv \rho_0, \quad S_1 = S_2^* \equiv \rho e^{i\varphi}, \quad S_3 = S_3^* \equiv \rho_3, \quad (4.1.1)$$

where we introduced

$$\rho \geq 0, \quad \rho_0, \rho_3, \varphi \in \mathbb{R}. \quad (4.1.2)$$

With this parametrization the unitarity equations (2.3.7) translate (see also Fig. 4.2) into

$$1 = (q-3)\rho_0^2 + \rho^2, \quad (4.1.3)$$

$$0 = (q-4)\rho_0^2 + 2\rho_0\rho \cos \varphi, \quad (4.1.4)$$

$$1 = (q-2)\rho^2 + \rho_3^2, \quad (4.1.5)$$

$$0 = (q-3)\rho^2 + 2\rho\rho_3 \cos \varphi. \quad (4.1.6)$$

Note that the equations contain q as a parameter which does not need to be integer, so that the scattering formalism realizes in the continuum the analytic continuation in q which we know from the cluster representation of the model. For q integer, the amplitudes involving a number of colors larger than that integer (S_0 for $q=3$, also S_1 and S_2 for $q=2$) are unphysical. All amplitudes, however,

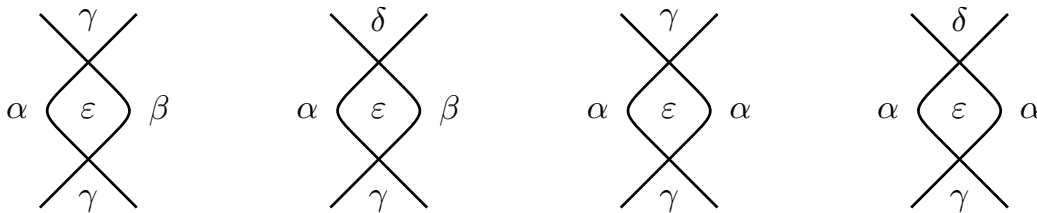


Figure 4.2: Pictorial representations associated to the unitarity equations (4.1.3), (4.1.4), (4.1.5), (4.1.6), in that order. The amplitude for the lower crossing multiplies the complex conjugate of the amplitude for the upper crossing, and sum over ε is implied.

enter the continuation to non-integer values of q . Various mechanisms of this continuation, in particular for the case $q \rightarrow 1$ is relevant for percolation, are illustrated in [36–40].

The solutions of the unitarity equations [3,29] are listed in Table 4.1 together with the range of q in which they satisfy the conditions (4.1.2). The sign doublings follow from the general fact that, given a solution of the unitarity and crossing equations (2.3.7) and (2.3.6), another solution is obtained reversing the sign of all amplitudes. In our notation, II_+ (II_-) corresponds to the solution with upper (lower) signs, and similarly for III, IV and V.

Solution I, which has φ as a free parameter, is defined for $q = 3$ only. Although S_0 is unphysical at $q = 3$, we quote the values of ρ_0 allowed by the equations for the purpose of comparison with solutions II, III and IV, which allow continuation away from $q = 3$.

We conclude this section observing that it follows in general from the amplitudes of Fig. 4.1 that the state $\sum_{\gamma \neq \alpha} A_{\alpha\gamma} A_{\gamma\alpha}$ scatters into itself with the amplitude

$$S = S_3 + (q - 2)S_2, \quad (4.1.7)$$

which is the phase entering (2.3.2).

Solution	Range	ρ_0	ρ	$2 \cos \varphi$	ρ_3
I	$q = 3$	$0, 2 \cos \varphi$	1	$\in [-2, 2]$	0
II $_{\pm}$	$q \in [-1, 3]$	0	1	$\pm\sqrt{3-q}$	$\pm\sqrt{3-q}$
III $_{\pm}$	$q \in [0, 4]$	± 1	$\sqrt{4-q}$	$\pm\sqrt{4-q}$	$\pm(3-q)$
IV $_{\pm}$	$q \in [\frac{7-\sqrt{17}}{2}, 3]$	$\pm\sqrt{\frac{q-3}{q^2-5q+5}}$	$\sqrt{\frac{q-4}{q^2-5q+5}}$	$\pm\sqrt{(3-q)(4-q)}$	$\pm\sqrt{\frac{q-3}{q^2-5q+5}}$
V $_{\pm}$	$q \in [4, \frac{7+\sqrt{17}}{2}]$	$\pm\sqrt{\frac{q-3}{q^2-5q+5}}$	$\sqrt{\frac{q-4}{q^2-5q+5}}$	$\mp\sqrt{(3-q)(4-q)}$	$\pm\sqrt{\frac{q-3}{q^2-5q+5}}$

Table 4.1: Solutions of Eqs. (4.1.3)-(4.1.6) with the conditions (4.1.2). They correspond to renormalization group fixed points of \mathbb{S}_q -invariant theories.

4.2 Ferromagnetic critical line

We saw that an important feature of the q -state Potts model is that the partition function admits the random cluster expansion (1.4.13), which allows analytical continuation to non-integer values of q . The cluster representation makes sense of the Potts model with non-integer q also in the antiferromagnetic case, in spite of the absence of a probabilistic interpretation¹ ($p < 0$). We start our discussion of the scattering solutions from the ferromagnetic case.

Since we know that the ferromagnetic phase transition in the two-dimensional q -state Potts model is of the second order up to $q = 4$ [25], the critical ferromagnetic line must correspond to one of the solutions in Table 4.1 having $q = 4$ as upper endpoint. The fact that in two dimensions the Ising model is a theory of free fermions implies $\rho_3 = -1$, and uniquely selects the solution III $_-$ [3]. We now recall how it is further characterized in the language of conformal field theory.

The four-state Potts model is a particular case of the Ashkin-Teller model (see [34] for the scattering description), which corresponds to two Ising models coupled by a four spin interaction and has $c = 1$. The critical line III $_-$ must then

¹Notice, on the other hand, that for $T \rightarrow 0$ the partition function of the Potts antiferromagnet counts the number of ways the sites of a lattice can be colored with q colors in such a way that nearest neighbors always have different colors (q -coloring problem, see [23]).

be able to account for a conformal field theory with central charge $c(q) \leq 1$. We saw that in this range of central charge a main physical role is played by the degenerate primary fields $\Phi_{m,n}(z)$ with conformal dimension $\Delta_{m,n}$ ($\bar{\Delta}_{m,n}$) given by the Kac formula (1.3.21). The strategy for relating this “colorless” conformal field theory to the \mathbb{S}_q -invariant scattering solution III₋ is the following (details are given in [3]). It can be argued that the energy density field $\varepsilon(x)$ for the ferromagnetic model is a degenerate field. Then, knowing that $\Delta_\varepsilon = 1/2$ at the Ising point ($c = 1/2$, $p = 3$), that ε cannot produce more relevant fields in the OPE with itself, and that it is odd under the high-low temperature duality characteristic of the model, one arrives at the identification $\Delta_\varepsilon = \Delta_{2,1}$. One then looks for the particle-creating field η as the most relevant chiral field local with respect to ε . It can be shown that also η needs to be degenerate, so that (1.3.23) can be used to obtain $\Delta_\eta = \Delta_{1,3}$. This result for Δ_η as a function of p can then be compared with that provided by (2.3.2) as a function of q (Eq. (4.1.7) gives $S = \mp e^{-4i\varphi}$ for the solutions III_±). This provides the relation

$$\sqrt{q} = 2 \sin \frac{\pi(p-1)}{2(p+1)} = 2 \cos \frac{\pi}{p+1}, \quad (4.2.1)$$

which determines the central charge as a function of q . This result coincides with that obtained in [11] from the exact lattice determination of scaling dimensions [12]; here it is derived in a self-contained way in the continuum limit. A slightly more general analysis involving nondegenerate fields [3] allows to find $\Delta_\sigma = \Delta_{1/2,0}$.

4.3 Ferromagnetic tricritical line

If the Potts Hamiltonian is generalized allowing for the presence of vacant sites, tricriticality can be realized. The tricritical line exists as long as the critical one exists, and the two lines meet at the common endpoint $q = 4$ [41]. The presence of vacancies preserves color permutational symmetry, so that the tricritical line must also correspond to one of the scattering solutions of section 4.1. Since the

solutions III_\pm are the only ones terminating at $q = 4$, and since they do not coincide at $q = 4$, we are again left with III_- as the only possibility.

Hence, besides that of the previous subsection, there should be another relation between solution III_- and conformal field theory with $c \leq 1$, a relation corresponding to the tricritical line. This is indeed found as follows. The energy density field on the tricritical line must have the same OPE and duality properties as on the critical line. We also know the value of Δ_ε at $q = 4$ where the two lines meet. This information then selects $\Delta_\varepsilon = \Delta_{1,2}$. Since this differs from the result on the critical line by exchange of the two indices, the form of the OPE (1.3.23) ensures that the search for η as a chiral field local with respect to ε has a solution with the same exchange, i.e. $\Delta_\eta = \Delta_{3,1}$; one can check that this is indeed the most relevant solution. We can now use this result in (2.3.2), with $S = e^{-4i\varphi}$ for solution III_- , to obtain

$$\sqrt{q} = 2 \sin \frac{\pi(p-2)}{2p} = 2 \cos \frac{\pi}{p}; \quad (4.3.1)$$

comparison with (4.2.1) shows that the same q corresponds to p on the critical line and to $p + 1$ on the tricritical one. For the order parameter one obtains $\Delta_\sigma = \Delta_{0,1/2}$. Again, these findings coincide with those of [11, 12].

4.4 Antiferromagnetic case

It is very interesting to consider also the antiferromagnetic case ($J < 0$). An antiferromagnet tries to find at low temperature a ground state in which nearest neighboring spins take different values. The number of such configurations can be zero, finite or infinite *depending on the lattice*. It follows that, in contrast with the universality exhibited by ferromagnets, antiferromagnetic critical behavior essentially depends on the lattice structure and needs to be investigated case by case (see e.g. the discussion in [42]). We saw that solution III_- corresponds to the ferromagnetic critical lines. As a matter of fact, however, it was shown in [29] that solution III_- is able to account also for the best known q -state Potts

$\mathbb{S}_q(\text{III}_-)$	Potts	c	Δ_ε	Δ_η	Δ_σ
$\sqrt{q} = 2 \cos \frac{\pi}{(p+1)}$	F critical	$1 - \frac{6}{p(p+1)}$	$\Delta_{2,1}$	$\Delta_{1,3}$	$\Delta_{\frac{1}{2},0}$
$\sqrt{q} = 2 \cos \frac{\pi}{p}$	F tricritical	$1 - \frac{6}{p(p+1)}$	$\Delta_{1,2}$	$\Delta_{3,1}$	$\Delta_{0,\frac{1}{2}}$
$\sqrt{q} = 2 \cos \frac{\pi}{(N+2)}$	AF square	$\frac{2(N-1)}{N+2}$	$\frac{N-1}{N}$	$\frac{2}{N+2}$	$\frac{N}{8(N+2)}$

Table 4.2: Realizations of the \mathbb{S}_q -invariant scattering solution III_- as Potts ferromagnetic (F) and square lattice antiferromagnetic (AF square) critical lines. The central charge and the conformal dimensions of the energy density, chiral, and order parameter fields are given together with the critical lines obtained by ε - η duality. The conformal dimensions $\Delta_{m,n}$ are specified through Kac formula (1.3.21).

antiferromagnet, that on the square lattice [25, 43–49] (see table 4.2).

The other solutions of table 4.1 should account for Potts antiferromagnetic criticality on lattices other than the square one. Remarkably, a lattice realization of solution I has recently been found [50]. A particularly interesting feature is that solution V leaves room for criticality in a $q = 5$ Potts antiferromagnet, while no previous theoretical results for criticality at $q > 4$ had been available. Very interestingly, numerical indication of criticality at $q = 5$ was given in [51], and infinite families of two-dimensional lattices that could allow for criticality at $q = 5$ have been considered in [52].

Chapter 5

Vector-Ising model

We show that scale invariant scattering allows to exactly determine the critical points of systems with coupled $O(N)$ and Ising order parameters. In particular, for $N = 1$ we exhibit three critical lines intersecting at the Berezinskii-Kosterlitz-Thouless transition point of the Gaussian model and related to the Z_4 symmetry of the isotropic Ashkin-Teller model. For $N = 2$ we classify the critical points that can arise in the XY-Ising model and provide exact answers about the critical exponents of the fully frustrated XY model.

5.1 Physical context

When a statistical mechanical system possesses two order parameters, phase transitions associated with each of them can take place at different points of the phase diagram. It is possible, however, that the two types of ordering set in at the same point, and that this gives rise to novel critical behavior with new critical exponents. The example of a vector order parameter for $O(N)$ symmetry coupled to a scalar (Ising) order parameter for Z_2 symmetry is paradigmatic of the combination of continuous and discrete symmetries and was addressed since the early days of the perturbative expansion in $4 - \varepsilon$ dimensions [53]. The case $N = 2$ (XY-Ising model) [54] has been highly debated in two dimensions also

because it shares the ground state degeneracy of the fully frustrated (FF) XY model [55] describing a Josephson-junction array in a magnetic field [56]. The problem of whether this case can originate new critical behavior has been studied numerically for decades, with open questions persisting to this day (see [57] for a review). A consensus in favor of two transitions occurring at close but distinct temperatures very slowly emerged for the FFXY model (see [58–60]), but disagreement on critical exponents remained even in the most extensive simulations (order 10^6 lattice sites) [60–62]. For the XY-Ising model, which has a larger parameter space, two transition lines are observed to approach each other, without that the numerical analysis could so far determine the nature of the meeting point, although evidence for universal crossover effects in both models [60] suggests the existence of a multicritical point with simultaneous criticality. The recent realization [63] with cold atoms of a two-dimensional system with the symmetries of the XY-Ising model opened the way to experimental investigations of the critical behavior, but also here the required level of accuracy calls for theoretical benchmarking. On the analytic side, however, the problem has been considered as intractable, since the distance from the upper critical dimension as well as the interplay with the Berezinskii-Kosterlitz-Thouless (BKT) physics do not provide small expansion parameters, while an exactly solvable lattice realization of the coupled symmetries has never been found (see [64]).

In this chapter we use scale invariant scattering to show that the critical points of coupled $O(N)$ and Ising order parameters in two dimensions can be determined in a general and exact way, directly in the continuum limit [65]. We determine the lines of renormalization group fixed points as a function of the variable N , which can be taken continuous, within a space of universal parameters. In particular, our results for $N = 2$ allow us to classify the multicritical points that can arise in the XY-Ising model, and to draw conclusions about the critical exponents in the FFXY model. For this purpose we consider the two-dimensional vector-Ising

model with lattice Hamiltonian

$$\mathcal{H} = - \sum_{\langle i,j \rangle} [(A + B\sigma_i\sigma_j)\mathbf{s}_i \cdot \mathbf{s}_j + C\sigma_i\sigma_j], \quad (5.1.1)$$

which is invariant under the rotations of the N -component unit vectors \mathbf{s}_i and the reversal of $\sigma_i = \pm 1$. We look for the points of simultaneous $O(N)$ and Z_2 criticality, where the correlators $\langle \mathbf{s}_i \cdot \mathbf{s}_j \rangle$ and $\langle \sigma_i\sigma_j \rangle$ behave as $|i - j|^{-2X_s}$ and $|i - j|^{-2X_\sigma}$, respectively, X_s and X_σ being the scaling dimensions.

5.2 Scattering formulation

Generalizing what we did for the $O(N)$ case, we are led to consider the scattering processes depicted in Fig. 5.1, where the vector degrees of freedom correspond to a multiplet of particles $a = 1, 2, \dots, N$, while the scalar corresponds to a particle whose trajectories we represent by dashed lines. The amplitudes S_1, \dots, S_7 are those allowed by the requirement that the tensor, vector or scalar character of the initial state is preserved in the final state.

Crossing symmetry takes the form

$$S_1 = S_3^* \equiv \rho_1 e^{i\phi}, \quad (5.2.1)$$

$$S_2 = S_2^* \equiv \rho_2, \quad (5.2.2)$$

$$S_4 = S_6^* \equiv \rho_4 e^{i\theta}, \quad (5.2.3)$$

$$S_5 = S_5^* \equiv \rho_5, \quad (5.2.4)$$

$$S_7 = S_7^* \equiv \rho_7, \quad (5.2.5)$$

and allows the parametrization in terms of the variables ρ_1 and ρ_4 non-negative, and $\rho_2, \rho_5, \rho_7, \phi$ and θ real. On the other hand, the unitarity equations now

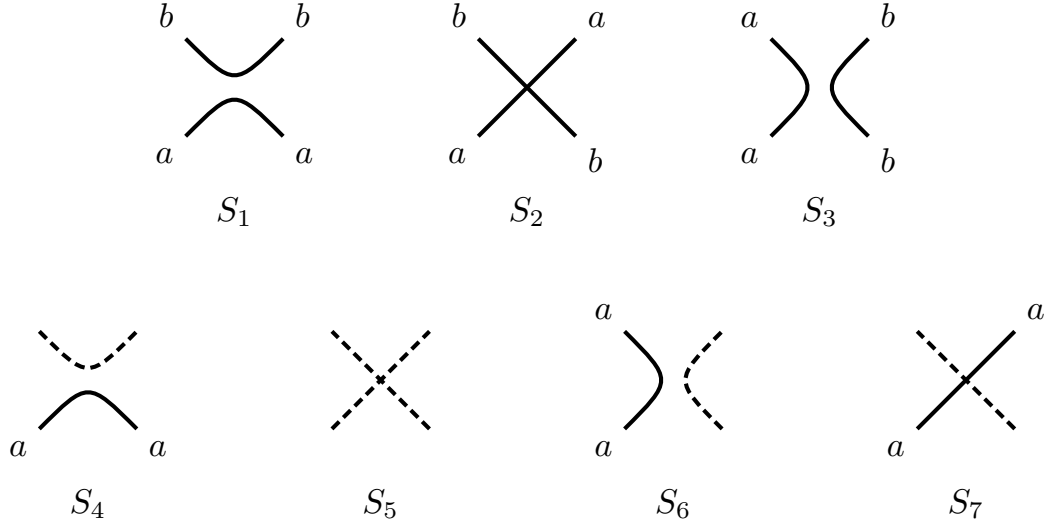


Figure 5.1: Scattering processes for a vector particle multiplet ($a = 1, 2, \dots, N$) and a scalar (dashed trajectories) at criticality. The amplitudes S_1, \dots, S_7 are invariant under time (up-down) and space (right-left) reflections.

read

$$1 = \rho_1^2 + \rho_2^2, \quad (5.2.6)$$

$$0 = \rho_1 \rho_2 \cos \phi, \quad (5.2.7)$$

$$0 = N \rho_1^2 + \rho_4^2 + 2 \rho_1^2 \cos 2\phi, \quad (5.2.8)$$

$$1 = \rho_4^2 + \rho_7^2, \quad (5.2.9)$$

$$1 = N \rho_4^2 + \rho_5^2, \quad (5.2.10)$$

$$0 = \rho_4 \rho_7 \cos \theta, \quad (5.2.11)$$

$$0 = \rho_4 [\rho_2 e^{-i\theta} + \rho_1 e^{-i(\phi+\theta)} + N \rho_1 e^{i(\phi-\theta)} + \rho_5 e^{i\theta}]. \quad (5.2.12)$$

For example, (5.2.10) follows from $1 = \langle \emptyset \emptyset | S S^\dagger | \emptyset \emptyset \rangle = \langle \emptyset \emptyset | S \sum_a | a a \rangle \langle a a | S^\dagger | \emptyset \emptyset \rangle + \langle \emptyset \emptyset | S | \emptyset \emptyset \rangle \langle \emptyset \emptyset | S^\dagger | \emptyset \emptyset \rangle = N |S_4|^2 + |S_5|^2$, where we denoted by \emptyset the scalar particle. Once again N enters the equations as a parameter that can be given real values.

Solution	N	ρ_2	$\cos \phi$	ρ_4	$\cos \theta$	ρ_5
D1 $_{\pm}$	\mathbb{R}	± 1	-	0	-	$(\pm)1$
D2 $_{\pm}$	$[-2, 2]$	0	$\pm \frac{1}{2}\sqrt{2-N}$	0	-	$(\pm)1$
D3 $_{\pm}$	2	$\pm\sqrt{1-\rho_1^2}$	0	0	-	$(\pm)1$
F1	1	0	$[-\frac{1}{2}, \frac{1}{2}]$	$\sqrt{1-4\cos^2\phi}$	0	$2\cos\phi$
F2	1	$[-1, 1]$	0	$\sqrt{1-\rho_2^2}$	0	ρ_2
F3	1	0	0	1	$[-1, 1]$	0
L1 $_{\pm}$	$[-3, 1]$	0	$\pm \frac{1}{2}\sqrt{1-N}$	1	$(\pm)\frac{1}{2}\sqrt{1-N}$	$\pm\sqrt{1-N}$
L2 $_{\pm}$	$[-3, 1]$	0	$\pm \frac{1}{2}\sqrt{1-N}$	1	$(\pm)\frac{1}{2}\sqrt{3+N}$	$\mp\sqrt{1-N}$
T1 $_{\pm}$	$(-\infty, 1]$	$\pm\sqrt{\frac{1-N}{2-N}}$	0	1	$\frac{(\pm)1}{\sqrt{2}}\sqrt{1+\frac{(\pm)1}{\sqrt{2-N}}}$	$(\pm)\sqrt{1-N}$
T2 $_{\pm}$	$[-3, -2]$	0	± 1	$\sqrt{-2-N}$	0	$\pm(N+1)$

Table 5.1: Solutions of the Eqs. (5.2.6)-(5.2.12) classifying the renormalization group fixed points of two-dimensional systems with coupled $O(N)$ and Ising order parameters. One also has $\rho_1 = \sqrt{1-\rho_2^2}$ and $\rho_7 = (\pm)\sqrt{1-\rho_4^2}$. Signs in parenthesis are both allowed.

5.3 Scattering solutions and classification of multicritical points

The solutions of the Eqs. (5.2.6)-(5.2.12) are given in Table 5.1 and provide the general and exact classification of the renormalization group fixed points that can arise in the theory (5.1.1). Their discussion conveniently begins with the solutions of type D (Fig. 5.2). These are characterized by $\rho_4 = 0$, amounting to decoupling between the vector and the scalar. Indeed, this yields $S_4 = S_6 = 0$ and, recalling also (5.2.9) and (5.2.10), $S_5 = S_7 = \pm 1$. We know that scattering in $1+1$ dimensions involves position exchange, and mixes statistics with interaction. It follows that $S_5 = -1$ corresponds for the decoupled scalar sector to Ising criticality, which in two dimensions is described by a neutral free fermion;

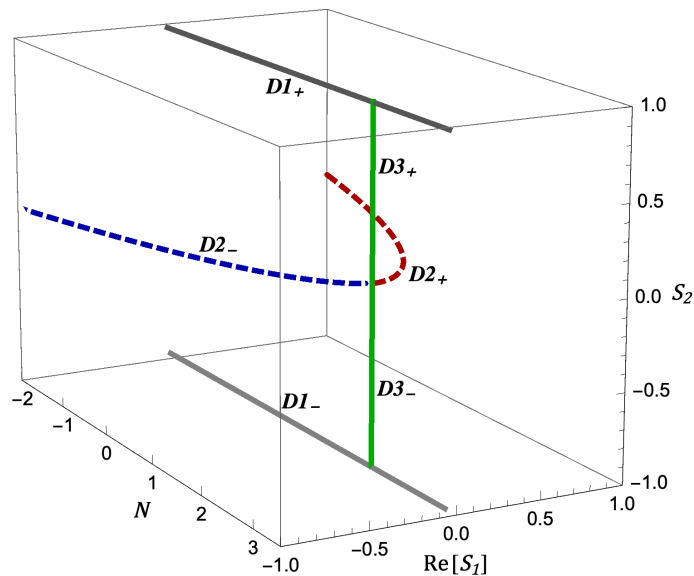


Figure 5.2: Solutions of type D in the parameter space of the vector sector. This is decoupled from the scalar sector and describes, in particular, the critical lines of the dilute ($D2_-$) and dense ($D2_+$) regimes of the gas of nonintersecting loops, the BKT phase of the XY model ($D3_+$), and the zero-temperature critical point of the $O(N > 2)$ ferromagnet ($D1_+$).

on the other hand, $S_5 = 1$ accounts for the trivial fixed point (free boson). $D1_\pm$ corresponds to free bosons/fermions. In particular, the vector part (amplitudes S_1, S_2, S_3) of $D1_+$ also describes the asymptotically free zero-temperature critical point of the $O(N > 2)$ ferromagnet, as we saw in previous chapters; hence, for $\rho_5 = 1$ the full solution $D1_+$ describes the zero-temperature critical point of the $O(N+1)$ model. The vector part of the solution $D2_\pm$ corresponds to nonintersecting trajectories ($S_2 = 0$) and we have already shown how it describes the critical lines of the gas of nonintersecting planar loops with fugacity N (self-avoiding walks for $N \rightarrow 0$) in its dilute ($D2_-$) and dense ($D2_+$) regimes.

The solution $D3_\pm$ is defined for $N = 2$ and contains ρ_1 as a free parameter. Its vector part then corresponds to the line of fixed points that accounts for the BKT transition in the XY model. We recall that this line is described by the Gaussian field theory with action (1.3.10) and energy density field $\varepsilon(x) = \cos 2b\varphi(x)$ with scaling dimension $X_\varepsilon = 2b^2$; b^2 provides the coordinate along the line, with the

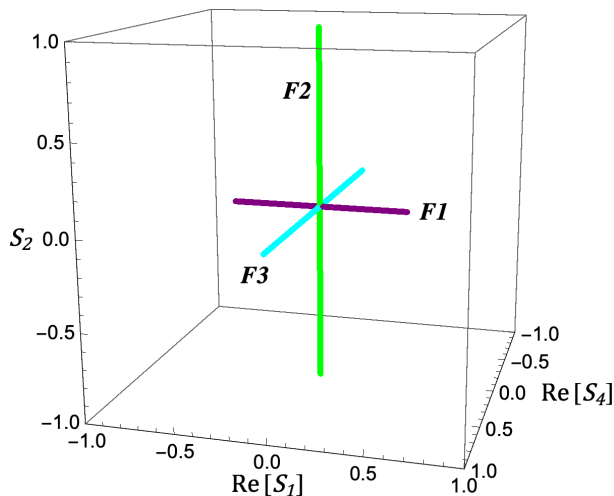


Figure 5.3: Critical lines at $N = 1$ due to the solutions of type F. They meet at the BKT transition point.

BKT transition point corresponding to $b^2 = 1$, where ε becomes marginal. In the Euclidean complex coordinates, the fields

$$U_m(x) = V_{\frac{m}{4b}, -\frac{m}{4b}}(x) = e^{i\frac{m}{2b}(\phi(z) - \bar{\phi}(\bar{z}))}, \quad m \in \mathbb{Z}, \quad (5.3.1)$$

with scaling dimension $m^2/8b^2$, satisfy the condition that $\langle \cdots \varepsilon(x) U_m(0) \cdots \rangle$ is single valued in x (see e.g. [4]). $(\phi - \bar{\phi})/2b$ is the $O(2)$ angular variable, and the vector field $\mathbf{s} = (s_1, s_2)$ corresponds to $s_1 \pm is_2 = U_{\pm 1}$. The mapping on the solution $D3_{\pm}$ is provided by $\rho_1 = \sin \frac{\pi}{2b^2}$ [3,4], so that the BKT phase corresponds to $D3_+$: it goes from the BKT transition point $b^2 = 1$ (contact point with $D2_{\pm}$ in Fig. 5.2) to the zero-temperature point $b^2 = \infty$ (contact point with $D1_+$).

With this understanding, we can continue the discussion of the results of Table 5.1. The solutions of type F are all defined for $N = 1$ and correspond to fixed points of two coupled Ising order parameters; the Hamiltonian (5.1.1) becomes that of the Ashkin-Teller (AT) model [66]. The “isotropic” ($A = C$) AT model is known to possess a line of fixed points that also maps on the theory (1.3.10), with continuously varying $X_{\varepsilon} = 2b^2$, fixed $X_s = X_{\sigma} = 1/8$, and b^2 nonuniversally related to the four-spin coupling B [25, 33, 34, 67]. In fact, all solutions of type

F possess a free parameter and describe three critical lines sharing a common point (Fig. 5.3). The identification of this point with the BKT transition point $b^2 = 1$ follows from the observation that F2 has S_1, S_2, S_3 equal to S_4, S_5, S_6 , respectively, so that it reconstructs the vector part of D3; then we know that $S_2 = 0$ corresponds to $b^2 = 1$. Further insight is obtained considering the theory with action

$$\mathcal{A} = \mathcal{A}_0 + \int d^2x \{ \lambda \varepsilon(x) + \tilde{\lambda} [U_4(x) + U_{-4}(x)] \}. \quad (5.3.2)$$

Since we saw that $U_{\pm 1}$ define the components of a $O(2)$ vector, the terms $U_{\pm 4}$ in (5.3.2) break $O(2)$ symmetry down to Z_4 . The scaling dimensions that we specified above imply that at $b^2 = 1$ all the fields in the integral in (5.3.2) are marginal. The renormalization group equations around $b^2 - 1 = \lambda = \tilde{\lambda} = 0$ were studied at leading order in [68] and give three lines of fixed points: $\lambda = \tilde{\lambda} = 0$ and $b^2 = 1$, $\lambda = \pm \tilde{\lambda}$. It was then conjectured in [69] that these lines may persist to all orders. Our exact result of Fig. 5.3 shows that this is indeed the case. The isotropic AT model does possess Z_4 symmetry: for $A = C$ the Hamiltonian (5.1.1), which contains the Ising variables s and σ , is invariant under rotations of the vector (s, σ) by angles multiples of $\pi/2$. The maximal value of b^2 realized in the square lattice AT model is $3/4$ [67], and only the line with varying b^2 plays a role.

The solutions of type L correspond to nonintersecting trajectories¹ ($S_2 = S_7 = 0$) and are defined for $N \in [-3, 1]$ (Fig. 5.4). Hence, they reproduce the critical lines of the nonintersecting loop gas (vector part of solution D2) through a mechanism in which the scalar provides the second component of the vector. Finally, the solutions of type T cannot be traced back to the decoupled $O(N)$ case, and necessarily correspond to new universality classes.

¹Notice that S_5 cannot distinguish between intersection and nonintersection.

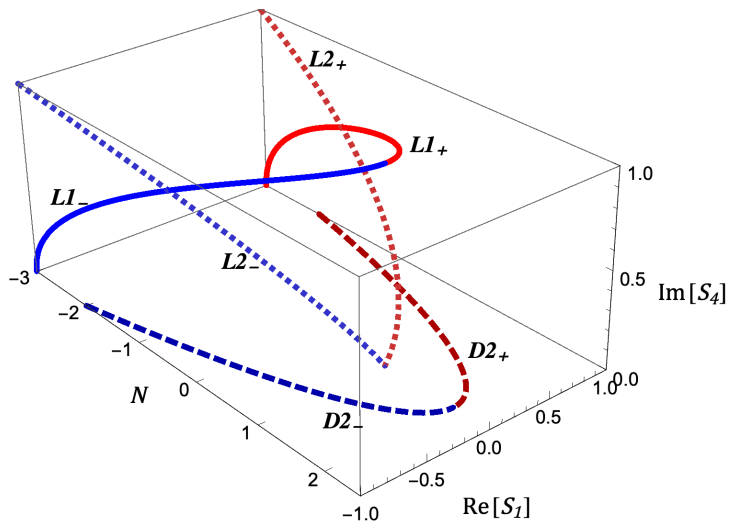


Figure 5.4: The solutions L1 and L2 (continuous and dotted curves, respectively). As the vector part of D2 (dashed), they correspond to critical lines of the gas of nonintersecting loops.

5.4 Implications for the fully frustrated XY model

Let us now focus on the theory (5.1.1) with $N = 2$, i.e. on the XY-Ising model. We see from Table 5.1 that the only allowed renormalization group fixed points are those of type D. We have already seen how the vector sector of D3 is related to the Gaussian theory (1.3.10) and its parameter b^2 ; the scalar sector describes a trivial or Ising fixed point depending on the sign of ρ_5 , with order parameter scaling dimension X_σ equal to 0 or $1/8$, respectively. The case $b^2 = \infty$, $\rho_5 = 1$, with $X_s = X_\sigma = 0$, describes the $O(3)$ zero-temperature critical point. Fig. 5.2 shows that for $N = 2$ the solution D3 includes as particular cases $D1_\pm$ ($b^2 = \infty$ and $1/2$) and $D2_\pm$ ($b^2 = 1$).

Besides the points of simultaneous $O(2)$ and Z_2 criticality, which we can call multicritical, the XY-Ising model possesses points where only one of the order parameters is critical. Even considering those, it follows from our results that the only possible values for X_σ at $N = 2$ are 0 and $1/8$, while X_s can vary con-

tinuously. However, since continuous symmetries do not break spontaneously in two dimensions, a vector “ordering” transition can only occur at $b^2 = 1$ through the BKT mechanism; hence, only the usual value $\eta_s = 2X_s = 1/4$ can arise at a vector transition point.

There will be in the parameter space of the XY-Ising model phase transition lines bifurcating from a multicritical point and ending in an Ising critical point on one side and a BKT transition point on the other side. The $O(3)$ fixed point is a natural candidate for a zero-temperature multicritical point. The FFXY model can be defined on the square lattice through the Hamiltonian $-\sum_{\langle i,j \rangle} J_{i,j} \mathbf{s}_i \cdot \mathbf{s}_j$ ($J_{i,j} = \pm J$), with ferromagnetic horizontal rows and alternating ferromagnetic and antiferromagnetic columns. The model has the same ground state degeneracy of the XY-Ising model [55], but possesses only the parameter J . On universality grounds, it then corresponds to a line within the parameter space of the XY-Ising model. Our classification of allowed critical behaviors at $N = 2$ implies that the exponents $0.2 \lesssim \eta_\sigma = 2X_\sigma \lesssim 0.4$, $0.8 \lesssim \nu_\sigma \lesssim 1$ measured over the years (see the survey in [60]) for the FFXY model are only consistent with the Ising universality class ($\eta_\sigma = 1/4$, $\nu_\sigma = 1$). Slow nonmonotonic approach to Ising exponents was observed in [60] for increasing system size. We have also shown that at the vector transition only the BKT transition value $\eta_s = 1/4$ is allowed. A check consistent with the BKT universality class was performed in [60], although η_s was not measured. The value $\eta_s \simeq 0.2$ found in [62] is instead not compatible with our results. Our conclusions on the FFXY exponents do not depend on simultaneous or separate transitions. The now accepted two-transition scenario suggests that the FFXY line intercepts the bifurcation originating from a multicritical point in XY-Ising parameter space.

Summarizing, we have shown how scale invariant scattering theory yields the exact solution to the longstanding problem of determining the renormalization group fixed points for two-dimensional systems with coupled $O(N)$ and Ising order parameters. For $N = 2$ this enabled us to classify the multicritical points allowed in the XY-Ising model and to provide exact answers about the FFXY

exponents. At $N = 1$ we have exhibited three lines of fixed points intersecting at the BKT transition point of the Gaussian theory and related to the Z_4 symmetry of the isotropic AT model. For $N \leq 1$ new universality classes appear that can be relevant for gases of intersecting loops.

Chapter 6

RP^{N-1} model

The Lebwohl-Lasher model describes the isotropic-nematic transition in liquid crystals. In two dimensions, where its continuous symmetry cannot break spontaneously, it is investigated numerically since decades to verify, in particular, the conjecture of a topological transition leading to a nematic phase with quasi-long-range order. We use scale invariant scattering to exactly determine the renormalization group fixed points in the general case of N director components (RP^{N-1} model), which yields the Lebwohl-Lasher model for $N = 3$. For $N > 2$ we show the absence of quasi-long-range order and the presence of a zero temperature critical point in the universality class of the $O(N(N+1)/2 - 1)$ model. For $N = 2$ the fixed point equations yield the Berezinskii-Kosterlitz-Thouless transition required by the correspondence $RP^1 \sim O(2)$.

6.1 Physical context

A liquid crystal cooled starting from its isotropic phase is generically expected to undergo a transition to a nematic phase with orientational order [70]. The head-tail symmetry of the elongated molecules distinguishes the isotropic-nematic (I-N) transition from the $O(3)$ ferromagnetic transition, and indeed in three dimensions the latter is second order while the former is observed to be first order,

although weakly so [70]. In two dimensions, on the other hand, the effect of fluctuations is stronger and the existence and nature of an I-N transition have been the object of ongoing debate. The absence of spontaneous breaking of continuous symmetries prevents a nematic phase with long range order, but leaves room for a defect-mediated (topological) transition similar to the BKT one. In absence of analytical approaches, the matter has been investigated experimentally [71–73] and, more extensively, through numerical simulations within the Lebwohl-Lasher (LL) lattice model [74], which encodes head-tail symmetry and successfully accounts for the weak first order transition in three dimensions [75]. The possibility in the two-dimensional model of a topological transition driven by “disclination” defects [76] and leading to a nematic phase with quasi-long-range order (QLRO) received support by some numerical studies [77–80], with others concluding for the absence of a true transition [81–85]. It was also argued [86–88] that in two dimensions the head-tail symmetry is not relevant for the critical behavior of the LL model, which should then coincide with that of the $O(3)$ model, with a zero-temperature critical point and exponentially diverging correlation length [8, 89]. On the other hand, the fact that the correlation length of the LL model was numerically found to be several orders of magnitude smaller than that of the $O(3)$ model in the same low-temperature range [90, 91] had been seen as an indication that the two models belong to different universality classes [91, 92].

We can use scale invariant scattering theory to study for the first time the problem of critical behavior in the two-dimensional LL model within an analytical framework [93]. Here we implement this program for the case in which the interaction symmetries are those of the LL model. Actually, we consider the more general case of N director components (RP^{N-1} model), which yields the LL model for $N = 3$. We show that for $N > 2$ there is no QLRO; there is instead a zero temperature critical point that falls in the $O(N(N + 1)/2 - 1)$ universality class.

The RP^{N-1} lattice model is defined by the reduced Hamiltonian

$$\mathcal{H} = -\frac{1}{T} \sum_{\langle i,j \rangle} (\mathbf{s}_i \cdot \mathbf{s}_j)^2, \quad (6.1.1)$$

where \mathbf{s}_i is a N -component unit vector located at site i , and T is the temperature. Head-tail symmetry is ensured by the invariance of the Hamiltonian under a *local* replacement $\mathbf{s}_i \rightarrow -\mathbf{s}_i$. As a consequence, \mathbf{s}_i effectively takes values on the unit hypersphere with opposite points identified, and this is the real projective space that gives the name to the model. The symmetry is conveniently represented through an order parameter variable which is quadratic in the vector components s_i^a and takes the form of the symmetric tensor [70]

$$Q_i^{ab} = s_i^a s_i^b - \frac{1}{N} \delta_{ab}. \quad (6.1.2)$$

$\sum_a s_i^a s_i^a = 1$ excludes the presence of an invariant linear in the order parameter components, while $\text{Tr} Q_i^{ab} = 0$ ensures that, upon diagonalization, the order parameter $\langle Q_i^{ab} \rangle$ vanishes in the isotropic phase in generic dimension.

6.2 Scattering formulation

In the continuum limit, the order parameter field is the symmetric tensor $Q_{ab}(x)$, which creates particles labeled by $\mu = ab$, with a and b running between 1 and N . It follows that the scattering amplitudes are those shown in figure 6.1. Recalling also the relations (2.3.4) and (2.3.5), the scattering matrix reads

$$\begin{aligned} S_{ab,cd}^{ef,gh} = & S_1 \delta_{(ab),(cd)}^{(2)} \delta_{(ef),(gh)}^{(2)} + S_2 \delta_{(ab),(ef)}^{(2)} \delta_{(cd),(gh)}^{(2)} + S_3 \delta_{(ab),(gh)}^{(2)} \delta_{(cd),(ef)}^{(2)} \\ & + S_4 \delta_{(ab)(gh),(cd)(ef)}^{(4)} + S_5 \delta_{(ab)(ef),(cd)(gh)}^{(4)} + S_6 \delta_{(ab)(cd),(ef)(gh)}^{(4)} \\ & + S_7 \left[\delta_{ab} \delta_{ef} \delta_{(cd),(gh)}^{(2)} + \delta_{cd} \delta_{gh} \delta_{(ab),(ef)}^{(2)} \right] + S_8 \left[\delta_{ab} \delta_{gh} \delta_{(cd),(ef)}^{(2)} + \delta_{cd} \delta_{ef} \delta_{(ab),(gh)}^{(2)} \right] \\ & + S_9 \left[\delta_{ab} \delta_{(cd),(ef),(gh)}^{(3)} + \delta_{cd} \delta_{(ab),(ef),(gh)}^{(3)} + \delta_{ef} \delta_{(cd),(ab),(gh)}^{(3)} + \delta_{gh} \delta_{(cd),(ef),(ab)}^{(3)} \right] \\ & + S_{10} \delta_{ab} \delta_{cd} \delta_{ef} \delta_{gh} + S_{11} \left[\delta_{ab} \delta_{cd} \delta_{(ef),(gh)}^2 + \delta_{ef} \delta_{gh} \delta_{(ab),(cd)}^2 \right], \quad (6.2.1) \end{aligned}$$

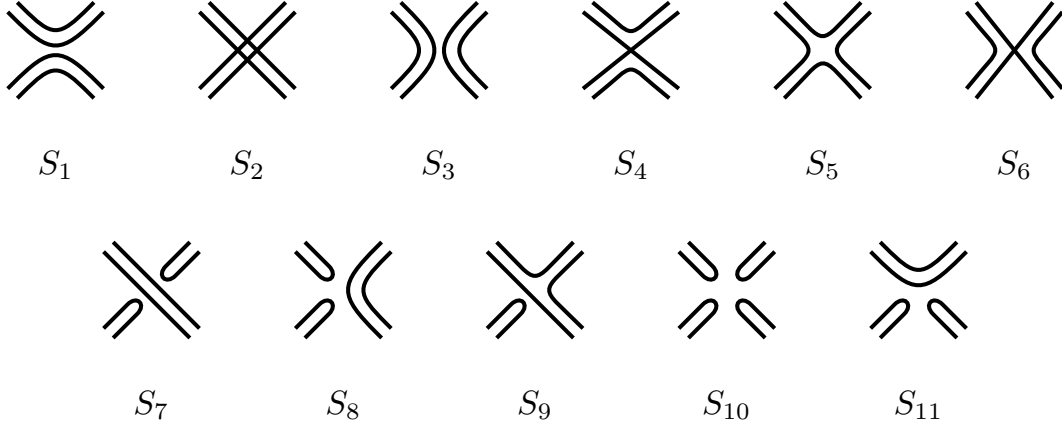


Figure 6.1: Scattering amplitudes appearing in (6.2.1). Time runs upwards.

where

$$\delta_{(ab),(cd)}^{(2)} \equiv (\delta_{ac}\delta_{bd} + \delta_{ad}\delta_{bc})/2, \quad (6.2.2)$$

$$\begin{aligned} \delta_{(ab),(cd),(ef)}^{(3)} \equiv & (\delta_{af}\delta_{bd}\delta_{ce} + \delta_{ad}\delta_{bf}\delta_{ce} + \delta_{ae}\delta_{bd}\delta_{cf} + \delta_{ad}\delta_{be}\delta_{cf} \\ & + \delta_{af}\delta_{bc}\delta_{de} + \delta_{ac}\delta_{bf}\delta_{de} + \delta_{ae}\delta_{bc}\delta_{df} + \delta_{ac}\delta_{be}\delta_{df})/8, \end{aligned} \quad (6.2.3)$$

$$\begin{aligned} \delta_{(ab)(cd),(ef)(gh)}^{(4)} \equiv & (\delta_{ah}\delta_{bf}\delta_{cg}\delta_{de} + \delta_{af}\delta_{bh}\delta_{cg}\delta_{de} + \delta_{ag}\delta_{bf}\delta_{ch}\delta_{de} + \delta_{af}\delta_{bg}\delta_{ch}\delta_{de} \\ & + \delta_{ah}\delta_{be}\delta_{c,g}\delta_{df} + \delta_{a,e}\delta_{bh}\delta_{cg}\delta_{df} + \delta_{ag}\delta_{be}\delta_{ch}\delta_{df} + \delta_{ae}\delta_{bg}\delta_{ch}\delta_{df} \\ & + \delta_{ah}\delta_{bf}\delta_{ce}\delta_{dg} + \delta_{af}\delta_{bh}\delta_{ce}\delta_{dg} + \delta_{ah}\delta_{be}\delta_{cf}\delta_{dg} + \delta_{ae}\delta_{bh}\delta_{cf}\delta_{dg} \\ & + \delta_{ag}\delta_{bf}\delta_{ce}\delta_{dh} + \delta_{af}\delta_{bg}\delta_{ce}\delta_{dh} + \delta_{ag}\delta_{be}\delta_{cf}\delta_{dh} + \delta_{ae}\delta_{bg}\delta_{cf}\delta_{dh})/4 \end{aligned} \quad (6.2.4)$$

take into account that, for a given process in figure 6.1, there are several ways of contracting the particle indices. The amplitudes $S_{i \geq 7}$ take into account that the indices of a particle aa can annihilate each other.

The amplitudes $S_{i \leq 3}$ satisfy the crossing equation (3.1.2), and we keep for them the same parameterization in terms of ρ_1 , ρ_2 and ϕ . For the other amplitudes

we have the crossing relations and parameterizations

$$S_4 = S_6^* \equiv \rho_4 e^{i\theta}, \quad (6.2.5)$$

$$S_5 = S_5^* \equiv \rho_5, \quad (6.2.6)$$

$$S_7 = S_7^* \equiv \rho_7, \quad (6.2.7)$$

$$S_8 = S_{11}^* \equiv \rho_8 e^{i\psi}, \quad (6.2.8)$$

$$S_9 = S_9^* \equiv \rho_9, \quad (6.2.9)$$

$$S_{10} = S_{10}^* \equiv \rho_{10}. \quad (6.2.10)$$

The fact that the field $Q_{ab}(x)$ that creates the particles is traceless is taken into account defining $\mathcal{T} = \sum_a aa$ and requiring

$$\mathbf{S}|(ab)\mathcal{T}\rangle = \pm|(ab)\mathcal{T}\rangle \quad (6.2.11)$$

for any particle state $|(ab)\rangle = |ab\rangle + |ba\rangle$, namely requiring that the trace mode \mathcal{T} is a noninteracting (and then decoupled) particle that can be discarded, thus restricting to the desired sector with $\text{Tr } Q_{ab} = 0$. Eq. (6.2.11) yields the relations

$$\begin{aligned} S_2 + S_9 + NS_7 &= \pm 1 \\ S_1 + S_9 + NS_{11} &= 0 \\ S_3 + S_9 + NS_8 &= 0 \\ 4(S_4 + S_5 + S_6) + NS_9 &= 0 \\ S_7 + S_8 + S_{11} + NS_{10} &= 0 \end{aligned}$$

which can be used to express the amplitudes $S_{i \geq 7}$ in terms of $S_{i \leq 6}$. In this way the unitarity equations (2.3.7), where now $\mu = ab$ and Kronecker deltas are replaced

by (6.2.2), take the form

$$1 = \rho_1^2 + \rho_2^2 + 4\rho_4^2, \quad (6.2.12)$$

$$0 = 2\rho_1\rho_2 \cos \phi + 4\rho_4^2, \quad (6.2.13)$$

$$\begin{aligned} 0 = & M_N \rho_1^2 + 2\rho_1^2 \cos 2\phi + 2\rho_1\rho_2 \cos \phi + 4 \left(1 - \frac{2}{N} + N\right) \rho_1\rho_4 \cos(\phi - \theta) \\ & + 4 \left(1 - \frac{2}{N}\right) \rho_1\rho_4 \cos(\phi + \theta) + \frac{32}{N^2} \rho_4^2 \cos 2\theta + 4 \left(1 - \frac{2}{N} + N\right) \rho_1\rho_5 \cos \phi \\ & + 8 \left(1 + \frac{8}{N^2}\right) \rho_4\rho_5 \cos \theta + 4 \left(1 + \frac{8}{N^2}\right) \rho_4^2 + 4 \left(1 + \frac{4}{N^2}\right) \rho_5^2, \end{aligned} \quad (6.2.14)$$

$$\begin{aligned} 0 = & 2\rho_2\rho_5 + 2\rho_1\rho_4 \cos(\phi + \theta) - \frac{8}{N} \rho_4^2 + 2 \left(1 - \frac{4}{N}\right) \rho_4^2 \cos 2\theta \\ & + 2 \left(3 - \frac{8}{N} + N\right) \rho_4\rho_5 \cos \theta - \frac{4}{N} \rho_5^2, \end{aligned} \quad (6.2.15)$$

$$\begin{aligned} 0 = & 2\rho_2\rho_4 \cos \theta + \left(2 - \frac{8}{N} + N\right) \rho_4^2 + 2 \left(1 - \frac{4}{N}\right) \rho_4^2 \cos 2\theta + 2\rho_1\rho_5 \cos \phi \\ & + 2 \left(1 - \frac{8}{N}\right) \rho_4\rho_5 \cos \theta + \left(2 - \frac{4}{N} + N\right) \rho_5^2, \end{aligned} \quad (6.2.16)$$

$$0 = 2\rho_1\rho_4 \cos(\phi - \theta) + 2\rho_2\rho_4 \cos \theta + 2\rho_4^2, \quad (6.2.17)$$

where

$$M_N \equiv \frac{1}{2}N(N+1) - 1. \quad (6.2.18)$$

6.3 Scattering solutions and implications for liquid crystals

The solutions of these equations give the fixed points allowed for the RP^{N-1} model. It is immediately clear that for $\rho_4 = \rho_5 = 0$ the equations (6.2.12)-(6.2.17) reduce to the $O(N)$ vector unitarity equations (3.1.3)-(3.1.5), with M_N “vector” components. This means that the RP^{N-1} model possesses, in particular, the fixed points of the $O(M_N)$ model. Notice that, since $M_2 = 2$, for $N = 2$ we recover the BKT transition required by the topological correspondence $RP^1 \sim$

$O(2)$. More generally, the RP^{N-1} model possesses the zero temperature FP of the $O(M_N)$ model. The equations (6.2.12)-(6.2.17) do not possess additional solutions for integer $N > 3$. The only additional solution for $N = 3$ is

$$\rho_1 = 2\rho_4 = \frac{2}{3}, \quad \phi = \theta = \frac{\pi}{2} \pm \frac{\pi}{2}, \quad \rho_2 = \rho_5 = \pm \frac{1}{3}, \quad (6.3.1)$$

and does not extend away from $N = 3$. Since a free parameter, namely a line of fixed points for N fixed, is necessary for QLRO, we see that there is no QLRO for integer $N > 2$.

Since the symmetry is continuous, the $N = 3$ solution (6.3.1) should not correspond to spontaneous breaking. The fact that such a solution exists only at $N = 3$ may suggest a topological origin. On the other hand, a topological transition is usually expected to lead to QLRO. The point is intriguing and will deserve further investigation.

The identification of a zero temperature fixed point in the $O(M_N)$ universality class provides a natural solution to the controversy about the suppression of the correlation length at low temperatures observed in [90, 91]. Since $M_N > N$ for $N > 2$, the RP^{N-1} and $O(N)$ universality classes are different. The correlation length in the $O(M > 2)$ model can be computed for $T \rightarrow 0$ from the non-linear sigma model (1.4.10) and reads [8, 89]

$$\xi_M \propto T^{1/(M-2)} e^{A/[(M-2)T]}, \quad (6.3.2)$$

where A is a positive constant. The dominant effect comes from the exponential factor, and we see that ξ_M diverges less rapidly as M increases. Hence, the identification of the RP^{N-1} zero temperature critical point with the $O(M_N > N)$ critical point explains the numerical observations that the correlation length of the RP^{N-1} model diverges less rapidly than that of the $O(N)$ model. The discrepancy increases exponentially as T decreases, and this explains that the suppression observed numerically involves several order of magnitudes. In addition, our result implies that, for T fixed, the correlation length suppression with

respect to the $O(N)$ case decreases as N increases, and this also agrees with the data of [91] for $N = 3, 4$. The correlation length in the RP^{N-1} model is determined by $\langle Q_{ab}(x)Q_{ab}(y) \rangle$, consistently with the fact that $\langle \mathbf{s}(x) \cdot \mathbf{s}(y) \rangle$ vanishes due to head-tail symmetry.

As we saw, zero temperature $O(M_N)$ criticality is associated with the vanishing of the parameters ρ_4 and ρ_5 . Away from criticality ($T > 0$) these parameters will normally acquire nonzero values, and for T not too small will make apparent a difference with the $O(M_N)$ behavior. This might produce some form of crossover at intermediate temperatures.

Summarizing, we used scale invariant scattering theory to exactly determine the renormalization group fixed points of the two-dimensional RP^{N-1} model. For $N > 2$ we showed the absence of QLRO and the presence of a zero temperature critical point belonging to the $O(N(N+1)/2-1)$ universality class. For $N = 2$ the equations yield the BKT transition required by the correspondence $RP^1 \sim O(2)$. These results answer questions debated in the literature over the last decades, in particular about the presence of a nematic phase with QLRO in two-dimensional liquid crystals with $N = 3$ and the ability of an extra local symmetry to change the low temperature critical behavior.

Chapter 7

Bond disordered Potts model

We consider the random bond q -state Potts model and illustrate how the framework of scale invariant scattering extends to systems with quenched disorder. In particular, we exhibit the line of stable fixed points induced by disorder for arbitrarily large values of q , and examine the renormalization group pattern for $q > 4$, when the transition of the pure model is first order.

7.1 Scale invariant scattering and replicas

The random bond q -state Potts model corresponds to the case in which the couplings J_{ij} in the lattice Hamiltonian (1.4.11) are random variables drawn from a probability distribution $P(J_{ij})$. As we saw, the average over disorder can be dealt with through the replica method [94]. The latter can be implemented *exactly* for two-dimensional critical systems within the scale invariant scattering approach [5], and we now show how this is done in the Potts case. With respect to the scattering description of the pure model (i.e. without disorder), which we saw is based on the particle basis $A_{\alpha\beta}$ ($\alpha, \beta = 1, 2, \dots, q; \alpha \neq \beta$), we now have to take into account that such an excitation can occur in any of the n replicas. Hence we consider the particles $A_{\alpha_i\beta_i}$, where $i = 1, 2, \dots, n$ labels the replicas. Now the trajectory of the particle $A_{\alpha_i\beta_i}$ separates a region characterized

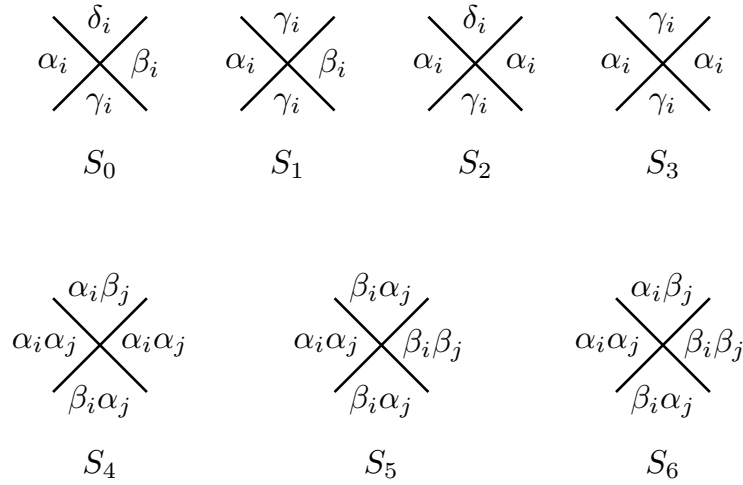


Figure 7.1: Scattering processes corresponding to the amplitudes $S_0, S_1, S_2, S_3, S_4, S_5, S_6$. Different latin indices correspond to different replicas, and different greek letters for the same replica correspond to different colors.

by colors $\alpha_1, \dots, \alpha_n$ for replicas $1, \dots, n$, respectively, from a region where replica i changed its color to β_i , with the colors of the other replicas unchanged. Then the requirement of invariance under permutations of the replicas and permutations of the colors within each replica ($\mathbb{S}_q \times \mathbb{S}_n$ symmetry) leaves us with the seven inequivalent amplitudes S_0, S_1, \dots, S_6 depicted in figure 7.1, where we only keep track of the replicas whose color changes in the scattering process. The four amplitudes in the upper part of the figure have all particles in the same replica and are the amplitudes entering the pure case; the three remaining amplitudes introduce interaction among the replicas.

As usual, crossing symmetry establishes a relation between amplitudes which are exchanged under exchange of time and space directions, and in the present case

takes the form

$$S_0 = S_0^* \equiv \rho_0, \quad (7.1.1)$$

$$S_1 = S_2^* \equiv \rho e^{i\varphi}, \quad (7.1.2)$$

$$S_3 = S_3^* \equiv \rho_3, \quad (7.1.3)$$

$$S_4 = S_5^* \equiv \rho_4 e^{i\theta}, \quad (7.1.4)$$

$$S_6 = S_6^* \equiv \rho_6, \quad (7.1.5)$$

where we introduced

$$\rho_0, \rho_3, \rho_6, \varphi, \theta \in \mathbb{R}, \quad \rho, \rho_4 \geq 0. \quad (7.1.6)$$

On the other hand, unitarity translates into the equations [5]

$$1 = \rho_3^2 + (q-2)\rho^2 + (n-1)(q-1)\rho_4^2, \quad (7.1.7)$$

$$0 = 2\rho\rho_3 \cos \varphi + (q-3)\rho^2 + (n-1)(q-1)\rho_4^2, \quad (7.1.8)$$

$$0 = 2\rho_3\rho_4 \cos \theta + 2(q-2)\rho\rho_4 \cos(\varphi + \theta) + (n-2)(q-1)\rho_4^2, \quad (7.1.9)$$

$$1 = \rho^2 + (q-3)\rho_0^2, \quad (7.1.10)$$

$$0 = 2\rho_0\rho \cos \varphi + (q-4)\rho_0^2, \quad (7.1.11)$$

$$1 = \rho_4^2 + \rho_6^2, \quad (7.1.12)$$

$$0 = \rho_4\rho_6 \cos \theta, \quad (7.1.13)$$

which correspond to the diagrams of figure 7.2. Equation (7.1.12) implies

$$\rho_4 = \sqrt{1 - \rho_6^2} \in [0, 1]. \quad (7.1.14)$$

It is important to note that now not only q , but also n appears in the equations as a parameter which can take real values, so that the limit $n \rightarrow 0$ required by the replica method can be taken without problems.

As required, the unitarity equations (7.1.7)–(7.1.13) reduce to those of the pure

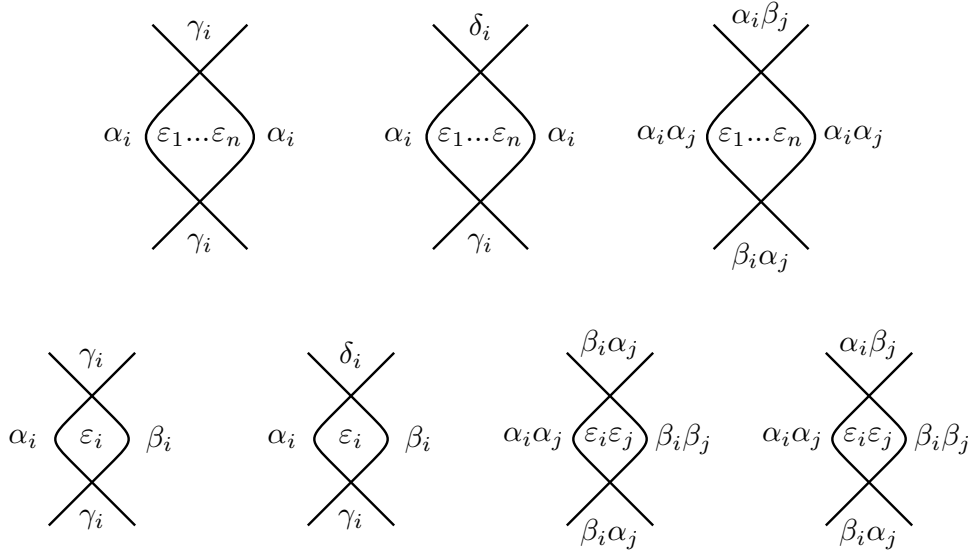


Figure 7.2: Pictorial representations associated to the unitarity equations (7.1.7)–(7.1.13), in the same order. The amplitude for the lower crossing multiplies the complex conjugate of the amplitude for the upper crossing, and sum over colors in the internal (i.e. closed) region is implied. Replicas which are not indicated keep the same color in the four external regions, and also in the internal region for the last four diagrams (bottom row).

model when n is set to 1 and the equations which still involve ρ_4 and/or ρ_6 are ignored. Another important property is that $\rho_4 = 0$ gives n non-interacting replicas, since it corresponds to $S_4 = S_5 = 0$ and, as a consequence of (7.1.12), to $S_6 = \pm 1$. As in the pure case, it is possible to build superpositions of two-particle states which diagonalize the scattering, i.e. scatter into themselves with amplitudes which, by unitarity, must be phases. In particular, the superposition $\sum_{i, \gamma_i} A_{\alpha_i \gamma_i} A_{\gamma_i \alpha_i}$ scatters into itself with the phase

$$S = S_3 + (q - 2)S_2 + (n - 1)(q - 1)S_4. \quad (7.1.15)$$

We call “neutral” this scattering channel involving excitations beginning and ending with the same color. In a similar way, the “charged” superpositions

$\sum_{\gamma_i} A_{\alpha_i \gamma_i} A_{\gamma_i \beta_i}$ and $A_{\alpha_i \beta_i} A_{\alpha_j \beta_j} + A_{\alpha_j \beta_j} A_{\alpha_i \beta_i}$ diagonalize the scattering with phases

$$\Sigma = S_1 + (q - 3)S_0, \quad (7.1.16)$$

$$\tilde{\Sigma} = S_5 + S_6, \quad (7.1.17)$$

respectively. As we know, the neutral phase is related to the conformal dimension Δ_η of the chiral field η which creates the massless particles as (2.3.2); bosonic and fermionic particles are obtained when Δ_η is integer and half-integer, respectively, and particles with generalized statistics otherwise¹.

7.2 Solutions of the unitarity equations

7.2.1 Generic number of replicas

The solutions of the unitarity equations (7.1.7)–(7.1.13) satisfying (7.1.6) and (7.1.14) correspond to renormalization group fixed points possessing the symmetry $\mathbb{S}_q \times \mathbb{S}_n$. It is a general consequence of the form of the crossing and unitarity equations that, given a solution, another solution is obtained reversing the sign of all the amplitudes; correspondingly, all the solutions we write below admit a choice between upper and lower signs. We already listed in table 4.1 the solutions for the pure case [29] which, as we said, is obtained setting $n = 1$ and ignoring the equations which still contain ρ_4 and/or ρ_6 .

Coming to solutions with n generic [99], (7.1.13) shows that we can distinguish two classes of solutions with coupled replicas ($\rho_4 \neq 0$), that with $\cos \theta = 0$ and that with $\rho_6 = 0$, which we now consider separately.

¹In the off-critical case, generalized statistics does not affect low energy phenomena (see e.g. [95]), but shows up in high energy asymptotics [96–98].

A. $\cos \theta = 0$

Up to sign doubling, there are four solutions defined in intervals of n which include $n = 0$. For all of them the maximal value of n is $\frac{2}{q-1}$ for² $q > 2$.

The first solution is defined for $q \geq 3$ and reads

$$\begin{aligned} \rho_0 = \rho_3 = 0, & & 2 \cos \varphi = \pm \frac{1}{q-2} \sqrt{\frac{n^2(q-1)(q-3)}{n-1} + 4}, \\ \rho = 1, & & \rho_4 = \sqrt{\frac{3-q}{(n-1)(q-1)}}. \end{aligned} \quad (7.2.1a)$$

The second solution is defined for $q > \sqrt{2}$ and reads

$$\begin{aligned} \rho_0 = 0, & & \rho_3 = 2 \cos \varphi = \pm \sqrt{\frac{n^2(q-1)(q-3) + 4(n-1)}{(n-q)(n-nq+q)}}, \\ \rho = 1, & & \rho_4 = |q-2| \sqrt{\frac{q+1}{(q-1)(q-n)(n-nq+q)}}. \end{aligned} \quad (7.2.1b)$$

The third solution is defined for $q \in [\frac{1}{2}(7 - \sqrt{17}), 4]$ and $q \geq \frac{1}{2}(7 + \sqrt{17})$, and reads

²The fact that solutions allowing the analytic continuation to $n = 0$ are defined for $n < 2$ when $q > 2$ is of interest for the perturbative studies of coupled Potts models (see [100] and references therein).

$$\begin{aligned}
\rho_0 = \rho_3 &= \pm \sqrt{\frac{(q-3)(q-1)n^2 + 4(n-1)}{(q-1)(q^2 - 5q + 5)n^2 + (q^2 - 6q + 6)^2(n-1)}}, \\
\rho &= \sqrt{\frac{(q-4)[(q-1)n^2 + (q^3 - 8q^2 + 16q - 12)(n-1)]}{(q-1)(q^2 - 5q + 5)n^2 + (q^2 - 6q + 6)^2(n-1)}}, \\
2 \cos \varphi &= \mp (q-4) \sqrt{\frac{(q-3)(q-1)n^2 + 4(n-1)}{(q-4)[(q-1)n^2 + (q^3 - 8q^2 + 16q - 12)(n-1)]}}, \\
\rho_4 &= \frac{|q-2|}{q-1} \sqrt{-\frac{(q-4)(q-1)(q^2 - 7q + 8)}{(q^2 - 5q + 5)n^2 + (q^2 - 6q + 6)^2(n-1)}}. \tag{7.2.1c}
\end{aligned}$$

For positive values of q , the fourth solution is defined in the ranges $q \in [\tilde{q} = 1.488\dots, 3]$ and $q \geq 4$, and reads

$$\begin{aligned}
\rho_0 &= \pm \sqrt{\frac{(q-3)(q-1)n^2 + 4(n-1)}{(q-3)(q-1)n^2 + (q^2 - 4q + 2)^2(n-1)}}, \\
\rho_3 &= \mp (q-3) \sqrt{\frac{(q-3)(q-1)n^2 + 4(n-1)}{(q-3)(q-1)n^2 + (q^2 - 4q + 2)^2(n-1)}}, \\
\rho &= \sqrt{\frac{(q-4)[-(q-3)(q-1)n^2 + (q^3 - 4q^2 + 4q - 4)(n-1)]}{(q-3)(q-1)n^2 + (q^2 - 4q + 2)^2(n-1)}}, \\
2 \cos \varphi &= \mp (q-4) \sqrt{\frac{(q-3)(q-1)n^2 + 4(n-1)}{(q-4)[-(q-3)(q-1)n^2 + (q^3 - 4q^2 + 4q - 4)(n-1)]}}, \\
\rho_4 &= \frac{|q-2|}{q-1} \sqrt{-\frac{(q-4)(q-3)(q-1)q}{(q-3)(q-1)n^2 + (q^2 - 4q + 2)^2(n-1)}}. \tag{7.2.1d}
\end{aligned}$$

The value \tilde{q} is a root of the equation $q^4 - 8q^3 + 20q^2 - 14q - 2 = 0$; below \tilde{q} the solution would not include the value $n = 0$.

For all solutions, it is understood that ρ_6 follows from ρ_4 through (7.1.14). Defining

$$\operatorname{sgn}(\sin \theta \sin \varphi) = (-1)^j, \tag{7.2.2}$$

all four solutions correspond to $j = 0$ below $q = 2$, and to $j = 1$ above.

B. $\rho_6 = 0$

There are two solutions in this class which admit continuation to $n = 0$. Both are defined for any q , have

$$\rho_0 = 0, \quad \rho = \rho_4 = 1, \quad \rho_3 = 2 \cos \varphi = \pm \sqrt{n(1-q) + 2}, \quad (7.2.3)$$

and differ in the value of $\cos \theta$. The first solution has

$$\cos \theta = \cos \varphi, \quad (7.2.4a)$$

and $j = 1$ in (7.2.2), while the second

$$2 \cos \theta = \pm \frac{\sqrt{n(1-q) + 2} (n(q-1) - q^2 + 2)}{(n(q-1)^2 - q^2 + 2q - 2)}, \quad (7.2.4b)$$

$j = 0$ for $q \in [2 - \sqrt{2}, 2 + \sqrt{2}]$, and $j = 1$ outside this range.

7.2.2 The limit of zero replicas

Specializing to $n = 0$ the four solutions (7.2.1a)-(7.2.1d) with $\cos \theta = 0$ we obtain that the first of them, defined for $q \geq 3$, reads

$$\rho_0 = \rho_3 = 0, \quad \rho = 1, \quad 2 \cos \varphi = \pm \frac{2}{q-2}, \quad \rho_4 = \sqrt{\frac{q-3}{q-1}}; \quad (7.2.5a)$$

the second, defined for $q > \sqrt{2}$, reads

$$\rho_0 = 0, \quad \rho = 1, \quad \rho_3 = 2 \cos \varphi = \pm \frac{2}{q}, \quad \rho_4 = \frac{|q-2|}{q} \sqrt{\frac{q+1}{q-1}}; \quad (7.2.5b)$$

the third, defined for $q \in [\frac{1}{2}(7 - \sqrt{17}), 4]$ and $q \geq \frac{1}{2}(7 + \sqrt{17})$, reads

$$\begin{aligned}\rho_0 = \rho_3 &= \pm \frac{2}{|q^2 - 6q + 6|}, \\ \rho &= \frac{\sqrt{(q-4)(q^3 - 8q^2 + 16q - 12)}}{|q^2 - 6q + 6|}, \\ 2 \cos \varphi &= \mp \frac{2(q-4)}{\sqrt{(q-4)(q^3 - 8q^2 + 16q - 12)}} \\ \rho_4 &= \frac{|q-2|\sqrt{(q-4)(q-1)(q^2 - 7q + 8)}}{(q-1)|q^2 - 6q + 6|};\end{aligned}\quad (7.2.5c)$$

finally the fourth solution, which for q positive is defined in the ranges $q \in [\tilde{q} = 1.488\dots, 3]$ and $q \geq 4$, reads

$$\begin{aligned}\rho_0 &= \pm \frac{2}{|q^2 - 4q + 2|}, & \rho &= \frac{\sqrt{(q-4)(q^3 - 4q^2 + 4q - 4)}}{|q^2 - 4q + 2|}, \\ \rho_3 &= \mp \frac{2(q-3)}{|q^2 - 4q + 2|}, & 2 \cos \varphi &= \mp \frac{2(q-4)}{\sqrt{(q-4)(q^3 - 4q^2 + 4q - 4)}}, \\ \rho_4 &= \frac{|q-2|\sqrt{(q-4)(q-3)(q-1)q}}{(q-1)|q^2 - 4q + 2|},\end{aligned}\quad (7.2.5d)$$

with $\rho_6 = 0$ at \tilde{q} .

For $n = 0$ the two solutions with $\rho_6 = 0$, which are defined for any q , read

$$\rho_0 = 0, \quad \rho = \rho_4 = 1, \quad \rho_3 = 2 \cos \varphi = 2 \cos \theta = \pm \sqrt{2}, \quad (7.2.6a)$$

and

$$\rho_0 = 0, \quad \rho = \rho_4 = 1, \quad \rho_3 = 2 \cos \varphi = \pm \sqrt{2}, \quad 2 \cos \theta = \pm \frac{\sqrt{2}(q^2 - 2)}{(q^2 - 2q + 2)}, \quad (7.2.6b)$$

7.3 Properties of the solutions

We have noted above how the scattering solutions with $\rho_4 = 0$ correspond to decoupled replicas. Since the replicas are coupled by the average over disorder, the parameter $\rho_4 \in [0, 1]$ gives a measure of the disorder strength within the scattering formalism. It follows that the two classes of solutions obtained in the previous section, that with $\cos \theta = 0$ and that with $\rho_6 = 0$, are physically distinguished by the dependence of the disorder strength on the parameter q . While the four solutions in the first class all admit weak disorder limits, the two solutions in the second class are strongly disordered for any q . We now separately discuss these two classes of solutions.

7.3.1 Critical lines with weak disorder limit

An important difference between the scattering solutions for the pure case and those for the random case is that, while in the first case there are no fixed points for $q > (7 + \sqrt{17})/2$, the second admits lines of fixed points extending to q infinite. This result then appears as the explicit and exact manifestation of the findings of [101, 102] that in two dimensions quenched bond randomness can soften first order phase transitions into second order ones. We also know that the pure and random ferromagnetic critical lines meet at $q = 2$, where randomness is marginally irrelevant [103], so that the scattering solution for the random ferromagnetic line should have $\rho_4 = 0$ at $q = 2$. Since the proof of [101] refers to integer values of q , these properties select two solutions³ among those of section 7.2.2, namely (7.2.5b) and (7.2.5d); the choice of lower signs in both cases ensures that S_3 , the only physical amplitude for the pure model at $q = 2$, takes the required value -1 at this point. On the other hand, numerical studies [104, 105] indicate that the ferromagnetic random critical line extends to real values of q , including the interval $q \in [3, 4]$. If this property is required, solution (7.2.5b) remains as the only admissible.

³Solution (7.2.5c) has $\rho_4 = 0$ at $q = 2$ but is not defined for $q = 5$.

A main property common to all solutions with $\cos \theta = 0$ is that (7.1.15) and (7.1.9) imply $\text{Im } S = 0$ at $n = 0$. This means that, while S is q -dependent for n generic, it becomes constant for $n = 0$, i.e. precisely in the limit required for the random case. This is visible in figure 7.3 for solution (7.2.1b), which has

$$\begin{aligned} S &= \frac{1}{2}(q\rho_3 + in(q-1)\rho_4 \sin \theta) \\ &= \exp[-i \operatorname{sgn}(n) \operatorname{sgn}(\sin \varphi) \operatorname{Arccos}(q \cos \varphi)], \end{aligned} \tag{7.3.1}$$

where $\operatorname{sgn}(0) = 1$.

This indicates that the symmetry sector of the state $\sum_{i,\gamma_i} A_{\alpha_i\gamma_i} A_{\gamma_i\alpha_i}$ becomes q -independent in the random case. This symmetry sector contains the fields which create the state $\sum_{i,\gamma_i} A_{\alpha_i\gamma_i} A_{\gamma_i\alpha_i}$, namely the \mathbb{S}_q -invariant fields like the energy density ε . This makes possible that the scaling dimensions of these fields remain constant along the random critical line. In particular, the correlation length critical exponent $\nu = 1/(2 - X_\varepsilon)$ can keep along the line the value 1 it takes at $q = 2$ (superuniversality) [5]. This value saturates the rigorous bound $\nu \geq 2/d$ for disordered systems in d dimensions [106]. On the other hand, the spin field carries a representation of \mathbb{S}_q symmetry and does not belong to the sector which becomes q -independent at $n = 0$. As a consequence, the magnetization exponent β , which depends on the spin field scaling dimension, depends on q . This subtle analytical mechanism finally sheds light on puzzling numerical observations [104, 105, 107–113] yielding q -dependent β and $\nu \approx 1$.

It must be noted that the q -independence of the scattering phase S emerges as a property of the *exact* solution at $n = 0$, and may not appear in an approximate calculation. Hence, the scenario of a constant exponent ν is not in contradiction with the very weak q -dependence exhibited by leading order perturbative expansion in powers of $q - 2$ for the random bond ferromagnet [114, 115]. The value $\nu = 1$ is also consistent with the exact conjecture of [116] for $q \rightarrow \infty$. Concerning the numerical estimates of ν for the random bond ferromagnet, they appear to have the value $\nu = 1$ within their error bars. The fact that this circumstance

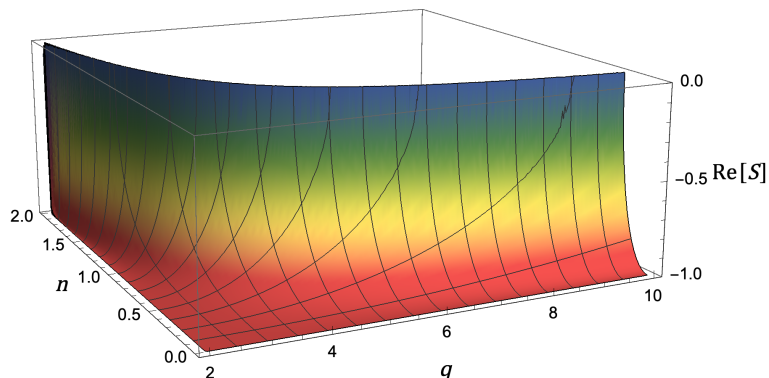


Figure 7.3: Real part of the scattering phase (7.1.15) for the solution (7.2.1b). It becomes q -independent in the limit $n \rightarrow 0$ corresponding to quenched disorder.

persists at large values of q [111–113], which are out of reach for the expansion in powers of $q - 2$, requires a non-perturbative mechanism, whose presence is confirmed by the appearance of the q -independent amplitude S in the exact scattering solution.

7.3.2 Critical lines without weak disorder limit

Consider now the two solutions with $\rho_6 = 0$. They are defined for all values of q and are always strongly disordered ($\rho_4 = 1$). Solution (7.2.6a) is characterized by complete q -independence, a peculiarity which is not unexpected within the space of solutions. Indeed, for a disorder probability distribution

$$P(J_{ij}) = p\delta(J_{ij} - J) + (1 - p)\delta(J_{ij}), \quad J > 0, \quad (7.3.2)$$

corresponding to a dilute ferromagnet, the energy receives contribution from clusters of spins connected by ferromagnetic bonds $J_{ij} = J$. At zero temperature, all the spins in such a cluster have the same color, different clusters are independently colored, and the total magnetization vanishes unless there is an infinite cluster; the latter appears when p exceeds the random percolation threshold p_c . Hence, the dilute ferromagnet has a zero-temperature transition in the universality class of random percolation, no matter the value of q . It is then natural

to associate this random percolation line to the q -independent solution (7.2.6a), for a suitable sign choice.

In the dilute ferromagnet, temperature is known to provide a relevant perturbation close to $T = 0$ (see e.g. [8]). For $q > 2$ this is consistent with a phase diagram with three fixed points along the paramagnetic/ferromagnetic phase boundary in the p - T plane (left panel of figure 7.4): two unstable fixed points at the endpoints of the phase boundary (that of the pure model at $p = 1$ and the percolative one at $T = 0$) and an intermediate, stable fixed point corresponding to the solution with q -dependent disorder strength of the previous subsection. When $q \rightarrow 2$, the latter fixed point coalesces with the pure one and the renormalization group flow directly goes from the zero temperature to the pure fixed point.

A different scenario occurs for a disorder probability distribution

$$P(J_{ij}) = p\delta(J_{ij} - J) + (1 - p)\delta(J_{ij} + J), \quad J > 0, \quad (7.3.3)$$

which allows for ferromagnetic and antiferromagnetic bonds. A phase boundary separating ferromagnetic and paramagnetic regimes is observed in the low- $(1-p)$ region of the p - T plane (right panel of figure 7.4). A main difference with the dilute ferromagnet is the presence of an additional fixed point located on the phase boundary between a zero-temperature fixed point and the random (resp. pure) ferromagnetic fixed point for $q > 2$ (resp. $q = 2$). For $q = 2$ a gauge symmetry [117] allows one to infer the presence of the additional fixed point, which is known as the Nishimori point. For $q > 2$ Nishimori gauge symmetry does not hold but the Nishimori-like fixed point is still expected, and has been exhibited numerically for $q = 3$ [118].

The Nishimori-like fixed point is strongly disordered and cannot correspond to the scattering solutions with variable disorder strength. It should then correspond to (7.2.6a) or (7.2.6b). While (7.2.6a) is completely q -independent, (7.2.6b) leads to q -independence of the scattering amplitude Σ given by (7.1.16); again, q -independence arises only at $n = 0$. The numerically estimated exponents

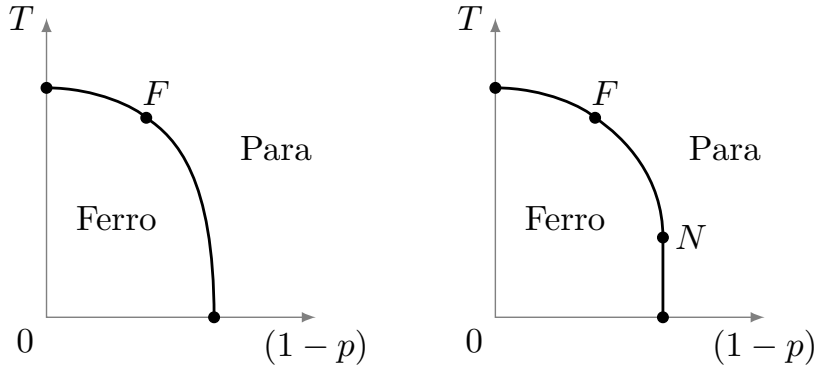


Figure 7.4: Qualitative phase diagrams and expected fixed points (dots) in the $q > 2$ two-dimensional Potts model with quenched bond distributions (7.3.2) (left) and (7.3.3) (right); N denotes the Nishimori-like fixed point. For $q = 2$ the fixed point F is absent and N is the Nishimori point.

at the Nishimori(-like) fixed point are $\nu \approx 1.5$, $\eta \approx 0.18$ for $q = 2$ [119–123], and $\nu = 1.28 - 1.36$, $\eta = 0.17 - 0.22$ for $q = 3$ [118]. These results appear to exclude the q -independent solution (7.2.6a), but are compatible with (7.2.6b). A model possessing Nishimori gauge property was introduced in [124] for the case of \mathbb{Z}_q symmetry (cyclic permutations) and a specific realization of disorder. This model was studied numerically⁴ for $q = 3$ in [126], where the value $\eta = 0.20 - 0.21$ was obtained at the Nishimori point.

Numerical study of the zero temperature fixed point for the distribution (7.3.3) indicates that it is no longer in the percolation universality class [121] and that it is stable under thermal perturbation [118], as required by the presence of the additional fixed point. Also the zero temperature fixed point is strongly disordered and should be described by (7.2.6a) or (7.2.6b), so that at least η could be q -independent. The numerical results $\nu = 1.35 - 1.45$, $\eta = 0.18(1)$ for $q = 2$ [118, 127, 128], and $\nu = 1.45 - 1.55$, $\eta = 0.18(1)$ for $q = 3$ [118] are consistent with this scenario and point to q -dependent ν , namely to (7.2.6b). Note that, even if the Nishimori-like and the zero temperature fixed points correspond to the same scattering solution, this does not imply that they have the same

⁴See also [125] for a study of the phase diagram.

critical exponents, since we already saw for the case of pure Potts that a single scattering solution accounts for ferromagnetic and square lattice antiferromagnetic criticality.

7.4 Softening of first order transition by disorder

Let us now look more closely [129] into the problem of the softening that disorder operates on the first order transition that the pure model possesses for $q > 4$. Indeed, having found the line of stable fixed points that extends to arbitrarily large values of q is not enough from the point of view of the renormalization group. Within the space of parameters, this line will be the large distance limit of a second order transition surface that has to originate somewhere else. For $q \leq 4$ it originates from the line of fixed points of the pure model, which is unstable under the action of disorder. Where does the surface originate from for $q > 4$? Since the correlation length is infinite on the second order surface, the latter cannot originate from the first order transition line of the pure model, along which the correlation length is finite. Given its generality, the scale invariant scattering framework should provide new elements also on this question. We will see that this is the case.

We know that the critical line of the pure ferromagnet corresponds to solution III₋ of table 4.1, which we rewrite for convenience:

$$\rho_0 = -1, \quad \rho = \sqrt{4-q}, \quad 2 \cos \varphi = -\sqrt{4-q}, \quad \rho_3 = q-3. \quad (7.4.1)$$

The Harris criterion implies that weak disorder is relevant for $q \in (2, 4]$, the upper extreme of the interval being the endpoint of second order criticality, and leads to a random fixed point that was studied perturbatively for $q \rightarrow 2^+$ [114, 115].

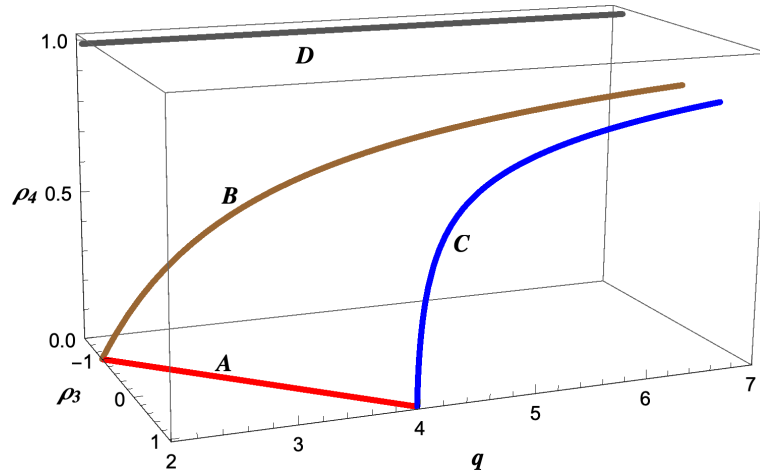


Figure 7.5: Lines of renormalization group fixed points with \mathbb{S}_q permutational symmetry associated to solutions of the equations (7.1.7)-(7.1.13) with $n = 0$. Absence of disorder corresponds to $\rho_4 = 0$, and A is the critical line of the pure Potts ferromagnet (7.4.1). The critical lines B and C correspond to the solutions (7.4.2) and (7.4.3), respectively. D corresponds to Nishimori-like and zero temperature fixed points, which are not distinguished in this parameter subspace.

We saw that this fixed point corresponds to the solution

$$\rho_0 = \cos \theta = 0, \quad \rho = 1, \quad \rho_3 = 2 \cos \varphi = -\frac{2}{q}, \quad \rho_4 = \frac{q-2}{q} \sqrt{\frac{q+1}{q-1}}, \quad (7.4.2)$$

which extends until $q = \infty$ (figure 7.5), in agreement with the result of [101, 102] on the softening of first order transitions by disorder. Hence, scale invariant scattering provides the first analytic verification of this expectation. It also provides the first exact verification that random critical points possess conformal invariance; numerical evidence of this fact for the critical line corresponding to our solution (7.4.2) had been given in [130].

The picture, however, cannot yet be considered as complete. Indeed, the Harris criterion implies that for $q \in (2, 4]$ there is a renormalization group flow from the pure ferromagnet (7.4.1) to the line of random fixed points (7.4.2). The latter, however, continues to be a line of infrared fixed points also for $q > 4$, where

the transition of the pure model is first order. If usual renormalization group mechanisms have to apply, the random model should possess for $q > 4$ a line of unstable fixed points from which the flow towards solution (7.4.2) originates. In this case, the equations (7.1.7)-(7.1.13) should admit a solution starting at $q = 4$ and extending until $q = \infty$. As a matter of fact, such a solution exists and reads

$$\begin{aligned}\rho_0 &= -\frac{2}{|q^2 - 4q + 2|}, & \rho &= \frac{\sqrt{(q-4)(q^3 - 4q^2 + 4q - 4)}}{|q^2 - 4q + 2|}, \\ \rho_3 &= \frac{2(q-3)}{|q^2 - 4q + 2|}, & 2 \cos \varphi &= \frac{2(q-4)}{\sqrt{(q-4)(q^3 - 4q^2 + 4q - 4)}}, \\ \rho_4 &= \frac{(q-2)\sqrt{(q-4)(q-3)(q-1)q}}{(q-1)|q^2 - 4q + 2|}, & \cos \theta &= 0.\end{aligned}\tag{7.4.3}$$

Notice that this solution coincides with that for the pure ferromagnet (7.4.1) at $q = 4$ (see figure 7.5).

In the same way, X_ε is expected to keep for $q > 4$ along the unstable line (7.4.3) the value 1/2 that it has at $q = 4$ in the pure model.

Notice also that the expressions (7.4.2) and (7.4.3) formally coincide at $q = \infty$. However, it is easy to check that the amplitude (7.1.15) calculated at $n = 0$ takes for $q \geq 4$ the value -1 for (7.4.2) and the value 1 for (7.4.3). This is possible because, due to the term $(q-2)S_2$, for both solutions this amplitude behaves for large q as $q \cos \varphi$, with $\cos \varphi$ vanishing as $-1/q$ for (7.4.2) and as $1/q$ for (7.4.3). Hence, due to the peculiarity of the limit, the stable and unstable critical lines do not really merge as $q \rightarrow \infty$.

The solution (7.4.3) is also defined for $q \in [2, 3]$, with ρ_4 vanishing at the extrema of this interval. At $q = 2$ it corresponds to the Ising free fermion with $X_\varepsilon = 1$; at $q = 3$, however, it does not correspond to the Potts ferromagnet but to a theory of two free neutral fermions, again with $X_\varepsilon = 1$ [129]. This difference at $q = 3$ means that this branch enters a sector of the multidimensional parameter space that is not related to the phase diagram we are considering, and for this reason

it is not shown in figure 7.5.

Putting all together, the properties of solution (7.4.3) are consistent with the scenario that it provides the starting point for the renormalization group flow ending on the stable critical line (7.4.2) for $q > 4$. This scenario suggests that for $q > 4$ the second order transition may set in above a q -dependent disorder threshold. Below this threshold the transition would occur with finite correlation length but, to comply with the rigorous result of [101], without discontinuity in the energy density.

Chapter 8

Bond disordered $O(N)$ model

We apply scale invariant scattering to the case of replicated $O(N)$ symmetry and determine the lines of renormalization group fixed points in the limit of zero replicas corresponding to quenched disorder. We emphasize the role of one of the two disorder parameters, which vanishes in the pure limit and is maximal for the solutions corresponding to Nishimori-like and zero temperature critical lines. Emergent superuniversality (i.e. N -independence) of some critical exponents in the disordered case and disorder driven renormalization group flows are also discussed.

8.1 Scattering formulation

We now consider the $O(N)$ Hamiltonian (1.4.1) with bonds J_{ij} drawn from a probability distribution $P(J_{ij})$. A particularly interesting distribution is that mixing ferromagnetic and antiferromagnetic bonds in the form

$$P(J_{ij}) = p\delta(J_{ij} - 1) + (1 - p)\delta(J_{ij} + 1); \quad (8.1.1)$$

the pure ferromagnet is recovered when the fraction $1 - p$ of antiferromagnetic bonds goes to zero. Figure 8.1 qualitatively shows the phase diagram obtained

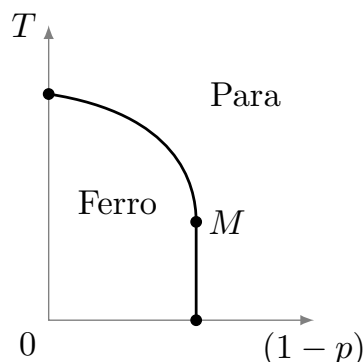


Figure 8.1: Qualitative phase diagram and expected fixed points for the two-dimensional Ising model with the disorder distribution (8.1.1). $1 - p$ is the amount of disorder with respect to the pure ferromagnet, and M indicates the multicritical (Nishimori) point.

by numerical simulations (see e.g. [121, 122]) for the two-dimensional Ising model with the disorder distribution (8.1.1). A ferromagnetic and a paramagnetic phase are separated by a phase boundary along which some fixed points of the renormalization group are located. Besides the pure fixed point and a zero temperature fixed point, the multicritical point known as Nishimori point is also present.

Similarly to what we did in the previous chapter for the disordered Potts model, we want to use scale invariant scattering to exactly implement the replica method. Generalizing our treatment of the pure $O(N)$ model, the particle basis is now given by excitations a_i , where $a = 1, 2, \dots, N$ labels the components of the vector multiplet, and $i = 1, 2, \dots, n$ labels the replicas. The product of two vectorial representations allows for the six scattering amplitudes shown in figure 8.2 [28, 132].

They amount to transmission and reflection of the particles in the same replica (S_2 and S_3 , respectively), or in different replicas (S_5 and S_6); it is also possible that two identical particles annihilate and produce another pair in the same replica (S_1) or in a different replica (S_4). The amplitudes are related under exchange of space and time directions by crossing symmetry, which yields the

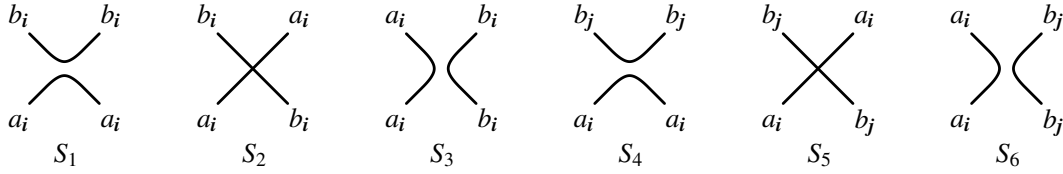


Figure 8.2: Scattering amplitudes of the replicated $O(N)$ theory. Time runs upwards, indices i and j label different replicas.

relations

$$S_1 = S_3^* \equiv \rho_1 e^{i\phi}, \quad (8.1.2)$$

$$S_2 = S_2^* \equiv \rho_2, \quad (8.1.3)$$

$$S_4 = S_6^* \equiv \rho_4 e^{i\theta}, \quad (8.1.4)$$

$$S_5 = S_5^* \equiv \rho_5, \quad (8.1.5)$$

and allows us to write the amplitudes in terms of the variables ρ_1 and ρ_4 non-negative, and ρ_2 , ρ_5 , ϕ and θ real. Unitarity is pictorially expressed in figure 8.3 and produces the equations

$$1 = \rho_1^2 + \rho_2^2, \quad (8.1.6)$$

$$0 = \rho_1 \rho_2 \cos \phi, \quad (8.1.7)$$

$$0 = N\rho_1^2 + N(n-1)\rho_4^2 + 2\rho_1\rho_2 \cos \phi + 2\rho_1^2 \cos 2\phi, \quad (8.1.8)$$

$$1 = \rho_4^2 + \rho_5^2, \quad (8.1.9)$$

$$0 = \rho_4 \rho_5 \cos \theta, \quad (8.1.10)$$

$$0 = 2N\rho_1\rho_4 \cos(\phi - \theta) + N(n-2)\rho_4^2 + 2\rho_2\rho_4 \cos \theta + 2\rho_1\rho_4 \cos(\phi + \theta). \quad (8.1.11)$$

Equations (8.1.6) and (8.1.9) yield the restrictions

$$0 \leq \rho_1 \leq 1, \quad -1 \leq \rho_2 \leq 1, \quad (8.1.12)$$

$$0 \leq \rho_4 \leq 1, \quad -1 \leq \rho_5 \leq 1, \quad (8.1.13)$$

Once again, not only N , but also n enters the equations as a parameter that can

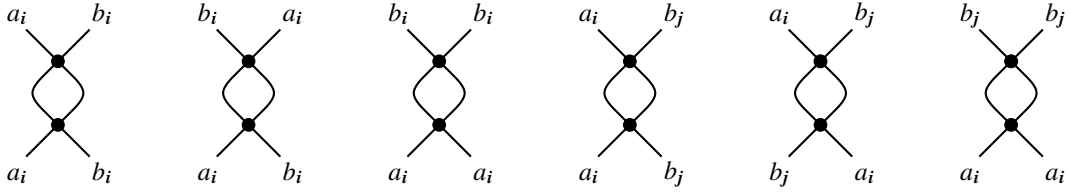


Figure 8.3: Pictorial representations associated to the unitarity equations (8.1.6)–(8.1.11), in the same order. The dotted scattering nodes stay for any of the amplitudes in figure 8.2. The lower amplitude multiplies the complex conjugate of the upper amplitude, and summation is performed over all intermediate particle labels compatible with the assigned external labels.

be treated as taking real values, so that the disorder limit $n \rightarrow 0$ can be taken without difficulty.

It is not difficult to check that the superposition of two-particle states $\sum_{a,i} a_i a_i$ scatters into itself with the amplitude

$$S = NS_1 + S_2 + S_3 + (n - 1)NS_4, \quad (8.1.14)$$

which has to be a phase by unitarity. Similarly, the superpositions $a_i b_i \pm b_i a_i$ and $a_i b_j \pm b_j a_i$ scatter into themselves with phases

$$\Sigma_{\pm} = S_2 \pm S_3, \quad (8.1.15)$$

$$\bar{\Sigma}_{\pm} = S_5 \pm S_6, \quad (8.1.16)$$

respectively.

8.2 Solutions of the fixed point equations

The solutions of the equations (8.1.6)–(8.1.11) correspond to renormalization group fixed points invariant under $O(N)$ transformations and replica permutations. In this section we give the solutions to these equations. We start from the case of n generic, which we then specialize to the disorder limit $n = 0$. The analysis will lead to the results for the solutions summarized in table 8.1. In this

table and in the whole discussion we take into account that equations (8.1.6) and (8.1.9) allow us to write

$$\rho_1 = \sqrt{1 - \rho_2^2}, \quad (8.2.1)$$

$$\rho_5 = \pm \sqrt{1 - \rho_4^2}, \quad (8.2.2)$$

so that the number of parameters characterizing the solutions is four. Two of them (ϕ and ρ_2) are sufficient to span the space of solutions for the pure case, while the remaining two (ρ_4 and θ) are disorder parameters. The quadratic nature of the unitarity equations leads to solution doublings according to the sign of some parameters. While these doublings are not expected to be always physical, it was shown in section 3.2 that in some cases they are.

8.2.1 Generic number of replicas

In the pure case only the amplitudes S_1 , S_2 , and S_3 , which involve a single replica, are physical, and we have only equations (8.1.6), (8.1.7), and (8.1.8), the latter with $n = 1$. Equivalently, the pure case can be regarded as that of n decoupled replicas ($S_4 = S_6 = 0$, $S_5 = \pm 1$), and is obtained for $\rho_4 = 0$. Since the replicas are coupled by the disorder, it follows that ρ_4 , to which we refer as “disorder modulus”, gives a measure of disorder strength¹. The solutions for the pure case were already given in table 3.1, and correspond to those of type P in table 8.1.

Interacting replicas require $\rho_4 \neq 0$, and (8.1.10) shows that we can distinguish two classes of solutions – one with $\cos \theta = 0$ and one with $\rho_5 = 0$. Below we restrict our attention to solutions defined in intervals of n containing $n = 0$, which are those of interest for the purpose of taking the disorder limit. In writing the solutions we take into account that the equations fix the relative sign of $\sin \phi$

¹For strong disorder, however, also the second disorder parameter θ becomes important, see below.

and $\sin \theta$, which we specify giving the value of

$$\gamma \equiv \operatorname{sgn}(\sin \phi \sin \theta). \quad (8.2.3)$$

Up to sign doublings, there are two solutions in the class with $\cos \theta = 0$. The first is defined for $N \in [-\sqrt{2} - 1, -2] \cup [\sqrt{2} - 1, \infty)$ and reads

$$\begin{aligned} \rho_2 = 0, \quad \rho_4 = |N - 1| \sqrt{\frac{N + 2}{N(Nn^2 + (N + 1)^2(1 - n))}}, \\ 2 \cos \phi = \pm \sqrt{\frac{4(1 - n) - N(N - 2)n^2}{(N + 1)^2(1 - n) + Nn^2}}, \end{aligned} \quad (8.2.4)$$

$$\begin{aligned} -\sqrt{2} - 1 \leq N \leq -2, \quad -\frac{2}{|N|} \leq n \leq \frac{N^2 + 2N - 1}{N}, \quad \gamma = +1 \\ \sqrt{2} - 1 = N_* \leq N < 1, \quad n \geq \frac{N^2 + 2N - 1}{N}, \quad \gamma = -1 \\ 1 < N \leq 2, \quad n \leq \frac{2}{N}, \quad \gamma = +1 \\ N > 2, \quad \frac{2}{2 - N} \leq n \leq \frac{2}{N}, \quad \gamma = +1, \end{aligned}$$

where, for different intervals of N , we specified the value of γ and the allowed interval of n . The second solution with $\cos \theta = 0$ is defined only for $N = 0$ and has

$$\rho_2 = \pm 1, \quad 0 \leq \rho_4 \leq 1; \quad (8.2.5)$$

it is n -independent and corresponds to a line of fixed points parametrized by ρ_4 .

Up to sign doublings, the class with $\rho_5 = 0$ contains four solutions. The first is defined for any N and reads

$$\begin{aligned} \rho_1 = \rho_4 = 1, \quad 2 \cos \phi = \pm \sqrt{2 - Nn}, \\ 2 \cos \theta = \pm \frac{\sqrt{2 - Nn}(N^2 - 1 + N(2 - n))}{N^2(1 - n) + 1}, \quad -\frac{2}{|N|} \leq n \leq \frac{2}{|N|}, \end{aligned} \quad (8.2.6)$$

with $\gamma = \pm 1$ when $(n - \bar{n}(N)) \operatorname{sgn}(N) \geq 0$, where $\bar{n}(N) = 2 - N + \frac{1}{N}$ is the boundary along which γ changes sign. The second solution is also defined for any N , differs from the previous one only in θ , and reads

$$\rho_1 = \rho_4 = 1, \quad 2 \cos \phi = 2 \cos \theta = \pm \sqrt{2 - Nn}, \quad \gamma = +1, \quad -\frac{2}{|N|} \leq n \leq \frac{2}{|N|}. \quad (8.2.7)$$

The third and fourth solutions with $\rho_5 = 0$ are defined only for $N \leq 0$ and again differ from each other only for the value of θ . We write them as

$$\begin{aligned} \rho_1 &= \sqrt{\frac{N(n-1)}{2-N}}, \quad \rho_2 = \pm \sqrt{\frac{2-Nn}{2-N}}, \quad \cos \phi = 0, \quad \rho_4 = 1, \\ \cos \theta &= \begin{cases} \mp \sqrt{\frac{2-Nn}{2-N} \frac{(N-1)\sqrt{N(n-1)(2+Nn)} + N(2-n)}{2(N^2(1-n)+1)}}, \\ \pm \sqrt{\frac{2-Nn}{2-N} \frac{(N-1)\sqrt{N(n-1)(2+Nn)} - N(2-n)}{2(N^2(1-n)+1)}}; \end{cases} \end{aligned} \quad (8.2.8)$$

the upper solution for $\cos \theta$ has $\gamma = 1$ and $-2/|N| \leq n \leq 2/(2-N)$, while the lower solution has $\gamma = -\operatorname{sgn}(n - \tilde{n}(N))$ and $-2/|N| \leq n \leq \min[2/|N|, 1]$, where $\tilde{n}(N) = 2[(N-1)^2 - \sqrt{2N^2 - 6N + 5}]/(N^2 - 2N)$.

8.2.2 Disorder limit

We now take the limit $n \rightarrow 0$ of the results of the previous subsection and obtain the solutions of type V and S in table 8.1.

The solution $V1_{\pm}$ is the limit of (8.2.4), and has $\gamma = -1$ for $N_* \leq N < 1$ and $\gamma = 1$ otherwise. $V2_{\pm}$ coincides with (8.2.5), which was n -independent. The solutions $S1_{\pm}$ and $S2_{\pm}$ are obtained from (8.2.6) and (8.2.7), respectively; γ is negative only for $S1_{\pm}$ in the interval $1 - \sqrt{2} < N < 1 + \sqrt{2}$. Finally, the solutions $S3_{\pm}$ and $S4_{\pm}$ are obtained from (8.2.8) and are specified in table 8.1 with

$$f_{\pm}(N) = \frac{\sqrt{-N}(N \pm \sqrt{-2N} - 1)}{\sqrt{2-N}(N^2 + 1)}; \quad (8.2.9)$$

Solution	N	ρ_2	$\cos \phi$	ρ_4	$\cos \theta$
$P1_{\pm}$	\mathbb{R}	± 1	-	-	-
$P2_{\pm}$	$[-2, 2]$	0	$\pm \frac{1}{2} \sqrt{2 - N}$	-	-
$P3_{\pm}$	2	$\pm \sqrt{1 - \rho_1^2}$	0	-	-
$V1_{\pm}$	$[-1 - \sqrt{2}, -2] \cup [\sqrt{2} - 1, \infty)$	0	$\pm \frac{1}{ N+1 }$	$ \frac{N-1}{N+1} \sqrt{\frac{N+2}{N}}$	0
$V2_{\pm}$	0	± 1	-	$[0, 1]$	0
$S1_{\pm}$	\mathbb{R}	0	$\pm \frac{1}{\sqrt{2}}$	1	$\pm \frac{N^2 + 2N - 1}{\sqrt{2}(N^2 + 1)}$
$S2_{\pm}$	\mathbb{R}	0	$\pm \frac{1}{\sqrt{2}}$	1	$\pm \frac{1}{\sqrt{2}}$
$S3_{\pm}$	$(-\infty, 0]$	$\pm \sqrt{\frac{2}{2-N}}$	0	1	$\mp f_+(N)$
$S4_{\pm}$	$(-\infty, 0]$	$\pm \sqrt{\frac{2}{2-N}}$	0	1	$\pm f_-(N)$

Table 8.1: Solutions corresponding to renormalization group fixed points with $O(N)$ symmetry in the pure (P type) and disordered (V and S types) cases. The functions $f_{\pm}(N)$ are given by (8.2.9).

γ is negative only for $S4_{\pm}$ in the interval $\tilde{N} < N \leq 0$, where $\tilde{N} \simeq -0.839$ is the real root of the polynomial $N^3 - 2N^2 + 2$.

8.3 Properties of solutions for the disordered case

8.3.1 Critical lines with varying disorder modulus

Random fixed points have disorder modulus $\rho_4 \neq 0$, and we first consider the solutions $V1_{\pm}$ of table 8.1. They possess the characteristic property that ρ_4 spans, as N varies, the range going from 0 (pure case) to the maximal value 1. More precisely, we focus on the solution $V1_-$, which for $N = 1$ coincides with the pure Ising model (point $N = 1$ of the solution $P2_-$). We know from the

Harris criterion that the scaling dimension of weak disorder is twice that of the energy density field of the pure model. Since the pure Ising model has $\Delta_\varepsilon = 1/2$, weak disorder is marginal² at $N = 1$. The fact that $\Delta_\varepsilon = \Delta_{1,3}$ along the solution $P2_-$ implies that weak disorder is weakly relevant slightly below $N = 1$, and that a random fixed point can be found perturbatively in this region; such a perturbative analysis is similar to that for $q \rightarrow 2^+$ in the Potts model [114, 115] and was performed in [134]. More generally, we conclude that the branch of the solution $V1_-$ extending from $N = 1$, where $\rho_4 = 0$, down to

$$N_* = \sqrt{2} - 1 = 0.414\dots, \quad (8.3.1)$$

where $\rho_4 = 1$, is a line of stable (infrared) fixed points. The existence of a lower endpoint N_* for the infrared critical line was argued in [134], where the estimate $N_* \approx 0.26$ was obtained in the two-loop approximation. The subsequent estimate $N_* \approx 0.5$ obtained in [135] within a numerical transfer matrix study is not far from our exact result.

For $N > 1$ the solution $V1_-$ becomes a line of unstable fixed points, weak disorder becoming irrelevant. Indeed the pure model has $\Delta_\varepsilon > 1/2$ both for $1 < N < 2$, where it corresponds to $P2_-$ with $\Delta_\varepsilon = \Delta_{1,3}$, and for $N > 2$, where it corresponds to $P1_+$ with $\Delta_\varepsilon = 1$.

Figure 8.4 shows the real part of the scattering phase (8.1.14) for the solution (8.2.4) of the fixed point equations, which in the limit $n \rightarrow 0$ becomes $V1_-$. We see (and it can be checked analytically) that S becomes N -independent at $n = 0$, meaning that the symmetry sector of the superposition $\sum_{a,i} a_i a_i$, which is invariant under $O(N)$ transformations and replica permutations, becomes superuniversal along the line of fixed points $V1_-$. Since the energy density field $\varepsilon(x)$ belongs to this symmetry sector, the dimension Δ_ε is expected to keep its $N = 1$ (pure Ising) value $1/2$ along the line $V1_-$. This is analogous to the result we have already seen for the correlation length critical exponent $\nu = [2(1 - \Delta_\varepsilon)]^{-1}$ in the

²It was shown in [103, 133] to be marginally irrelevant.

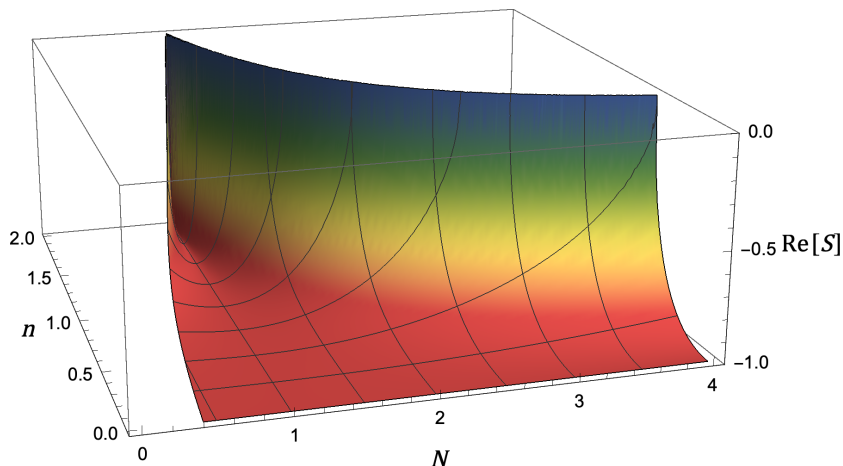


Figure 8.4: The scattering phase (8.1.14) exhibits superuniversality (N -independence) in the limit $n \rightarrow 0$ corresponding to the solution $V1_-$.

random bond q -state Potts ferromagnet. On the other hand, the spin field does not fall into the superuniversal sector and its dimension Δ_s is expected to vary along the critical line $V1_-$. This dimension was measured in [135] for $N = 0.55$ on the infrared fixed line and found to be consistent with the two-loop result of [134].

8.3.2 Critical lines with maximal disorder modulus

The last class of solutions in table 8.1 is characterized by a maximal value $\rho_4 = 1$ of the disorder modulus and corresponds to critical lines that stay strongly disordered as N varies. We focus on the solutions $S1$ and $S2$, whose range of definition includes N positive. Continuing the physical considerations of the previous subsection, we see that the infrared branch of the solution $V1_-$ coincides at its endpoint N_* with the solution $S1_-$ (see figure 8.5). This indicates that for $N > N_*$ $S1_-$ is a line of unstable fixed points. There are renormalization group trajectories that emanate from this line and end on the line $V1_-$ for $N \in (N_*, 1)$, and on the pure model for $N > 1$ (figure 8.6). The point $N = 1$ on the line $S1_-$ then corresponds to the Nishimori multicritical point M in the Ising phase diagram of figure 8.1. A line of strongly disordered fixed points

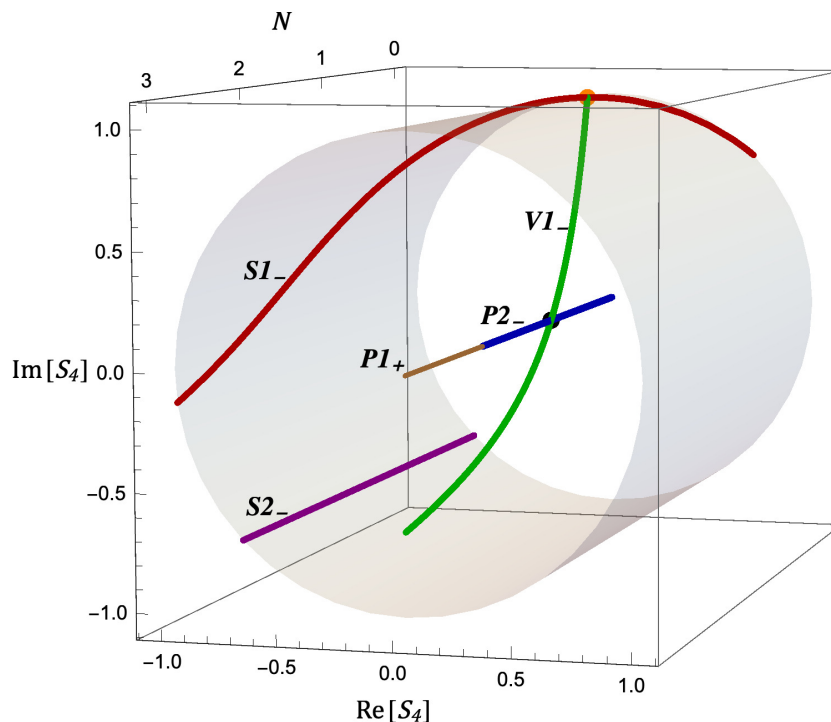


Figure 8.5: Critical lines in the space of the two disorder parameters. The pure case corresponds to $S_4 = 0$, while lines that are strongly disordered for any N lie on the cylinder $|S_4| = \rho_4 = 1$.

extending for $N > N_*$ was in deed observed numerically in [135], and its universal properties at $N = 1$ were found to be quantitatively consistent with those of the Nishimori point. We refer to the portion $N > N_*$ of the critical line $S1_-$ as a line of Nishimori-like multicritical points, implying by this that, from the renormalization group point of view, the points on this line play a role analogous to that of the Nishimori point at $N = 1$, while the lattice gauge symmetry characteristic of the $\pm J$ Ising model [117] is in general absent for $N \neq 1$. We also notice that the symmetry sector corresponding to the scattering phases (8.1.15) is N -independent along $S1_-$.

When we say that for $N > 1$ there is a renormalization group flow from the Nishimori-like critical line $S1_-$ to the pure model, we mean solution $P2_-$ for $N \in (1, 2)$, and solution $P1_+$ for $N > 2$. At $N = 2$ the flow from the Nishimori-

like point can end on any point of the line of fixed points $P3_+$. This explains the BKT phase observed in numerical studies (see e.g. [136, 137]) of the disordered XY model³. These studies find a phase diagram analogous to that of figure 8.1, with a BKT phase replacing the ferromagnetic phase.

It is a consequence of our analysis that, having $\rho_4 = 1$, the Nishimori-like critical line never approaches the pure case. It follows that the zero temperature fixed point of figure 8.1 must have the same property, and must also belong to the class of solutions with $\rho_4 = 1$. Excluding $S3$ and $S4$, which are not defined for N positive, the main candidate for a zero temperature critical line appears to be $S2_-$, which differs from $S1_-$ only for the θ -dependence. Notice that this solution actually is completely N -independent, so that conformal dimensions and critical exponents should not vary along it. Hence, $S2_-$ is expected to be a line of infrared fixed points for any N . It follows that for $-2 < N < N_*$, where the pure solution is unstable and the solution $V1_-$ is not defined, the flow from the pure model should end directly on the zero temperature line $S2_-$.

The pattern of disorder driven flows discussed in this section is schematically summarized in figure 8.6. For $N_* < N < 1$ there is a sequence of three flows between four fixed points ($P2_- \rightarrow V1_- \leftarrow S1_- \rightarrow S2_-$) that accounts for the pattern observed numerically at $N = 0.6$ in [135]. The flows observed in [135] in the ranges $0 < N < N_*$ and $1 < N < 2$ also match those following from our identifications. Our results also explain why the flow from the pure model to the Nishimori-like point is not observed in [135] for $N > 2$. The reason is that for $N > 2$ the hexagonal lattice loop model studied in that paper cannot see the critical point of the pure $O(N)$ model⁴. Indeed, we saw that this corresponds to $P1_+$, a purely transmissive ($S1 = S3 = 0$) solution that is not realized on the hexagonal lattice.

³The model studied in [136, 137] is the random phase XY model, which has $\mathbf{s}_i = (\cos \alpha_i, \sin \alpha_i)$, nearest neighbor interaction $-\cos(\alpha_i - \alpha_j + A_{ij})$, and random variables A_{ij} drawn from a distribution $P(A_{ij}) \propto e^{-A_{ij}^2/\sigma}$; σ replaces $1-p$ in figure 8.1. Since our formalism relies only on symmetry, it applies also to this type of disorder.

⁴It sees instead a critical point with Z_3 symmetry inherited from the lattice structure [138].

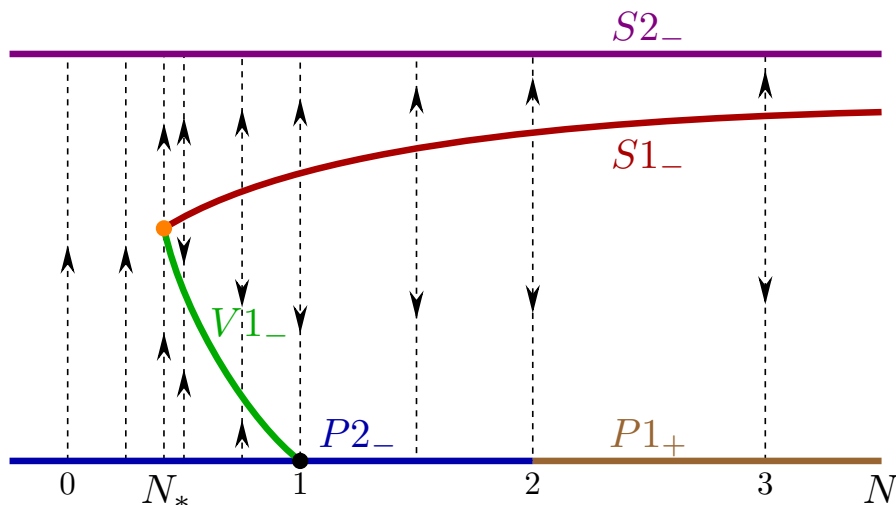


Figure 8.6: Schematic illustration of lines of fixed points and renormalization group flows between them. The critical pure model is at the bottom ($P2_-$, $P1_+$), and is connected to the Nishimori-like multicritical line $S1_-$ by the line of stable fixed points $V1_-$, which spans the interval $N \in (N_* = \sqrt{2} - 1, 1)$. $S2_-$ is a line of zero temperature stable fixed points. For $N = 1$ the renormalization group trajectories correspond to the phase boundary of figure 8.1.

The fact that for $N > 2$ both the pure fixed point and that corresponding to $S2_-$ fall at zero temperature suggests that in this range also the Nishimori-like fixed point should be at zero temperature. In this respect it is interesting to notice that *two* zero temperature disordered fixed points were found in [135] for $N = 8$.

One implication of our results is that the large distance physics of self-avoiding walks in a random medium ($N = 0$) is controlled by the fixed point on $S2_-$. Consistently, the amplitudes S_2 and S_5 corresponding to intersecting walks vanish for this solution.

The scale invariant scattering approach to random criticality in two dimensions initiated in [5] has shown, when such an outcome no longer seemed likely, that exact results can be obtained for this problem. In particular, it shows that random fixed points possess conformal invariance, which in the particle description is responsible for the elasticity of scattering processes. It also emerges that the

CFT's of random fixed points allow for superuniversal (symmetry independent) sectors, a circumstance that has no counterpart in the pure case. Probably this peculiarity has contributed to the difficulty of identifying CFT's of random criticality but, having been recognized, could also serve as a guide towards the remaining goal – completing for the random solutions a table of conformal data similar to table 3.2 for the pure ones.

Bibliography

- [1] P. Di Francesco, P. Mathieu, and D. Senechal, Conformal Field Theory, New York: Springer-Verlag (1997).
- [2] A.A. Belavin, A.M. Polyakov, and A.B. Zamolodchikov, Infinite conformal symmetry in two-dimensional quantum field theory, Nucl. Phys. B 241 (1984) 333.
- [3] G. Delfino, Parafermionic excitations and critical exponents of random cluster and $O(n)$ models. Ann. Phys. 333 (2013) 1.
- [4] G. Delfino, Fields, particles and universality in two dimensions, Annals of Physics 360 (2015) 477.
- [5] G. Delfino, Exact Results for Quenched Bond Randomness at Criticality, Phys. Rev. Lett. 118 (2017) 250601.
- [6] L.P. Kadanoff, Scaling laws for Ising models near T_c . Phys. 2 (1966) 263.
- [7] K.G. Wilson and J. Kogut, The renormalization group and the ϵ expansion, Phys. Rep. 12 (1974) 75.
- [8] J. Cardy, Scaling and renormalization in statistical physics, New York: Cambridge University Press (1996).
- [9] A.M. Polyakov, Conformal Symmetry of Critical Fluctuations. (Originally published in Russian Volume 12, Number 11) Sov. JETP Lett. 12 (1970) 381.

- [10] A.B. Zamolodchikov, Irreversibility of the Flux of the Renormalization Group in a 2D Field Theory, JETP Lett. 43 (1986) 730.
- [11] Vl.S. Dotsenko and V.A. Fateev, Conformal algebra and multipoint correlation functions in 2D statistical models, Nucl. Phys. B 240 (1984) 312.
- [12] B. Nienhuis, Coulomb gas formulation of two-dimensional phase transitions in: C. Domb, J.L. Lebowitz (Eds.), Phase Transitions and Critical Phenomena, Vol. 11, London: Academic Press (1987) p. 1.
- [13] B. Nienhuis, Critical behavior of two-dimensional spin models and charge asymmetry in the Coulomb gas, J. Stat. Phys. 34 (1984) 731.
- [14] B. Nienhuis, Exact Critical Point and Critical Exponents of $O(n)$ Models in Two Dimensions. Phys. Rev. Lett. 49 (1982) 1062.
- [15] P.G. de Gennes, Exponents for the excluded volume problem as derived by the Wilson method, Phys. Lett. A 38 (1972) 339.
- [16] N.D. Mermin and H. Wagner, Absence of Ferromagnetism or Antiferromagnetism in One- or Two-Dimensional Isotropic Heisenberg Models, Phys. Rev. Lett. 17 (1966) 1133.
- [17] P.C. Hohenberg, Existence of Long-Range Order in One and Two Dimensions, Phys. Rev. 158 (1967) 383.
- [18] S. Coleman, There are no Goldstone bosons in two dimensions, Commun.Math. Phys. 31 (1973) 259.
- [19] V.L. Berezinsky, Destruction of long range order in one-dimensional and two-dimensional systems having a continuous symmetry group. I. Classical systems, Sov.Phys.JETP 32 (1971) 493.
- [20] J.M. Kosterlitz and D.J. Thouless, Ordering, metastability and phase transitions in two-dimensional systems, J. Phys. C: Solid State Phys. 6 (1973) 1181.

-
- [21] S. Coleman, Quantum sine-Gordon equation as the massive Thirring model, *Phys. Rev. D* 11 (1975) 2088.
- [22] S. Mandelstam, Soliton operators for the quantized sine-Gordon equation, *Phys. Rev. D* 11 (1975) 3026.
- [23] F.Y. Wu, The Potts model, *Rev. Mod. Phys.* 54 (1982) 235.
- [24] C.K. Fortuin and P.W. Kasteleyn, On the random-cluster model: I. Introduction and relation to other models, *Physica* 57 (1972) 536.
- [25] R.J. Baxter, *Exactly Solved Models of Statistical Mechanics*, London: Academic Press (1982).
- [26] A.B. Harris, Effect of random defects on the critical behaviour of Ising models, *J. Phys. C: Solid State Phys.* 7 (1974) 1671.
- [27] R.J. Eden, P.V. Landshoff, D.I. Olive, J.C. Polkinghorne, *The Analytic S-matrix*, Cambridge: Cambridge University Press (1966).
- [28] G. Delfino and N. Lamsen, Critical lines in the pure and disordered $O(N)$ model. *J. Stat. Mech.* (2019) 024001.
- [29] G. Delfino and E. Tartaglia, Classifying Potts critical lines, *Phys. Rev. E* 96 (2017) 042137.
- [30] A.B. Zamolodchikov, Renormalization group and perturbation theory about fixed points in two-dimensional field theory, *Sov. J. Nucl. Phys.* 46 (1987) 1090.
- [31] J.L. Jacobsen, N. Read and H. Saleur, Dense Loops, Supersymmetry, and Goldstone Phases in Two Dimensions, *Phys. Rev. Lett.* 90 (2003) 090601.
- [32] A.B. Zamolodchikov, Exact S-matrix associated with self-avoiding polymer problem in two dimensions, *Mod. Phys. Lett. A* 6 (1991) 1807.
- [33] G. Delfino, Off-critical correlations in the Ashkin-Teller model, *Phys. Lett. B* 450 (1999) 196.

- [34] G. Delfino and P. Grinza, Universal ratios along a line of critical points. The Ashkin–Teller model, Nucl. Phys. B 682 (2004) 521.
- [35] L. Chim and A. Zamolodchikov, Integrable Field Theory of the q -state Potts Model with $0 < q < 4$, Int. J. Mod. Phys. A 07 (1992) 5317.
- [36] G. Delfino and J. Viti, On three-point connectivity in two-dimensional percolation, J. Phys. A: Math. Theor. 44 (2011) 032001.
- [37] G. Delfino, J. Viti and J. Cardy, Universal amplitude ratios of two-dimensional percolation from field theory, J. Phys. A: Math. Theor. 43 (2010) 152001.
- [38] G. Delfino and J. Viti, Potts q -color field theory and scaling random cluster model, Nucl. Phys. B 852 (2011) 149.
- [39] G. Delfino and J. Viti, Crossing probability and number of crossing clusters in off-critical percolation, J. Phys. A: Math. Theor. 45 (2011) 032005.
- [40] G. Delfino and P. Grinza, Confinement in the q -state Potts field theory, Nucl. Phys. B 791 (2008) 265.
- [41] B. Nienhuis, A.N. Berker, E.K. Riedel and M. Schick, First- and Second-Order Phase Transitions in Potts Models: Renormalization-Group Solution, Phys. Rev. Lett. 43 (1979) 737.
- [42] J. Salas and A.D. Sokal, Absence of phase transition for antiferromagnetic Potts models via the Dobrushin uniqueness theorem, J. Stat. Phys. 86 (1997) 551.
- [43] R. J. Baxter, Critical antiferromagnetic square-lattice Potts model, Proc. R. Soc. London. A. 383 (1982) 43.
- [44] H. Saleur, The antiferromagnetic Potts model in two dimensions: Berker-Kadanoff phase, antiferromagnetic transition, and the role of Beraha numbers, Nucl. Phys. B 360 (1991) 219.

- [45] J. Cardy, J.L. Jacobsen and A.D. Sokal, Unusual Corrections to Scaling in the 3-State Potts Antiferromagnet on a Square Lattice, *J. Stat. Phys.* 105 (2001) 25.
- [46] G. Delfino, Sine-Gordon description of the scaling three-state Potts antiferromagnet on the square lattice, *J. Phys. A: Math. Gen.* 34 (2001) L311.
- [47] G. Delfino, Field Theory of Scaling Lattice Models: The Potts Antiferromagnet in: A. Cappelli, G. Mussardo (Eds.) *Statistical Field Theories. NATO Science Series II, Vol. 73*, Amsterdam: Kluwer Academic Publishers (2002), p. 3.
- [48] J.L. Jacobsen and H. Saleur, The antiferromagnetic transition for the square-lattice Potts model, *Nucl. Phys. B* 743 (2006) 207.
- [49] Y. Ikhlef, The antiferromagnetic potts model, *Mod. Phys. Lett. B* 25 (2011) 291.
- [50] J.-P. Lv, Y. Deng, J.L. Jacobsen and J. Salas, The three-state Potts antiferromagnet on plane quadrangulations, *J. Phys. A: Math. Theor.* 51 (2018) 365001.
- [51] Y. Deng, Y. Huang, J.L. Jacobsen, J. Salas and A.D. Sokal, Finite-Temperature Phase Transition in a Class of Four-State Potts Antiferromagnets, *Phys. Rev. Lett.* 107 (2011) 150601.
- [52] Y. Huang, K. Chen, Y. Deng, J.L. Jacobsen, R. Kotecký, J. Salas, A.D. Sokal and J.M. Swart, Two-dimensional Potts antiferromagnets with a phase transition at arbitrarily large q , *Phys. Rev. E* 87 (2013) 012136.
- [53] D.R. Nelson, J.M. Kosterlitz, and M.E. Fisher, Renormalization-Group Analysis of Bicritical and Tetracritical Points, *Phys. Rev. Lett.* 33 (1974) 813.
- [54] E. Granato, J.M. Kosterlitz, J. Lee, M.P. Nightingale, Phase transitions in coupled XY-Ising systems. *Phys. Rev. Lett.* 66 (1991) 1090.

Bibliography

- [55] J. Villain, Two-level systems in a spin-glass model. I. General formalism and two-dimensional model. *J. Phys. C: Solid State Phys.* 10 (1977) 4793.
- [56] S. Teitel, C. Jayaprakash, Phase transitions in frustrated two-dimensional XY models, *Phys. Rev. B* 27 (1983) 598.
- [57] J.M. Kosterlitz, Kosterlitz–Thouless physics: a review of key issues, *Rep. Prog. Phys.* 79 (2016) 026001.
- [58] W.Y. Shih, D. Stroud, Superconducting arrays in a magnetic field: Effects of lattice structure and a possible double transition, *Phys. Rev. B* 30 (1984) 6774.
- [59] P. Olsson, Two Phase Transitions in the Fully Frustrated XY Model, *Phys. Rev. Lett.* 75 (1995) 2758.
- [60] M. Hasenbusch, A. Pelissetto, E. Vicari, Multicritical behaviour in the fully frustrated XY model and related systems, *J. Stat. Mech.* (2005) P12002.
- [61] Y. Ozeki and N. Ito, Nonequilibrium relaxation analysis of fully frustrated XY models in two dimensions *Phys. Rev. B* 68 (2003) 054414.
- [62] S. Okumura, H. Yoshino and H. Kawamura, Spin-chirality decoupling and critical properties of a two-dimensional fully frustrated XY model, *Phys. Rev. B* 83 (2011) 094429.
- [63] J. Struck *et al.*, Engineering Ising-XY spin-models in a triangular lattice using tunable artificial gauge fields, *Nature Physics* 9 (2013) 738.
- [64] Y.M.M. Knops, B. Nienhuis, H.J.F. Knops and H.W.J. Blote, 19-vertex version of the fully frustrated XY model, *Phys. Rev. B* 50 (1994) 1061.
- [65] G. Delfino and N. Lamsen, Critical points of coupled vector-Ising systems. Exact results. *J. Phys. A: Math. Theor.* 52 (2019) 35LT02.
- [66] J. Ashkin and E. Teller, Statistics of Two-Dimensional Lattices with Four Components, *Phys. Rev.* 64 (1943) 178.

- [67] L.P. Kadanoff and A.C. Brown, Correlation functions on the critical lines of the Baxter and Ashkin-Teller models, *Ann. Phys.* 121 (1979) 318.
- [68] J.V. José, L.P. Kadanoff, S. Kirkpatrick and D.R. Nelson, Renormalization, vortices, and symmetry-breaking perturbations in the two-dimensional planar model, *Phys. Rev. B* 16 (1977) 1217.
- [69] L.P. Kadanoff, Multicritical behavior at the kosterlitz-thouless critical point, *Ann. Phys.* 120 (1979) 39.
- [70] P.G. de Gennes and J. Prost, *The Physics of Liquid Crystals*, Oxford: University Press (1993).
- [71] P.J. Yoo, K.T. Nam, J. Qi, S.-K. Lee, J. Park, A.M. Belcher and P.T. Hammond, Spontaneous assembly of viruses on multilayered polymer surfaces, *Nat. Mater.* 5, 234 (2006).
- [72] L. Isa, J.M. Jung and R. Mezzenga, Unravelling adsorption and alignment of amyloid fibrils at interfaces by probe particle tracking, *Soft Matter* 7, 8127 (2011).
- [73] S. Jordens, L. Isa, I. Usov and R. Mezzenga, Non-equilibrium nature of two-dimensional isotropic and nematic coexistence in amyloid fibrils at liquid interfaces, *Nature Comm.* 4: 1917 (2013).
- [74] P.A. Lebwohl and G. Lasher, Nematic-Liquid-Crystal Order—A Monte Carlo Calculation, *Phys. Rev. A* 6 (1972) 426.
- [75] Z. Zhang, O.G. Mouritsen and M. Zuckermann, Weak first-order orientational transition in the Lebwohl-Lasher model for liquid crystals, *Phys. Rev. Lett.* 69 (1992) 2803.
- [76] N.D. Mermin, The topological theory of defects in ordered media, *Rev. Mod. Phys.* 51, 591 (1979).

- [77] H. Kunz and G. Zumbach, Topological phase transition in a two-dimensional nematic n-vector model: A numerical study, *Phys. Rev. B* 46 (1992) 662.
- [78] A.I. Farinas-Sanchez, R. Paredes and B. Berche, Evidence for a topological transition in nematic-to-isotropic phase transition in two dimensions, *Phys. Lett. A* 308 (2003) 461.
- [79] S. Dutta and S.K. Roy, Phase transitions in two planar lattice models and topological defects: A Monte Carlo study, *Phys. Rev. E* 70 (2004) 066125.
- [80] S. Shabnam, S.D. Gupta and S.K. Roy, Existence of a line of critical points in a two-dimensional Lebwohl Lasher model, *Phys. Lett. A* 380 (2016) 667.
- [81] C. Chiccoli, P. Pasini and C. Zannoni, A Monte Carlo investigation of the planar Lebwohl-Lasher lattice model, *Physica A* 148 (1988) 298.
- [82] R. Paredes R., A.I. Farinas-Sanchez and R. Botet, No quasi-long-range order in a two-dimensional liquid crystal, *Phys. Rev. E* 78 (2008) 051706.
- [83] A.I. Farinas-Sanchez, R. Botet, B. Berche and R. Paredes, On the critical behaviour of two-dimensional liquid crystals, *Condens. Matter Phys.* 13 (2010) 13601.
- [84] Y. Tomita, Finite-size scaling analysis of pseudocritical region in two-dimensional continuous-spin systems, *Phys. Rev. E* 90 (2014) 032109.
- [85] B. Kamala Latha and V.S.S. Sastry, Two Phase Transitions in the Two-Dimensional Nematic Three-Vector Model with No Quasi-Long-Range Order: Monte Carlo Simulation of the Density of States, *Phys. Rev. Lett.* 121 (2018) 217801.
- [86] F. Niedermayer, P. Weisz and D.-S. Shin, Question of universality in RP^{n-1} and $O(n)$ lattice σ models, *Phys. Rev. D* 53 (1996) 5918.
- [87] M. Hasenbusch, $O(N)$ and RP^{N-1} models in two dimensions, *Phys. Rev. D* 53 (1996) 3445.

-
- [88] S.M. Catterall, M. Hasenbusch, R.R. Horgan, R. Renken, Nature of the continuum limit in the 2D RP^2 gauge model, Phys. Rev. D 58 (1998) 074510.
- [89] J. Zinn-Justin, Quantum Field Theory and Critical Phenomena, Oxford: Clarendon Press (2002).
- [90] D.K. Sinclair, Monte Carlo calculations for an $O(3)/Z_2$ lattice spin model in 2 dimensions, Nucl. Phys. B 205 (1982) 173.
- [91] S. Caracciolo, R.G. Edwards, A. Pelissetto and A.D. Sokal, Possible failure of asymptotic freedom in two-dimensional RP^2 and RP^3 σ -models, Nucl. Phys. B (Proc. Suppl.) 30 (1993) 815.
- [92] S. Caracciolo, R.G. Edwards, A. Pelissetto and A.D. Sokal, New universality classes for two-dimensional σ -models, Phys. Rev. Lett. 71 (1993) 3906.
- [93] G. Delfino, Y. Diouane, and N. Lamsen, Absence of nematic quasi-long-range order in two-dimensional liquid crystals with three director components, arXiv:2005.06307 [cond-mat].
- [94] S.F. Edwards and P.W. Anderson, Theory of spin glasses, J. Phys. F 5 (1975) 965.
- [95] G. Delfino and A. Squarcini, Phase Separation in a Wedge: Exact Results, Phys. Rev. Lett. 113 (2014) 066101.
- [96] F. Smirnov, Quantum groups and generalized statistics in integrable models, Commun. Math. Phys. 132 (1990) 415.
- [97] G. Delfino, On the space of quantum fields in massive two-dimensional theories, Nucl. Phys. B 807 (2009) 455.
- [98] G. Delfino and G. Niccoli, The composite operator $\bar{T}T$ in sinh-Gordon and a series of massive minimal models, JHEP 05 (2006) 035.
- [99] G. Delfino and E. Tartaglia, On superuniversality in the q-state Potts model with quenched disorder J. Stat. Mech. (2017) 123303.

Bibliography

- [100] V. Dotsenko, J.L. Jacobsen, M.-A. Lewis and Marco Picco, Coupled Potts models: Self-duality and fixed point structure, Nucl. Phys. B 546 [FS] (1999) 505.
- [101] A. Aizenman and J. Wehr, Rounding of first-order phase transitions in systems with quenched disorder, Phys. Rev. Lett. 62 (1989) 2503.
- [102] K. Hui and A.N. Berker, Random-field mechanism in random-bond multicritical systems, Phys. Rev. Lett. 62 (1989) 2507.
- [103] V.S. Dotsenko and V.I.S. Dotsenko, Critical behaviour of the phase transition in the 2D Ising Model with impurities, Adv. Phys. 32 (1983) 129.
- [104] J. Cardy and J.L. Jacobsen, Critical Behavior of Random-Bond Potts Models, Phys. Rev. Lett. 79 (1997) 4063.
- [105] J.L. Jacobsen and J. Cardy, Critical behaviour of random-bond Potts models: a transfer matrix study, Nucl. Phys. B 515 (1998) 701.
- [106] J.T. Chayes, L. Chayes, D.S. Fisher and T. Spencer, Finite-Size Scaling and Correlation Lengths for Disordered Systems, Phys. Rev. Lett. 57 (1986) 2999.
- [107] S. Chen, A.M. Ferrenberg and D.P. Landau, Randomness-induced second-order transition in the two-dimensional eight-state Potts model: A Monte Carlo study, Phys. Rev. Lett. 69 (1992) 1213.
- [108] S. Chen, A.M. Ferrenberg and D.P. Landau, Monte Carlo simulation of phase transitions in a two-dimensional random-bond Potts model, Phys. Rev. E 52 (1995) 1377.
- [109] E. Domany and S. Wiseman, Critical behavior of the random-bond Ashkin-Teller model: A Monte Carlo study, Phys. Rev. E 51 (1995) 3074.
- [110] M. Kardar, A.L. Stella, G. Sartoni and B. Derrida, Unusual universality of branching interfaces in random media, Phys. Rev. E 52 (1995) R1269.

- [111] C. Chatelain and B. Berche, Magnetic critical behavior of two-dimensional random-bond Potts ferromagnets in confined geometries, *Phys. Rev. E* 60 (1999) 3853.
- [112] T. Olson and A.P. Young, Monte Carlo study of the critical behavior of random bond Potts models *Phys. Rev. B* 60 (1999) 3428.
- [113] J.L. Jacobsen and M. Picco, Large- q asymptotics of the random-bond Potts model, *Phys. Rev. E* 61 (2000) R13.
- [114] A.W.W. Ludwig, Infinite hierarchies of exponents in a diluted ferromagnet and their interpretation, *Nucl. Phys. B* 330 (1990) 639.
- [115] V. Dotsenko, M. Picco and P. Pujol, Renormalisation-group calculation of correlation functions for the 2D random bond Ising and Potts models, *Nucl. Phys. B* 455 (1995) 701.
- [116] J.-Ch. Anglès d'Auriac and F. Igloi, Phase Transition in the 2D Random Potts Model in the Large- q Limit, *Phys. Rev. Lett.* 90 (2003) 190601.
- [117] H. Nishimori, Internal Energy, Specific Heat and Correlation Function of the Bond-Random Ising Model, *Prog. Theor. Phys.* 66 (1981) 1169.
- [118] E.S. Sorensen, M.J.P. Gingras and D.A. Huse, Non-trivial fixed-point structure of the two-dimensional $\pm J$ 3-state Potts ferromagnet/spin glass, *Europhys. Lett.* 44 (1998) 504.
- [119] F. Merz and J.T. Chalker, Two-dimensional random-bond Ising model, free fermions, and the network model, *Phys. Rev. B* 65 (2002) 054425.
- [120] S.L.A. de Queiroz, Multicritical point of Ising spin glasses on triangular and honeycomb lattices, *Phys. Rev. B* 73 (2006) 064410.
- [121] M. Picco, A. Honecker and P. Pujol, Strong disorder fixed points in the two-dimensional random-bond Ising model, *JSTAT* (2006) P09006.

- [122] M. Hasenbusch, F. Parisen Toldin, A. Pelissetto and E. Vicari, Multicritical Nishimori point in the phase diagram of the $\pm J$ Ising model on a square lattice, Phys. Rev. E 77 (2008) 051115.
- [123] F. Parisen Toldin, A. Pelissetto and E. Vicari, Strong-Disorder Paramagnetic-Ferromagnetic Fixed Point in the Square-Lattice $\pm J$ Ising Model, J. Stat. Phys. 135 (2009) 1039.
- [124] H. Nishimori and M.J. Stephen, Gauge-invariant frustrated Potts spin-glass, Phys. Rev. B 27 (1983) 5644.
- [125] M. Ohzeki and J.L. Jacobsen, High-precision phase diagram of spin glasses from duality analysis with real-space renormalization and graph polynomials J. Phys. A 48 (2015) 095001.
- [126] J.L. Jacobsen and M. Picco, Phase diagram and critical exponents of a Potts gauge glass, Phys. Rev. E 65 (2002) 026113.
- [127] W.L. McMillan, Domain-wall renormalization-group study of the two-dimensional random Ising model, Phys. Rev. B 29 (1984) 4026.
- [128] W.L. McMillan, Domain-wall renormalization-group study of the three-dimensional random Ising model, Phys. Rev. B 30 (1984) 476.
- [129] G. Delfino and N. Lamsen, On the phase diagram of the random bond q -state Potts model. Eur. Phys. J. B 92 (2019) 278.
- [130] J.L. Jacobsen, P. Le Doussal, M. Picco, R. Santachiara and K.J. Wiese, Phys. Rev. Lett. 102 (2009) 070601.
- [131] V. Gorbenko, S. Rychkov and B. Zan, Walking, Weak first-order transitions, and Complex CFTs II. Two-dimensional Potts model at $Q > 4$, SciPost Phys. 5, 050 (2018).
- [132] G. Delfino and N. Lamsen, Exact results for the $O(N)$ model with quenched disorder. J. High Energ. Phys. (2018) 77.

- [133] V.S. Dotsenko and V.I.S. Dotsenko, Phase transition in the 2D Ising model with impurity bonds, *Sov. Phys. JETP Lett.* 33 (1981) 37.
- [134] H. Shimada, Disordered $O(n)$ loop model and coupled conformal field theories, *Nucl. Phys. B* 820 (2009) 707.
- [135] H. Shimada, J.L. Jacobsen and Y. Kamiya, Phase diagram and strong-coupling fixed point in the disordered $O(n)$ loop model, *J. Phys. A* 47 (2014) 122001.
- [136] V. Alba, A. Pelissetto and E. Vicari, Magnetic and glassy transitions in the square-lattice XY model with random phase shifts *J. Stat. Mech.* (2010) P03006.
- [137] Y. Ozeki, S. Yotsuyanagi, T. Sakai and Y. Echinaka, Numerical studies on critical properties of the Kosterlitz-Thouless phase for the gauge glass model in two dimensions, *Phys. Rev. E* 89 (2014) 022122.
- [138] W. Guo, H.W.J. Blote and F.Y. Wu, Phase Transition in the $n > 2$ Honeycomb $O(n)$ Model, *Phys. Rev. Lett.* 85 (2000) 3874.